Durham E-Theses

The influence of interchain interactions on the photophysics of conjugated polymers

Hintschich, Susanne Ilona

How to cite:

Hintschich, Susanne Ilona (2002) *The influence of interchain interactions on the photophysics of conjugated polymers*, Durham theses, Durham University. Available at Durham E-Theses Online: http://etheses.dur.ac.uk/3949/

Use policy

The Influence of Interchain Interactions

on the Photophysics of Conjugated Polymers

Susanne Ilona Hintschich

A thesis submitted to the University of Durham for the degree of Master of Science by Research and Thesis

1 0 NOV 2003

University of Durham

Department of Physics

December 2002

DECLARATION

All material contained in this thesis is original and is the result of my own work except where explicit reference is made. Material from work of others has been suitably indicated.

This thesis has not been submitted in whole or in part for the award of a degree at this or any other university.

The copyright of this thesis rests with the author. No quotation from it should be published without their prior consent and information derived from in acknowledged.

ACKNOWLEDGEMENTS

Probably I could add about 400 single spaced pages to this thesis just thanking all the people who supported me during my M.Sc. thesis – when I tried to be short. The first 399 1/2 of these would of course be devoted to Carst, who has been my motor (I tried hard to find a positive expression here) not only since I joined the OEM group and is the actual reason why I came to Durham. However, as the reader would probably want to skip these pages, I will use this space to thank all the persons who have been responsible to make sure that I don't regret my stay in Durham.

First of all, my family gave me the financial start to go abroad and have supported me in many other non-material ways since then.

Professor Andy P. Monkman. He keeps the OEM group together, adds a member now and then but still has an open ear for everyone. Thank you for all this good advice and your patience.

Ben, George, Jian, L-O, Micha, Naveed, Sinha and Sophie, who are all somehow related to the OEM group. Thank you for your help and sympathy with experimental and non-experimental matters, and for your company.

Norman and Davy. They have been the general organisers, problem solvers and persons to ask not only when equipment is broken. Your help was very important to me.

I hope that all of these people have contributed to something worth reading.

ABSTRACT

This thesis presents findings on the photoluminescence properties of two conjugated polymers with special interest paid to interchain interactions and chemical degradation.

The delayed luminescence of thin films of poly(3-methyl-4-octyl-thiophene) (PMOT) has been observed via time-resolved photoluminescence spectroscopy (TRS) in different temperature regimes. While at 15 K the emission consists of delayed fluorescence (DF) and phosphorescence (Ph) originating from radiatively decaying singlet and triplet excitons, room temperature emission is red-shifted with respect to the DF and originates from excimers. Supportingly, photo-induced absorption experiments detect very long-lived excitations allocated to the triplet counterparts of the emitting excimers.

Furthermore, the influence of the photo-oxidisation of polyfluorenes on their luminescence is investigated. A series of polyfluorene/polyfluorenone co-polymers (PFO/PFl) with varying percentages of fluorenone repeat units was analysed via TRS as well as steady-state absorption, photoluminescence and photoexcitation spectroscopy in solid state and solution. Fluorenone repeat units (or keto defects) arising from polyfluorene photo-oxidation are the origin of the green luminescence band affecting the colour purity and quantum yield of polyfluorene devices. Fluorenone triplets play a major role and can be directly photo-excited. Moreover, they form upon polyfluorene degradation. Efficient energy transfer takes place from PFO singlets to fluorenone triplets entailing two types of triplet-triplet interaction processes, which lead to the formation of fluorenone excimers as well as polyfluorene-fluorenone exciplexes. Two types of the green emission can be assigned to emission from these states. This could be confirmed by the decay kinetics, thermal behaviour and keto level dependence of the emissions.

1. INTRODUCTION

Decades ago artificially synthesised polymers replaced wood or metal wherever cheap and easy to fabricate bulk materials were needed. Their versatility satisfied applications as different as plastic bags or window frames, mainly owing to an extreme chemical and morphological complexity: Polymers encompass a whole class of organic chemistry with infinite chemical variety – their properties can be tuned to suit whatever purpose is intended.

This concerned the application of polymers as bulk materials; the use of their electrical properties was restricted to insulating layers in condensators or shoes until, in the late seventies it was discovered that a certain class of polymers – called the conjugated polymers – is able to conduct electricity. Combined with the enormous advantages of polymers regarding their processing this opened the prospect for a whole new field of electrical applications including conducting organic fibres or prints. However, these remained in the research laboratories when commercial interest faded after it became obvious that the conducting properties of a conjugated polymer could never match those of a metal.

Interest revived in 1990 when another breakthrough in polymer physics was achieved with the discovery of electroluminescence in thin films of poly(phenylenevinylene) (PPV) by Burroughes et al.[1]. Until then the spectrum of display technologies only included inorganic materials such as semiconductors or liquid crystals. Carried out under extremely high temperatures the fabrication of semiconductor displays is complicated and energy consuming. On the other hand, the easier to produce liquid crystal displays exhibit only a narrow viewing angle as they do not emit themselves but serve as the mask for the active layer. Getting polymer displays to work could remove all of these problems. Taking advantage of decades of experience with the processing of polymers, flexible displays might be produced commercially simply by printing the active polymer layer at room temperature – large viewing angles would be no problem anymore. Or, how about home-printed displays, glowing wallpaper or screens on your T-shirt?

Several steps towards these rather utopic applications have been taken since 1990 by commercial and institutional research. More and more efficient polymers have been synthesised as well as techniques to fabricate polymer light emitting diodes (PLEDs) and a new type of displays based on them[2, 3]. However, the requirements of a commercial application of PLEDs are still high: For displays, which are composed according to the RGB system, one needs saturated emission colours; moreover they have to be sufficiently bright and the emission must be efficient – with a stability for a time span of years.

Indeed, PLEDs are more efficient than their inorganic counterparts. Still, at least 75 percent of the input energy are "lost" between the moment of the injection of charge carriers into the

PLED and the emission of radiation. According to general theoretical considerations, this intrinsic limit arises during the recombination of charge carriers in a working device: Only 25 percent of the resulting excitations are actually singlet states, which can emit luminescence. The remaining 75 percent exhibit triplet character – and cannot contribute to emission. Several methods have been developed to circumvent this problem including the doping of PLEDs in order to transfer triplet energy to guest molecules, which can emit luminescence. Thus using otherwise lost energy the quantum yield of PLEDs could be improved – in some cases. Mostly, one encounters side effects such as interference of the dopant with the polymer singlets yielding the contrary effect of a reduction of quantum yield. Additionally, more sophisticated studies of the recombination of charge carriers have shown that the formation of singlets can exceed 25 percent by far (up to 60 percent). Both, the difficulties to use dopants and the uncertainty about the realistic singlet-triplet ratio show that actually little is known about the photophysics going on inside a conjugated polymer, especially regarding triplet excitons.

Apart from device architecture, it has become obvious that the processes determining the colour of emission, the brightness and stability of a PLED largely depend on the chemical composition and the morphology of the conjugated polymer. On one side, this is an advantage making it possible to chemically tune emission colours, which is unthinkable for semiconductors with their fixed bandgap. On the other side, the complexity of polymers, which consist of long disordered chain molecules instead of regular crystals, causes the difficulty to describe them physically and mathematically. Recent studies of long-lived photoexcitations in several conjugated polymers[4-7] have shown that these materials are not simply a sum of isolated macromolecules but that there are interactions between the single chains which have to be considered. Mechanisms such as aggregation or the formation of excimers are not found in inorganic systems but can affect polymer photophysics to a great extent. As they occur especially in the solid state – where interchain distances are minimised – they are of crucial importance to device photophysics.

Finally, chemistry adds some more unknown parameters as polymers are always subject to degradation i.e. via oxidisation. This leads to colour and brightness instability especially for the blue emitters. Despite all efforts to prolong the PLED lifetime by sealing, a stability of years is still hard to achieve – accounting for the lack of blue emitters which would be required for the production of colour displays. Therefore, understanding interchain interactions and chemical degradation of conjugated polymers is not only the key to understanding why different polymers emit differently. It can also be the fundament of a chemical optimisation of the emitters and, finally, of an improvement in PLED technology. In this context, special attention must be paid to the investigation of the solid state.

This work studies the influence of interchain interactions and photo-degradation on the photoluminescence of mainly two conjugated polymers, a polythiophene and a polyfluorene, with distinctive morphological and chemical properties. After an introduction into the

theoretical background and a description of the utilised experiments, sections four and five present the experimental results of the investigated substances for solid state and solution, discussion always running parallel and each section closing with conclusions and prospects to further work for the investigated polymer.

2. THEORY

2.1. The electronic orbitals of a conjugated polymer

2.1.1. The hybridisation of the carbon atom

Conjugated polymers are organic compounds built of thousands of repeat units, chemically bound together. They mainly consist of carbon atoms, which are found both in the polymer backbone and in the side chains attached to it.

The four outer electrons of a carbon atom are located in $2s^1$ and $2p^3$ orbitals. The energy step between them is so small that in the case of bond formation the orbitals can be hybridised yielding sp, sp^2 or sp^3 hybrid orbitals depending on the valence and number of the bond partners.
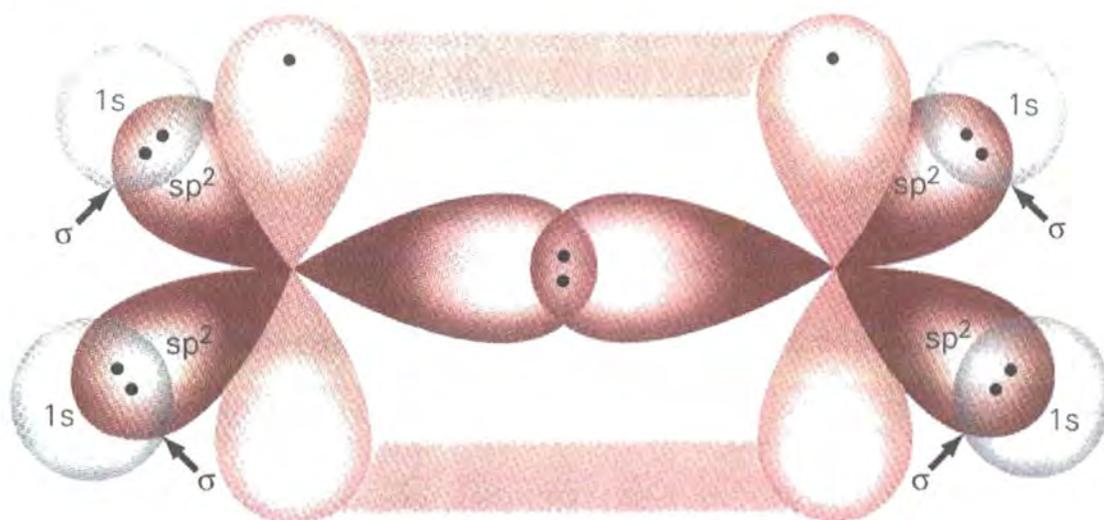
Figure 2.1 The bonding system of an ethene molecule[8]. *Gray*: Hydrogen orbitals; *Dark Red*: Carbon hybrid orbitals; *Light Red*: Carbon p_z orbitals.

The fundament of a conjugated polymer is the sp^2-hybrid: The three orbitals overlap with hydrogen or other carbon atoms to form strong σ bonds. The linear combination of the partners' electron densities leads to the creation of a *bonding* σ-and an *anti-bonding* σ*-orbital.

The remaining p_z-states are oriented orthogonally with respect to the hybrid electrons. Nevertheless, neighbouring p_z orbitals can overlap sideways to form a weak π bond in addition

to an already existing σ bond. Its weakness entails a pronounced delocalisation of the bound electrons located in a bonding π-and an anti-bonding π*-orbital. The former contains both π electrons in the ground state.

The above describes the basic structure of a conjugated polymer, with sp^2-hybridised carbon atoms as well as σ and π bonds. This is also found in the ethene molecule, shown in Figure 2.1[8]. Moreover, the repeat units of a conjugated polymer may also contain atoms with a valence different from four i.e. nitrogen that contribute *non-bonding* or *n orbitals* to the electron system. When they are excited, n electrons can be accommodated in π* orbitals.
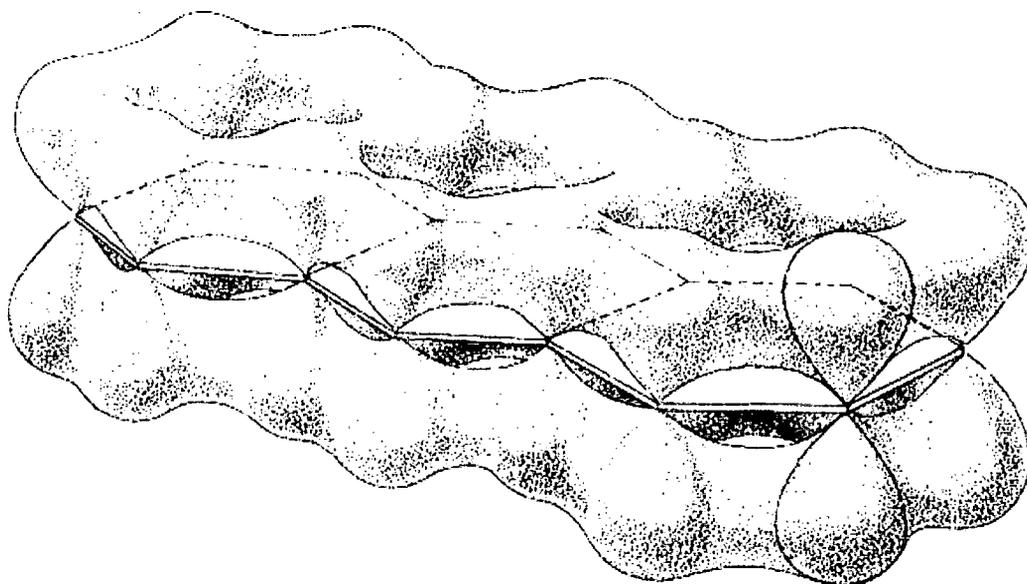
Figure 2.2 The delocalisation of π electrons over the three benzene ring orbitals of an anthracene molecule[9].

2.1.2. The conjugation of a polymer chain

Being the simplest of all conjugated polymers polyacetylene $(CH)_n$ is the macromolecular pendant of the ethene molecule. The polymer chains exhibit a structure with alternating single (only σ) and double (σ and π) bonds between the carbon atoms. Here, not only adjacent π orbitals overlap but – due to the structural periodicity – all π electrons are theoretically delocalised over the whole chain. This effect called *conjugation* is illustrated in Figure 2.2[9].

In reality, delocalisation is limited to an *effective conjugation length* located between 10 and 40 repeat units[10, 11]. The origin of this effect lies in chemical chain defects and impurities, which interfere with the conjugation system, but can also be found in twists between the repeat units[12], which force the neighbouring p_z orbitals out of plane and reduce their spatial overlap.

2.2. Excited states in conjugated polymers

This chapter will provide an introduction into the pseudo particles that exist in an excited conjugated polymer but also discuss the models, which are used to describe them.

2.2.1. Models for the electronic properties of conjugated polymers

Basically two models are employed to explain the electronic properties of conjugated polymers. The older theory considers the similarities between conjugated polymers and inorganic semiconductors. In both types of materials one encounters periodic structures – these extend in three isotropic dimensions for semiconductor crystals, whereas the linearity of polymer chains only allows for a one-dimensional periodicity provided that inter-chain interaction can be neglected.

In 1980, Su, Schrieffer and Heeger[13] modified the conventional semiconductor *band model* to be applied to one-dimensional chains of polyacetylene. As a result, the electronic structure of the polymer was made up of an occupied valence band and an unoccupied conduction band, which offered the first possibility to explain *conduction* phenomena in polymer materials.

However, the assumptions made for this model hold disadvantages. They include the negligibility of inter-chain contacts compared to intra-chain interactions, the dominance of nearest neighbour exchange for the latter but also the existence of free electrons. Consequently, Coulomb interactions of electron-hole pairs (*excitons*, see chapter 2.2.2) but also between exciton and polymer chain can only be considered to a limited extent.

Several experimental observations, particularly those concerning optical phenomena, contradict the assumptions. Vibrational modes occur in the luminescence spectra of many conjugated polymers e.g. MeH-PPV or PFO, which cannot be explained by a band model despite modifications that have been added to it in order to approach the reality of conjugated polymers.

Dealing with the optical spectroscopy of these materials, this thesis prefers the correlated or *exciton model* proposed by Bässler *et al.*[14]. Here, polymer chains are no longer required to be rigid and aligned. The delocalisation of π electrons can be imperfect caused by chain defects and twists (chapter 2.1.2). Therefore, the excitation of the polymer will not result in the formation of free or loosely bound charge carriers. Instead, an excited electron will still interact with its correlated hole via Coulombic forces to form an exciton localised on a conjugated segment of polymer chain.

This model allows for a detailed explanation of luminescence phenomena (chapter 2.3.4) and energy transport of conjugated polymers (chapter 2.4.3).

The nature of band and exciton model is so different that their validity can be evaluated considering only one parameter – the interaction or *binding energy* E_B of an exciton. The band model implies a generally low Coulomb interaction, corresponding to excitons of the Wannier-Mott type (next chapter). Values of ~0.1 eV would argue in favour of the semiconductor description, whereas a binding energy of >0.4 eV can only be realised with a majority of localised states.

Despite such clarity proponents of both models have found E_B values in favour of their side, e.g. for poly(phenylenevinylene) (PPV)[15, 16]. Less variation is observed for the ladder type poly(para-phenylene) (MeL-PPP), where the exciton model is favoured with E_B~0.3-0.4eV[15, 16].

2.2.2. Classification of excitons

The term *exciton* describes a pseudo-particle: a pair of electron and hole, which attract each other by their Coulombic potential. In contrast to a geminate pair they form a quantum mechanical unit i.e. the correlation of their spins. Excitons can be classified with respect to their binding energy, which is the energy an exciton needs to dissociate into independent charge carriers. In organic crystals one distinguishes between three types of excitons:

- The *Frenkel* type, where electron and hole are bound to the same molecular unit with a separation distance smaller than 5 Å[9]. Effectively no exciton dipole moment is observed due to such localisation. Electron and hole are strongly correlated with a binding energy of the order of several electron volts. Frenkel excitons in a conjugated polymer are located in a single conjugated region. Their recombination is supposed to be responsible for the emission of luminescence.
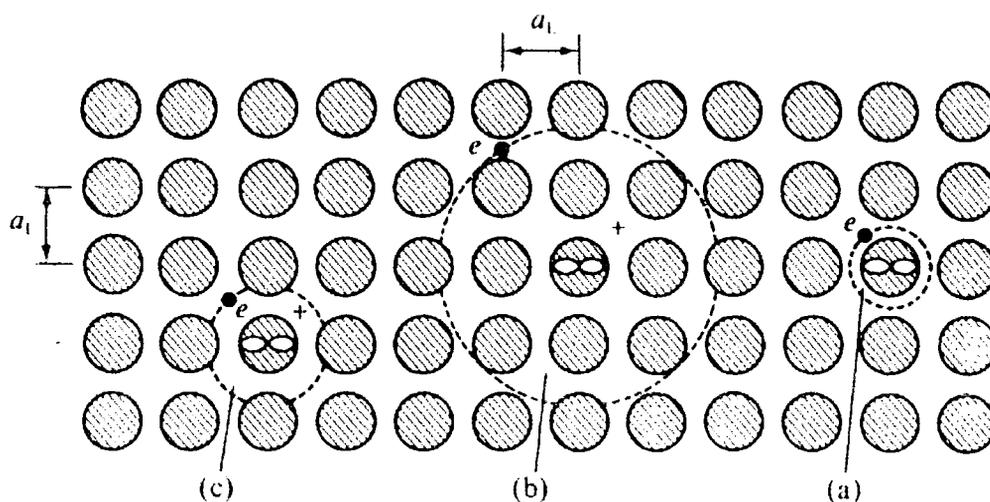
Figure 2.3 Excitons in an organic crystal: (a) Frenkel, (b) Wannier-Mott, (c) charge-transfer state[9].

- One refers to a *charge-transfer exciton* when the electron or hole has been transferred to a neighbour chain via excitation. Hence, the exciton possesses a permanent dipole moment but is still strongly correlated. Electron and hole might migrate independent of each other but also, similar to a geminate pair, recombine to emit delayed fluorescence.

- For *Wannier-Mott* type excitons the large mean separation distance between electron and hole of 40 to 100 Å[9] leads to a reduced Coulombic attraction. Correspondingly, these excitons exhibit a low binding energy (0.1 eV). Both charges can migrate rather freely, which inhibits the formation of a permanent dipole moment.

2.2.3. Polarons and geminate pairs

According to the Bässler model, excitons are created after the excitation of a conjugated polymer. If they finally recombine, they can give off their electrical energy in the form of radiation, a process which is called *luminescence*, see chapter 2.3.4.
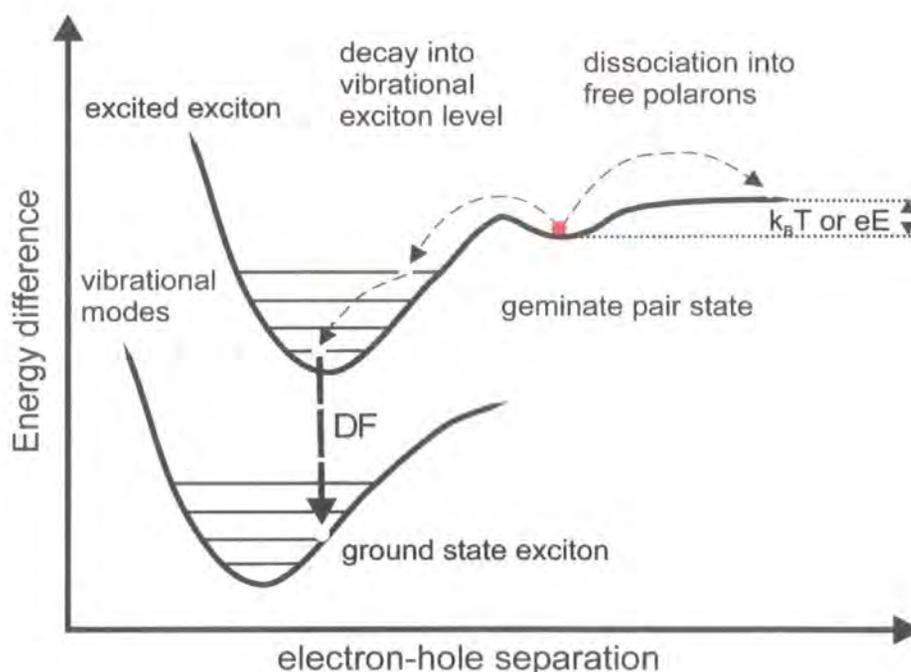
Figure 2.4 Relations between the potential energy of polarons, geminate pairs and exciton states. A transition from geminate pair to exciton can result in the emission of delayed fluorescence (DF)[17].

Beside this, further excitation might exceed the exciton binding energy and lead to its dissociation into an electron and hole, which then move independently through the polymer as single charge carriers on separate polymer chains. The polymer molecules carrying these single charges deform; their orbitals are disturbed in the presence of a new Coulomb potential so that

the bonding system has to find a new equilibrium. Compared to the surrounding electrically neutral molecules the charged chain is deformed at a length of about 20 repeat units[18]. Together, the charged polymer chain and the deformation pattern are termed *polaron*. Virtually, there are no free charges in the exciton model for conjugated polymers so that every single charge has to be treated as a polaron.

Being similar to a charge-transfer exciton, a *geminate pair (gp)* is an intermediate state between polaron and exciton. One can imagine it as a pair of oppositely charged polarons located on adjacent polymer chains: Their Coulomb potentials interact but they do not form an exciton. Thermal activation (which excites the pair by means of vibrational motion) or an applied electric field (which forces migration making use of the electrical dipole moment) can lead to the dissociation of a geminate pair into the original polarons.

As thermal excitation is also required to overcome the potential barrier between gp and exciton, the former can exist a long time (microsecond range) after it was created. Consequently, at these time scales in the presence of geminate pairs there is still a non-zero probability of exciton formation entailing the emission of *delayed fluorescence (DF)[19]*. Another DF channel, triplet-triplet annihilation, is described in chapter 2.5.1.

Figure 2.4[17] illustrates difference between excitons, geminate pairs and polarons with respect to the changes in potential energy required for the transitions between them.

2.3. Spectroscopy of conjugated polymers

Techniques like absorption or luminescence spectroscopy are essential for the understanding of the electronic structure and the electrical processes in a conjugated polymer. This section introduces into these spectroscopic methods and into the terminology that is necessary to describe the observed phenomena.

2.3.1. Absorption

Excited states in conjugated polymers can either be formed via *electroexcitation*, which stands for the injection and recombination of charge carriers, or via *photoexcitation*, which involves the absorption of radiation.

When electromagnetic radiation penetrates matter, it can be transmitted or absorbed. The fraction of the transmitted radiation is determined according to the law of Lambert and Beer:

Equation 2.1

$$I_x = I_0 \cdot \exp(-\alpha \cdot c \cdot x)$$

In Equation 2.1 the intensity of the transmitted radiation I_x is proportional to the intensity of the incident (monochromatic) radiation I_0, the concentration c of the absorber and the length x of the path of light in the material. The *absorption coefficient* α is introduced as the proportional factor. α can vary over several orders of magnitude for different wavelengths. Each material has its own characteristic absorption spectrum $\alpha(\lambda)$, which contains the information at which wavelength which amount of light can be absorbed. The product $A = \alpha cx$ is called the *absorbance* or *optical density* of the absorbing sample.

2.3.2. Allowed and forbidden transitions

Absorption is strong and α is high when the energy of the incident photons coincides with transition energies in the material. At these positions the absorption spectrum of smaller molecules exhibit sharp peaks imbedded into otherwise flat regions of low absorption. The height of these peaks is a measure of how *allowed* the corresponding transitions are. Maxima in the absorption of conjugated polymers appear in the visible spectrum (vis) up to the near ultraviolet (UV) and can be evaluated in the same way. However, these usually appear as broad bands; hence it is necessary to integrate the absorption coefficient over the frequencies v of the band region[20]:

Equation 2.2

$$f = 6.25 \times 10^{-19} \cdot \int_{v_1}^{v_2} \alpha(v) dv \cdot \frac{mol}{m^2 s}$$

The normalised outcome of this integration is termed *oscillator strength*, *f*, of the transition represented by the absorption band. f has the meaning of the probability of this transition; hence a value of f equal to 1 corresponds to fully allowed and f equal to 0 to fully forbidden events. The values of f between 1 and 0 can be further classified using quantum mechanical calculations.

In most cases, the Hamiltonian of the system has to be simplified in order to solve it and calculate probabilities of transitions. This also applies to the system of an exciton state in a *polyatomic molecule*. The corresponding Hamiltonian is separated into a set of *decoupled* sub-

Hamiltonians, which describe spin, parity, momentum properties and spatial dimensions of the orbitals. A general solution is independently an eigenfunction of all sub-Hamiltonians. Therefore separate transition probabilities p_i are found for spin (p_s), parity (p_p), momentum (p_m) and orbital symmetry (p_o).

Then the oscillator strength f of a transition from the π to the π^* orbital of a polyatomic molecule, i.e. benzene, can be written as:

Equation 2.3

$$f = p_s p_p p_m p_o f_a$$

where f_a is the oscillator strength of a fully allowed transition. The probabilities p_i can be summarised into *selection rules*. These are the selection rules for optical transitions:

- *Spin conservation* – Transitions which change the spin of a system are *spin forbidden*. This can be lifted due to disturbances of the system in the presence of heavy or paramagnetic atoms[9] – when the sub-Hamiltonians of the system are no longer separated due to *spin-orbit* coupling or *magnetic-spin* coupling. In most conjugated polymers the oscillator strength of transitions between states of different multiplicity (e.g. from a singlet to a triplet state) is weaker by a factor of $p_s=10^{-5}$ compared to those between states of equal multiplicity[21].

- *Inversion of parity* – Transitions between orbitals of opposite parity are probable. For the even π orbital of benzene a transition to the odd π^* state is *parity allowed*. The rule is lifted in most cases due to vibrations of the system which are not completely symmetrical.

- *Conservation of momentum* – When a photon is absorbed, no (elastic case) or only a small amount of momentum (inelastic case with phonon interaction) is added to the system. Transitions that involve *major* changes in the angular or linear momentum are *momentum forbidden*.

- *Orbital overlap* – A good spatial overlap of initial and final orbitals must be guaranteed for an allowed transition i.e. in the benzene ring a π-π^* transition, where both orbitals are located in the same plane. When the areas of electron probability between initial and final state are too different the transition is space or *overlap forbidden*.

Points 1 to 4 give some reasons, why a transition between two states might be forbidden. If this is the case, then the rate of the absorption process (or its reversal, the emission process) is decreased significantly due to the low transition probability. Other processes might occur faster and can dominate the absorption or emission due to forbidden transitions, so that the latter signals are often immeasurably weak.
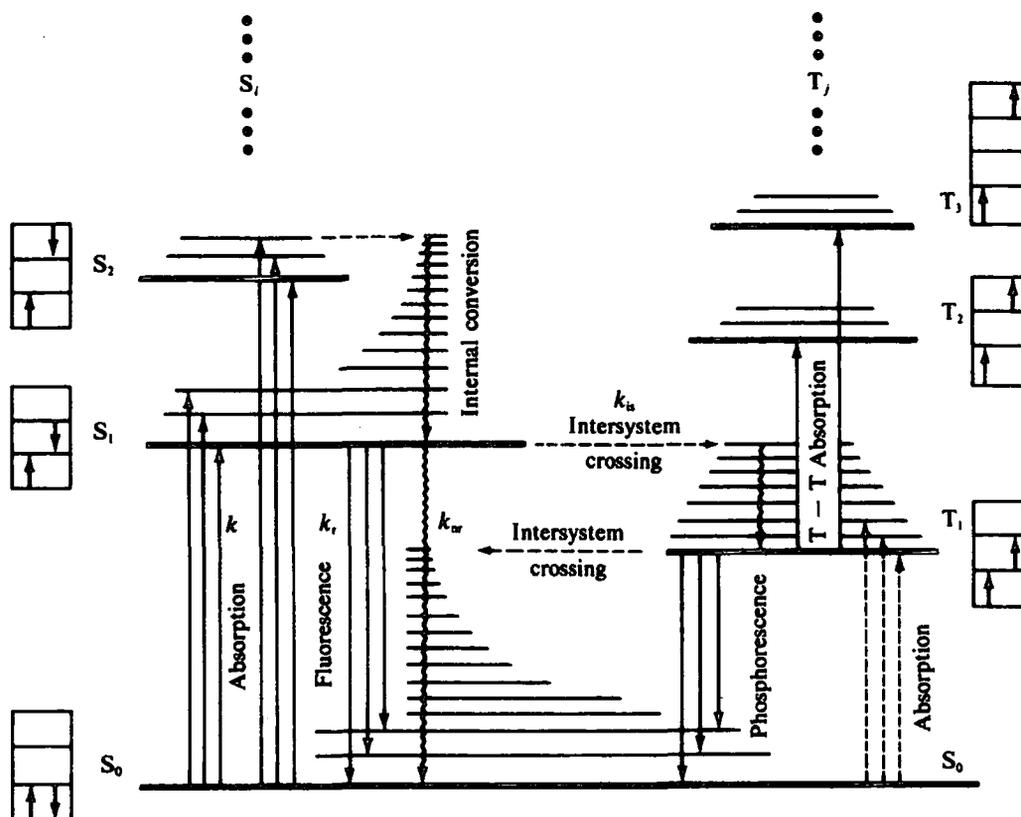
Figure 2.5 Jablonski diagram.

2.3.3. Photoexcitation of a conjugated polymer

This section will reconstruct the *photo-excitation* processes in a conjugated polymer and the following deactivation of excited states.

Electronic transitions are excited in the *chromophores* (electroactive parts) of a conjugated polymer when it is exposed to electromagnetic radiation of a suitable frequency. Then an electron of the chromophore (which might belong to the conjugated π- or to a non-bonding n-orbital) is transferred to the π^*-orbital. It leaves behind its corresponding hole but they are still correlated and form an exciton unless there is a further supply of excitation energy to dissociate it into two polarons (see chapter 2.2.2).

The energy levels of an exciton are illustrated in the *Jablonski diagram*, Figure 2.5[9]: For each main state there are a number of overtones, which represent the quantised sub-levels of vibrational energy that can be adopted by the molecule. Whereas the main exciton levels are separated by energy values in the UV or vis, the energy gap between the vibronics is usually found in the near infrared (IR). For example, it amounts to 180 meV for the C-C stretch mode of conjugated polymers containing benzene rings as chromophores[22].

In general, excitons exist in two multiplicities, *singlets* with a total spin of zero and *triplets*, where the total spin equals one. The energy level of a triplet T_1 lies approximately 1 eV below the S_1 state[23]. In most chemically stable compounds the ground state is a singlet. A nonzero multiplicity would cause the molecule to be highly reactive i.e. oxygen molecules exhibit a triplet ground state. In terms of the Jablonski diagram the ground state is represented by the symbol S_0^0 where S stands for singlet, S_0 for the lowest singlet exciton level of the molecule and S_0^0 for the lowest vibronic level of the lowest singlet state. In non-excited material at room temperature the majority of molecules are found in the ground state and do not possess excess energy. Hence all natural absorption processes (not induced absorption) start from a singlet state resulting in the creation of excitons which are again of singlet character since optical transitions that change the spin of a system are spin forbidden. The creation of excited triplet excitons via photon absorption only occurs very slowly with a probability of 10^{-5} (see chapter 2.3.2).
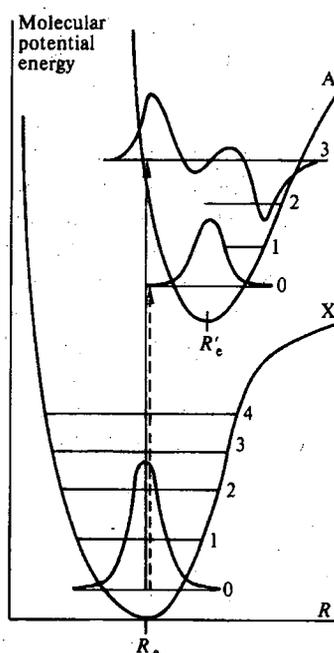
Figure 2.6 Illustration of the Franck-Condon-Principle for the absorption of a photon[20].

Photon absorption is so fast ($\tau \sim 10^{-15}$ s) that a vibrating molecule ($\tau \sim 10^{-13}$ s) can be considered rigid during the absorption process[20], which is a concept known as the *Franck-Condon-Principle*. Transitions take place between the states S_0^0 and S_n^k, where k is the vibrational level of S_n that has the highest spatial overlap with the S_0^0 electron density in the moment of absorption, see Figure 2.6. Here, the 0-0 transition route is much less probable than the 0-3 route. Thus, vibrational energy is taken up but it degrades into thermal motion when the 'hot' molecule relaxes back to the S_n^0 state within 10^{-12} s after the transition[24].

In Figure 2.6, R_e stands for the equilibrium distance of electron and hole in the exciton. Obviously, the excited state A is much more delocalised than the ground state X.

2.3.4. Deactivation processes

Excited states have finite lifetimes. Once in the S_n^0 state, the molecule tends to pass over to its stable ground state or, considering the Franck-Condon-principle, to a higher vibronic level of S_0. Theoretically, this could be accomplished with the emission of a photon:

Radiative transitions between states of equal multiplicity are called *fluorescence (F)*. The spin forbidden ones between states of unlike multiplicity are termed *phosphorescence (Ph)*.

However, these radiative transitions compete with *radiationless* deactivation processes: Radiationless transitions between states of equal multiplicity are termed *internal conversion (IC)*, whereas those between states of different multiplicity are known as *intersystem crossing (ISC)*.
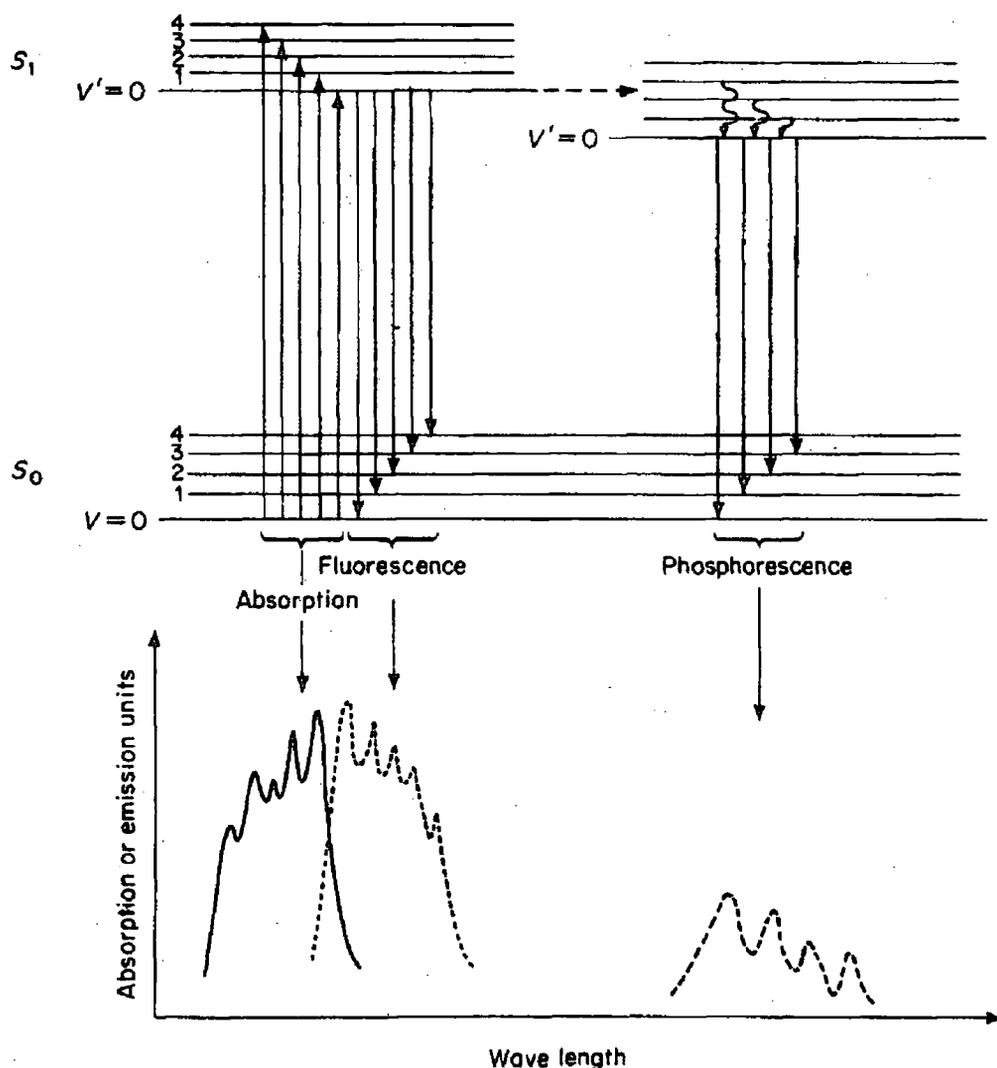
Figure 2.7 Vibrational modes in the luminescence spectra. Mirror symmetry of absorption and fluorescence spectrum[25].

The latter have in common that phonons are emitted instead of photons, which is the reason why they are favoured where only small energy gaps have to be bridged. This is given between adjacent singlet or triplet levels of high values of n. For this reason the deactivation $S_n \rightarrow S_1$ and $T_n \rightarrow T_1$ occurs almost exclusively via internal conversion within 10^{-13} s[25].

The remaining step is accomplished within less than a nanosecond[26] less dominated by IC and most of the singlets emit *fluorescence*, $S_1 \rightarrow S_0$. Since the Franck-Condon-Principle is also valid for fluorescence transitions these proceed from $S_1{}^0$ to one of the vibronics $S_0{}^n$. Consequently the typical fluorescence spectrum of a conjugated polymer i.e. polyfluorene (PFO)[27] or ladder type poly(para-phenylene) (PPP)[28] consists of several vibronical modes, whose distance corresponds to the energy gap between the vibronic levels. Usually, the highest of these modes originates from the transition to $S_0{}^0$.

Due to the energy which is lost by the vibrational relaxation of a molecule after absorption and emission, the emitted fluorescence is of lower energy than the initially absorbed photons. The energy difference between the first mode of the absorption and the emission spectra is called *Stokes shift*. Both spectra are arranged mirror symmetrically around the energy value of the $S_0{}^0$ level, see Figure 2.7[25].
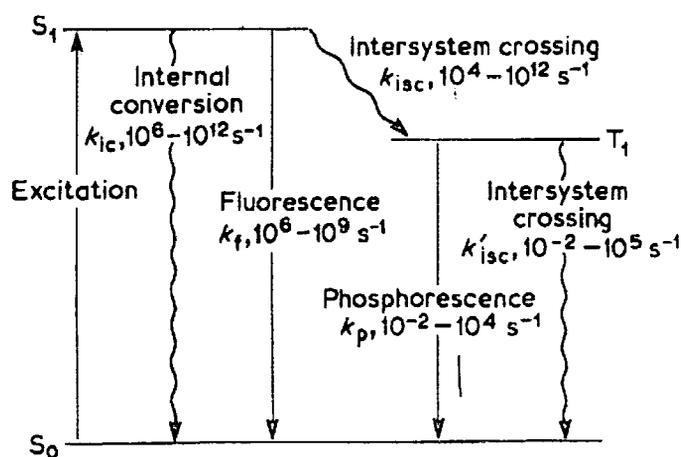
Figure 2.8 Compendium of the rates of radiative and radiationless deactivation processes[21].

Triplet excitons are not created via photon absorption. Consequently, the only possibility to populate the triplet manifold via photo-excitation is constituted by intersystem crossing from excited singlet levels. As this process requires a spin flip of the electron or hole of an exciton it runs slowly but accelerates in the presence of heavy atoms i.e. for conjugated polymers of the polythiophene family, which contain sulphur atoms. Here, the ISC quantum yield can reach more than 50 percent in solution[29], whereas in polyfluorenes it does not exceed 3 percent[29]. Most probably, ISC transitions occur from the $S_1{}^0$ state to $T_n{}^k$ as internal conversion rapidly reduces the number of higher excited singlets.

After vibrational relaxation the molecule reaches the lowest triplet state $T_1{}^0$. Now the spin of the exciton has to be changed to transfer it back to the ground state. Therefore, the few triplet excitons created via ISC are extremely *long-lived* (with a radiative lifetime of microseconds up

to seconds[6, 7]) compared to singlet excitons, whose radiative lifetime is measured in nano-or microseconds[21]. Nevertheless, if ISC occurs then phosphorescence from T_1^0 to S_0^k is not completely forbidden. If the process is not disturbed by triplet quenching it is observable and exhibits mono-exponential decay kinetics corresponding to the characteristic radiative triplet lifetime. Phosphorescence appears as a long-lived emission red-shifted to the fluorescence but exhibiting the same vibronic mode structure[6, 7].

The detection of phosphorescence can only be accomplished with very sensitive instrumentation since it is extremely weak and triplet creation via ISC is additionally slow. Non-radiative transitions from triplet to singlet (ISC) dominate it. Figure 2.8[21] gives an overview of typical transition rates of all radiative and radiationless deactivation channels described in this chapter.

2.3.5. Triplet-triplet-absorption

Although the formation of triplet excitons is restricted, their intrinsic radiative lifetime might suffice to establish concentrations of T_1 states, which are detectable if one uses a suitable method. Phosphorescence measurements are limited to the detection of the few emitting triplets and can only succeed when the emission is not disturbed by radiationless deactivation. This reduces the applicability of the method to low temperatures, where most of the phonon activity is 'frozen'.

It is more promising to measure the *photoinduced absorption* (*PIA*) signals due to spin allowed transitions from T_1 to higher triplet states, see Figure 2.5. This method can observe all triplets, either radiative or non-radiatively decaying, and does not fail at room temperature. The obtained absorption spectra can give information about the energy and symmetry of higher triplet states, which are involved into ISC. Moreover, the effective triplet lifetime and the decay kinetics are a key to estimating the importance of quenching mechanisms. Therefore, PIA of triplet excitons has been carried out in solution as well as on thin films of conjugated polymers.

An important component of triplet-triplet absorption measurements is the identification of the origin of the observed signals as triplet excitons. Other excited species, e.g. excimers, might give similar signals. If observable, the phosphorescence kinetics should coincide with those obtained from PIA. One might also introduce sensitiser molecules with a sufficient ISC rate and higher triplet energy than the investigated polymer to populate the triplet manifold. However, the safest way to check, is an EPR control measurement of the $\Delta m = 2$ transition resulting from the threefold multiplicity of the triplet.

2.3.6. Triplet formation via electroexcitation

Why should one be interested in the properties of triplet excitons when the main emission originates from singlets? It must be emphasised that section 2.3.4 dealt with the so-called *photoluminescence (PL)* – the fluorescence and phosphorescence emitted after *optical* excitation. There, the triplet manifold can only be populated via intersystem crossing.

In contrast to this, technical applications of the luminescence of conjugated polymers (as polymer light emitting diodes or *PLEDs*) involve the *electrical* excitation of the material. Charge carriers are injected at electrodes; they migrate into the polymer and when holes and electrons recombine at a polymer molecule they form excitons as an intermediate state. All of these undergo the radiative and non-radiative processes described above. However, the initial number of excited singlet and triplet excitons is determined by the recombination of charge carriers. According to very simple quantum statistics there are four equally probable possibilities of two spin-carrying particles to do this: The spin of the resulting exciton can be $\uparrow\downarrow$, $\uparrow\uparrow$, $\downarrow\downarrow$ or a mixed state $\uparrow\downarrow+\downarrow\uparrow$. Since the latter three are triplet states 75 percent of all created excitons will be triplets. The quantum yield of fluorescence can theoretically not exceed 25 percent and most of the electrical energy put into triplet excitons will be "lost" to non-radiative intersystem crossing from T_1 to S_0 since p_s for a radiative transition is still of the order of 10^{-5}. Consequently, *electroluminescence (EL)* is less efficient than photoluminescence – practically the electroluminescence quantum yield (ELQY) is diminished to around 10 percent due to non-radiative losses, which are aggravated by the presence of free charge carriers.

Even though latest quantum mechanical calculations have shown that up to 60 percent of all created excitons can be singlets when charge carrier recombination is not statistical but spin dependent[30] still the major loss of electrical energy is caused by the existence of triplet excitons. Hence their luminescence properties must be investigated.

2.4. Transport of energy in conjugated polymers

Chapter 2.3 illustrated the processes that contribute to the deactivation of an excited polymer molecule. It mentioned *intrinsic* radiative transitions (fluorescence, phosphorescence) and radiationless processes (internal conversion, intersystem crossing), for which it is not important whether they occur in isolated molecules or on polymer chains with close neighbours. However, one observes a different luminescence behaviour for polymer solutions and solid state polymer films. The luminescence output of a polymer sample can be strongly affected (quenched) in the presence of impurities or chain defects. Additionally, luminescence emission originating from such impurities i.e. metals can occur even when these are not directly excited.

To explain these effects, the present chapter describes a number of mechanisms which are responsible for the transport of energy along a polymer chain (intramolecular) and also between different molecules (intermolecular).

2.4.1. The reabsorption of luminescence

The first of these mechanisms is the reabsorption of radiation inside the polymer sample. An excited molecule, to be called the *donor D* (D* is the donor in its excited state), emits luminescence according to the processes described in chapter 2.3.3:

$$D^* \rightarrow D + h \cdot v_{lum}$$

The luminescence photon of the energy $h \cdot v_{lum}$ (where h is Planck's constant and v_{lum} the frequency of the photon) travels through the polymer solution or film but does not reach its surface as it is absorbed by an *acceptor* particle A that is excitable at the frequency v_{lum}:

$$A + h \cdot v_{lum} \rightarrow A^*$$
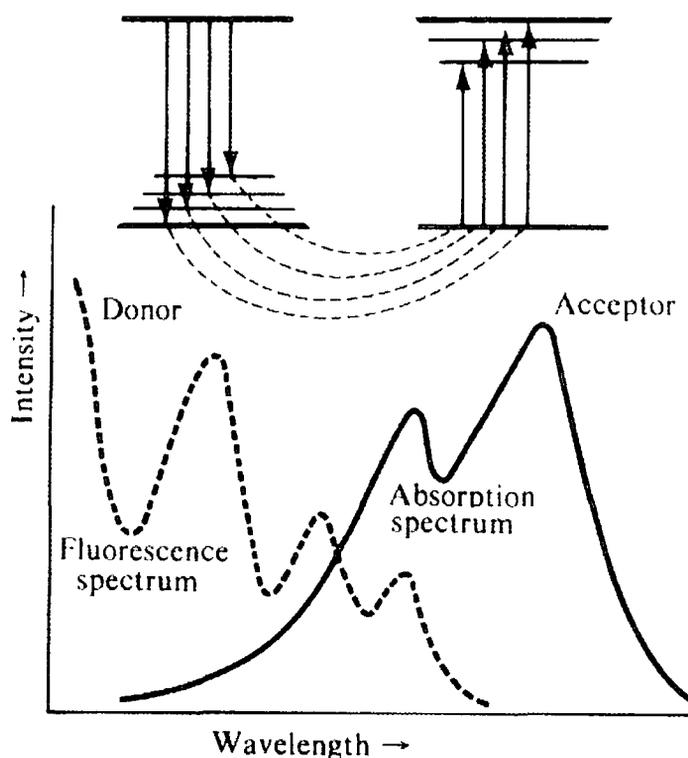
Figure 2.9 Overlap between donor emission (left) and acceptor absorption (right) must be given to enable Förster transfer (above)[9].

Now the acceptor itself can undergo internal conversion, intersystem crossing and luminescence processes. Of course, step two of the reabsorption is only possible when the emission spectrum of the donor and the absorption spectrum of the acceptor overlap sufficiently. As Figure 2.7 showed, this is usually the case when D and A, are polymer molecules of the same sort. Here, the strongest overlap is found between the absorption spectrum and the first fluorescence mode. As a consequence, the total emission of the polymer sample out of this vibronical mode is reduced[31].

Many reabsorption processes occur especially when the average path of light in a sample is long i.e. in polymer films with thicknesses of several hundred nanometers. Then the fluorescence spectrum will effectively consist of a low first vibronic and a relatively high second mode, in contrast to the fluorescence spectra of thin films which reflect the intrinsic emission patterns, which usually favour emission from the first mode.

2.4.2. Resonance and Förster energy transfer

Similar to the reabsorption, *Förster* or *resonant energy transfer* involves an energy donor D and an acceptor A. Again, the emission spectrum of the former has to overlap with the absorption spectrum of the latter to enable transfer. However, this process does not require the intermediate step of photon emission as two transitions take place simultaneously: the deactivation of the donor and the excitation of the acceptor:

$$D* + A \rightarrow D + A*$$
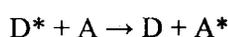
The term *resonant* transfer originates from the physical principle behind it: The dipole moments of donor and acceptor orbitals interact. Especially the vibronics of the acceptor state couple to the excited donor state, which entails that the coupling is not coherent: When the energy of the donor coincides with a transition energy of the acceptor both are in resonance and energy can be transferred. Afterwards the excited acceptor quickly relaxes back to the zero vibronic level, which makes the transfer an *irreversible* process.

In 1959 it was Förster[32] who found a mathematical description of the corresponding rate constant. Equation 2.5 gives the *very weak coupling limit*, which is of relevance for conjugated polymers:

Equation 2.4

$$K_{D \to A} = \frac{1}{\tau_D} \frac{1}{R^6 n_0^4} \left(\frac{3}{4\pi} \int \frac{c^4}{\omega^4} F_D(\omega) \delta_A(\omega) d\omega \right)$$

τ_D represents the donor lifetime in absence of the acceptor and R is the distance between donor and acceptor. The integral calculates the overlap between the normalised emission spectrum of D and the absorption spectrum of A. This *overlap integral* must be nonzero to enable Förster transfer, which is illustrated by Figure 2.9.

Resonant energy transfer does not make use of photons as mobile energy carriers like reabsorption. Instead, a minimum distance must be kept between donor and acceptor. The *Förster radius R_F* is defined as the distance where the transfer rate equilibrates the total decay rate of the donor:

Equation 2.5

$$K_{D \to A} = \frac{1}{\tau_D} \frac{R_F^6}{R^6}$$

$$\Rightarrow \quad R_F^6 = \frac{3}{4\pi n_0^4} \int \frac{c^4}{\omega^4} F_D(\omega) F_A(\omega) d\omega$$

In conjugated polymers, R_F can amount up to 50 Å[33], which suffices to allow intermolecular transfer. Unlike reabsorption, Förster transfer does not affect the shape of the emission spectrum of the donor because intermediate emission does not happen. Rather, the intensity of all modes is equally affected.

2.4.3. Exciton migration via Förster transfer

An important application of Förster transfer is the case where both D and A are molecules or chain segments of the same sort of polymer. Then the exciton state in D is deactivated while another exciton in A becomes excited. No triplets can be created via Förster transfer because a spin forbidden resonance transition is improbable during the short interaction time between the orbitals of D and A. One possible transfer route is *singlet-singlet transfer (SST)*:

$$D^* (S_n^0, \text{probably } S_1^0) + A (S_0^0) \quad \to \quad D (S_0^0) + A^* (S_m^k)$$
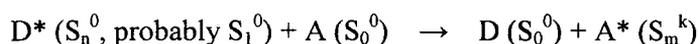
The SST rate is high enough to make sure that during their lifetime of $\sim 10^{-9}$ s singlets undergo many of these transfers. The excited state is now regarded as a particle that moves spatially:

singlet *migration* takes place. The process is also termed *hopping* since it consists of separate transfer steps. The hopping rates between two neighbour sites D and A can be described as[34]:

Equation 2.6

$$v_{DA} = A(r_{DA}) \exp\left(-\frac{e_A - e_D}{k_B T} \right) \quad , \quad e_A \geq e_D$$

$$v_{DA} = A(r_{DA}) \quad\quad\quad\quad , \quad e_A \leq e_D$$
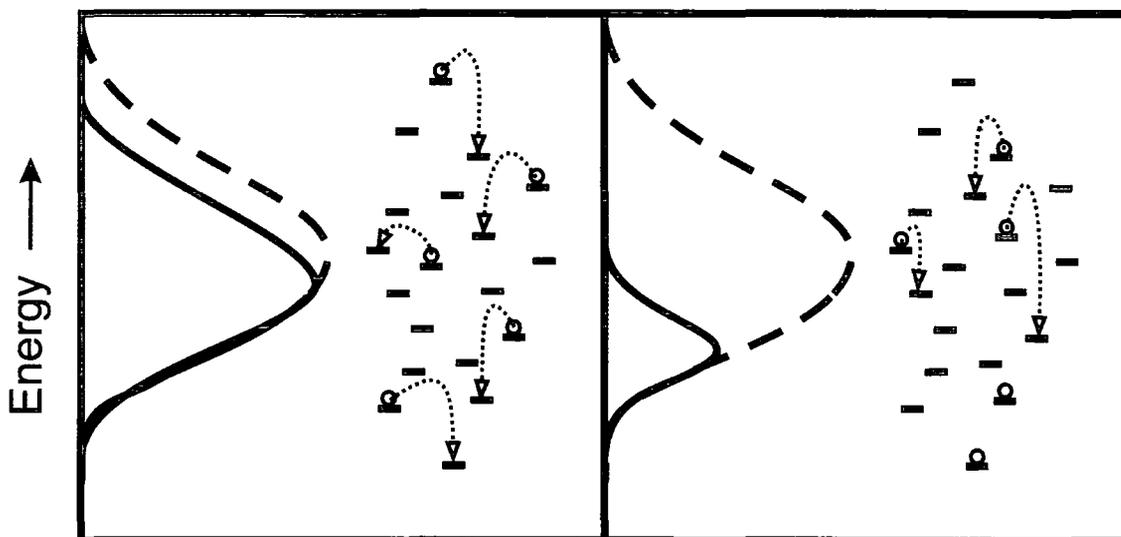
Figure 2.10 *Down-hill migration*: dashed line – initial distribution of exciton site energies; left picture – the random energy distribution shortly after excitation; right picture – after long-time migration only the sites of lowest energy are occupied, most excitons have decayed[17].

The terms e_D and e_A stand for the energy of donor and acceptor site, which are not necessarily equal. Rather, the energy of exciton sites is subject to a broad distribution represented by $A(r_{DA})$, which is caused by local deviations in the effective conjugation length l_{eff}. The longer it is, the lower is the energy[10]. Via dipole-dipole interaction every exciton senses this distribution among the sites within its Förster radius. As the jump rates above favour transfer to the least energy, the migration of singlet excitons is halted when it reaches a local minimum of site energy. At long times after photo-excitation this results in a red-shift of the initial exciton distribution[26], illustrated by Figure 2.10. l_{eff} also varies between different polymers due to their chemical bonding structure which can inhibit or prefer a twisted chain geometry. Upon mixing two polymers, singlet excitons will migrate to the molecular species which is less twisted, better aligned and therefore more conjugated[35].

Additionally, chemical or morphological chain defects can be responsible for the occurrence of local minima in site energy, whose energy difference to the surroundings is much larger than the width of the distribution described above. Only rarely, excitons migrating to such sites can

overcome the potential barrier for further migration, which means that they are *trapped*. The presence of many traps reduces the average mobility of excitons and thus the probability of annihilation processes, see section 2.5. Luminescence emitted from traps is not necessarily isoenergetic to the 'normal' luminescence but can be red-shifted due to the low site energy or exhibit a completely different spectrum if the emission originates from chemical defects i.e. keto groups.Defects exist in every polymer sample as well as impurities, which can be metal ions that remain inside the material after synthesis but also oxygen that diffuses into the surface of thin polymer films when these are not sealed against air contact. These can also act as traps – as a consequence, there are always unwanted Förster or Dexter interactions (see section 2.4.5) between excitons and impurities, which draw energy off the polymer and quench its luminescence. Triplets are affected as well as singlets, whereas the latter are efficiently quenched by oxygen via fast Förster transfer –oxygen atoms are paramagnetic, which breaks the spin forbiddeness of the transfer reaction.

The presence of oxygen can additionally lead to chemical reactions i.e. the formation of keto defects by oxidation of polyfluorene (PFO) repeat units[36]. In turn these defects attract excitons in their surroundings and eventually use the transferred energy to emit keto fluorescence. As keto emission is found in the green, red-shifted to the bright blue PFO fluorescence the chemical degradation of the polymer is followed by colour instability[36, 37].

2.4.4. Doping in conjugated polymers

A useful application of the quenching effect is the *doping* of polymer LEDs. The investigation of devices made of the presently available materials has shown that in most cases various improvements are needed for their final technical application: First, their emission quantum yield must be increased and second, the emission spectra are broadened by vibronics and inhomogeneous broadening that always occurs during optical transitions. Pure, saturated colours, which can be integrated into the RGB system, are a precondition for the application of LEDs in a commercial display. Moreover, the device lifetime and emission stability is a major problem[36] but this will not be addressed here.

To overcome these problems, some research groups investigated the introduction of *dopant* compounds into polymer devices. Their aim is to transfer excitation energy from the host polymer to the guest. To enable a fast Förster transfer, a suitable dopant must exhibit an absorption spectrum well overlapping with the host emission. Transfer must effectively compete with the deactivation channels of the polymer, including fluorescence. In this sense, energy is harvested for the dopant, which now emits instead of the host fluorescence.

Only a sufficient dopant concentration must be provided to guarantee an average host-guest distance smaller than the Förster radius. To improve the PLED, dopant emission must show a high quantum yield. Moreover, the emission spectrum should yield an attractive emission colour suitable for technical application. Unfortunately, there is always a red-shift from host to guest fluorescence as the emission spectrum of the former overlaps with the absorption spectrum of the latter to enable Förster transfer. Blue-emitting LEDs are not likely to be created via doping[38, 39].

Triplet excitons are the major limiting factor for the efficiency of polymer electroluminescence devices. Research groups have tried to find appropriate dopants to harvest their excitation energy as it would otherwise be lost to the thermal motion of molecules. However, the problem one has to overcome here is the spin forbiddeness of such Förster transfer. Both possibilities to break it have their disadvantages: Dopants exhibiting a triplet ground state would be too reactive and limit the device lifetime. On the other hand, raising the ISC rate also quenches the polymer fluorescence[38].

Summarising, one can say that the method of doping faces difficulties but might improve polymer LEDs. Apart from that, it is very useful to investigate the function of Förster transfer.

2.4.5. Dexter electron exchange transfer

The Förster mechanism does not allow *triplet-triplet transfer*:

$$D^* (T_n^0) + A (S_0^0) \rightarrow D (S_0^0) + A^* (T_m^k)$$
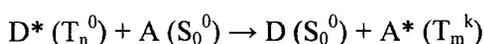
It is spin-forbidden and forbidden by the dipole-dipole interaction, as the triplet absorption only contributes values of 10^{-5} to the overlap integral of Equation 2.5. Still, triplet excitons are not immobile. There is another if slower transfer mechanism termed *Dexter transfer* or *electron exchange*, which occurs when a donor D and an acceptor site A are very close. Then their orbitals overlap and there is a probability for an electron from one site to appear on the other. In this context, a theory for triplet-triplet transfer was developed by Dexter[40], who calculated the rate for this process as:

Equation 2.7
$$k_{D \rightarrow A} = \frac{2\pi}{\hbar} |\beta_{D \rightarrow A}|^2 \int F_D(E) F_A(E) dE$$

$\beta_{D \rightarrow A}$ represents the exchange energy term between donor and acceptor. The overlap integral does not contain the fluorescence but the normalised phosphorescence spectrum of the donor

$F_D(E)$ and the normalised absorption spectrum of the acceptor $F_A(E)$. Since the total spin of the system is conserved, the electron exchange transfer is spin-allowed. Although $k_{D \rightarrow A}$ appears to be rather low, the rate of triplet decay is even slower so that transfer sequences are possible, which might enable a migration of triplets similar to the hopping migration of singlets. Still triplet-triplet transfer is lacking experimental evidence in conjugated polymers due to the weak phosphorescence signals – so far this has only been obtained for organic crystals[34, 41].

Singlet migration as described for Förster transfer is possible via electron exchange as well. However, the Förster radius for such a transition is much larger than the D-A separation required for Dexter transfer (10 to 15 Å); hence the latter process is less probable for singlets.

2.5. Bimolecular processes of excitons

2.5.1. Triplet-triplet annihilation

Triplet migration becomes important when triplet concentrations are very high. This is found especially in electroluminescence devices, where charge carrier recombination favours triplet formation (see chapter 2.3.6). However, the fact that all transitions, radiationless and radiative, of a triplet to the ground state are spin forbidden can cause relatively high triplet concentrations in photoexcited polymer samples as well.

Under such conditions, collisions between the independently migrating triplet excitons become probable and *triplet-triplet annihilation (TTA)* occurs[42]. Since Dexter transfer requires the proximity of two excitons of at least 15 Å, collisions of triplets located on different polymer chains are rather improbable. Instead, electron exchange takes place between neighbouring triplets on the same polymer chain:

$$T_1 + T_1 \rightarrow \begin{cases} \dfrac{8}{9}(S_0 + T_n) \\ \dfrac{1}{9}(S_0 + S_n) \end{cases}$$
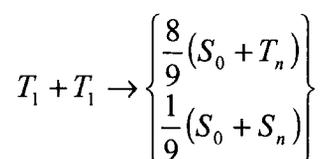
The energy of one T_1 is transferred to the other forming one ground state exciton and one highly excited exciton. For eight in nine cases this is a triplet – the upper equation gives a summary of the transfer reaction and does not denote all the occurring intermediate quadruple states but only the final state.

TTA is an important triplet quenching mechanism in polymer solutions[43] but has also been identified as the second source of solid-state delayed fluorescence (DF)[7] in conjugated polymers

beside geminate pair recombination (GPR): Considering the one case where a highly excited singlet is formed, S_n undergoes all the deactivation steps of a freshly excited exciton including the emission of fluorescence from S_1^0 to S_0^k. This increases the fluorescence lifetime up to the microsecond range. The mechanism has also been confirmed by work in the organic crystal field[42].

One can distinguish between TTA and GPR by the excitation dose dependency of DF and Ph: The former always requires the annihilation of two triplets to create one singlet. Thus the excitation dose dependency of the DF should be the square of the corresponding curve of the triplet signal (e.g. the phosphorescence). For DF originating from geminate pairs the relation between both is linear.

2.5.2. Singlet-triplet annihilation

As mentioned above, one encounters triplet concentrations in electroluminescence devices so high that triplets annihilate each other. Still, triplets outlive the singlet excitons by orders of magnitude, so that they can quench the singlet state via *singlet-triplet annihilation (STA)*[44].
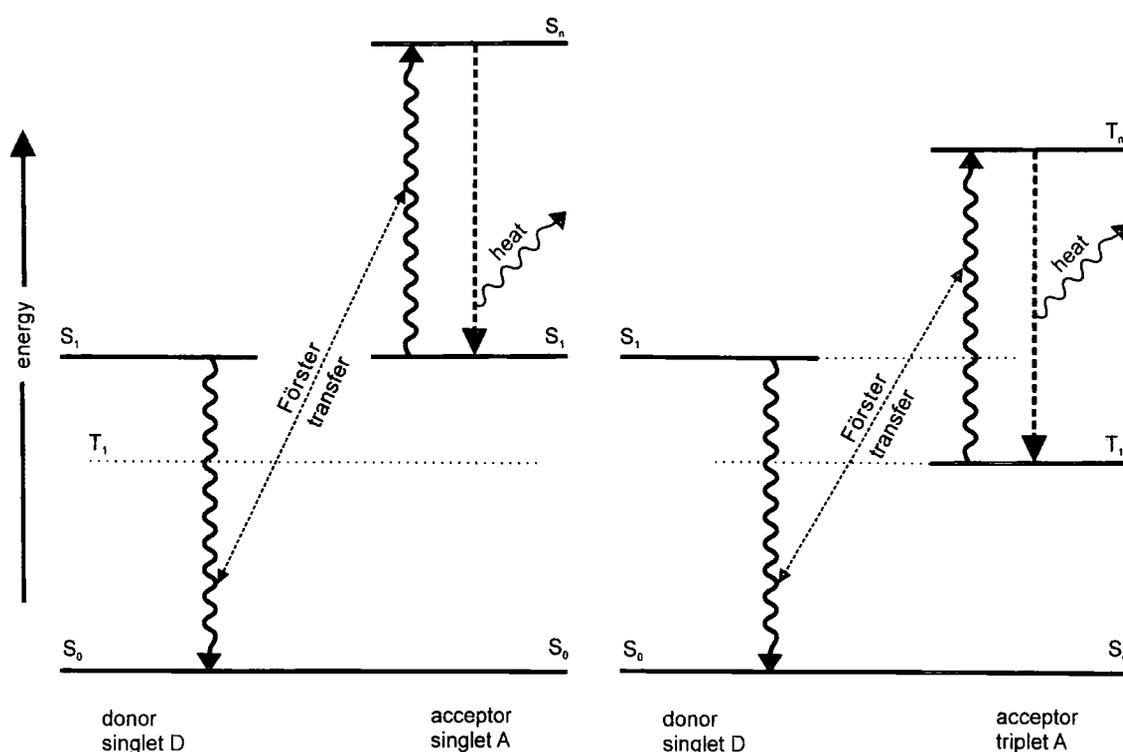
Figure 2.11 Illustration of the SSA (left) and STA (right) mechanisms, adapted from ref.[17].

Figure 2.11 illustrates the singlet-triplet annihilation process. Since the faster moving of the two exciton species are singlets, STA is controlled by Förster transfer. For that purpose, an overlap between singlet fluorescence and triplet-triplet absorption is required.

When an excited singlet S_1 and a triplet come closer than their Förster radius, a spin-allowed transfer reaction occurs, during which the singlet passes its energy to the triplet, raising it from T_1 to an upper triplet state:

$$S_1 + T_1 \rightarrow S_0 + T_n \quad , \qquad T_n \rightarrow T_1 + heat$$

As a reverse transfer, triplet energy might also be given to the singlet state but this includes a transition from T_1 to S_0 and is spin forbidden.

2.5.3. Singlet-singlet annihilation

Another *homomolecular* annihilation process like TTA is *singlet-singlet annihilation (SSA)*. The process is controlled by Förster transfer and occurs when the singlet concentration is very high.

When two singlet excitons collide in the sense of approaching each other closer than their Förster radius, one of them can transfer its energy to the other. In analogy to TTA, the reaction can be summarised as:

$$S_1 + S_1 \rightarrow S_0 + S_n \quad , \qquad S_n \rightarrow S_1 + heat$$
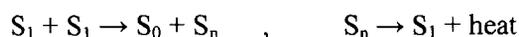
If SSA occurs, which is the case at very high excitation doses, the excitation dose dependency of the fluorescence is non-linear and the singlet lifetime is reduced. The scheme of Figure 2.11 illustrates the annihilation process.

2.6. Morphological effects

2.6.1. Aggregation, dimer and excimer

The emission of aggregated species can give a major contribution to the total emission of a polymer sample, especially in solid-state thin films. It appears when conjugated segments of

different polymer chains (or of one coiled chain) get close enough to interact physically and sometimes chemically forming a weak bond. Attracted by their mutual Coulomb potentials electron density partly drawn off the backbones constituting a break of conjugation.
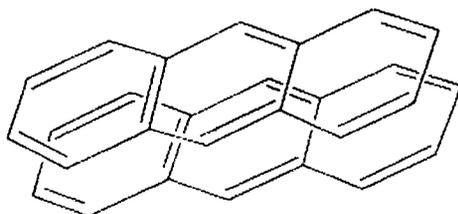
Figure 2.12 The sandwich geometry of an anthracene dimer[9].

One refers to a *dimer* when two identical molecules aggregate in their *ground state*; a possible geometry is illustrated by Figure 2.12 showing the 'sandwich' of two dimerised anthracene molecules. Dimers possess an absorption spectrum because the ground state wave functions of the contributing molecules interact. It resembles the monomer absorption spectrum although it is subject to significant broadening, which also applies for the emission spectrum. In addition, the latter are red-shifted with respect to the monomer emission as the major contribution arises from the $v = 1$ vibronic instead of $v = 0$.

An *excimer* can be formed by the interaction of a ground state molecule with one in an *excited* state. Its ground state is repulsive. Depending on the chemical ability of a polymer to form excimers, an exciton migrating along a polymer chain might find a ground state partner to interact with. Consequently, no absorption spectrum can be attributed to the excimer. Excimer emission involves a transition to the repulsive ground state; hence it is red shifted and appears featureless without vibrational modes[11]. An excimer formed between chemically molecules or repeat units is called *exciplex*.
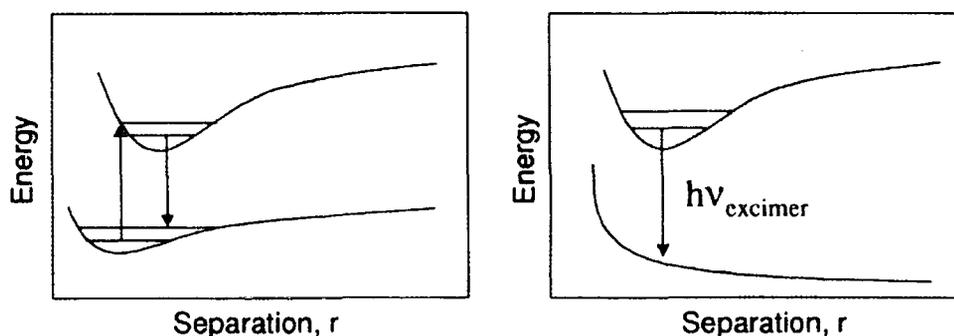
Figure 2.13 An excimer exhibits a dissociate ground state; hence its luminescence emission does not show vibrational modes[45].

On account of the thermal energy required to overcome the potential barrier during excimer association, an increasing quantum yield is observed with rising temperature. Excimers act as structural traps; they emit on cost of the polymer fluorescence. Considering the resulting broad and red-shifted spectra polymer without the tendency to form excimers are preferred for PLED application.

2.6.2.   Morphology of thin films and solution

A polymer solution consists of polymer chains imbedded in solvent molecules. Depending on their molecular weight, the chains are able to diffuse. Chain contacts and with it inter-chain energy migration as well as a range of bimolecular processes are linked to the concentration of polymer molecules. In dilute solution, every molecule takes its independent equilibrium formation, mostly they tend to coil. Aggregation effects might occur here but are much more probable in poor solution, where the solute is not sufficiently shielded by solvent molecules[46].

The morphology and hence the luminescence of a thin polymer film is influenced by the quality of the solution it is made of[47], by the film fabrication as well as further treatment it has undergone[48]. No solvent is present in the sample so that the chains are densely packed, which stimulates aggregation when the molecules try to find their equilibrium position.

In general, aggregation plays a much larger role in solid state compared to solution. It can be inhibited when molecular contacts are avoided by imbedding the polymer chains into matrix molecules which separate them.

Chain diffusion is not possible in solid state but also not necessary to establish energy transport as frequent molecular contacts guarantee the efficiency of energy transport via resonant transfer and electron exchange. Therefore, excitons show a high inter-chain mobility in solid-state conjugated polymers. This is supported by the orientation of chains parallel to the sample surface, which is observed especially for spin coated films[49]. Additionally, there are methods to align the chains, e.g. to fabricate lasering films of polyfluorene.

3. EXPERIMENT

3.1. Polymers

3.1.1. Polyfluorene

The conjugated polymer mainly investigated in this study is polyfluorene. Electrically excited or hit by UV radiation this material exhibits a bright, saturated blue fluorescence emission (see [37] and section 5.3) with relatively high quantum yields and a low intersystem crossing rate (up to 3 percent[29]). Its synthesis is described in the literature[50]. Commonly two octyl side chains are substituted to the repeat unit (PFO) but also other versions exist e.g. the ethylhexyl substituted poly[9,9-di(ethylhexyl)fluorene] (PF2/6). Several batches of the latter have been kindly provided by R. Guentner from the research group of Prof. U. Scherf at the University of
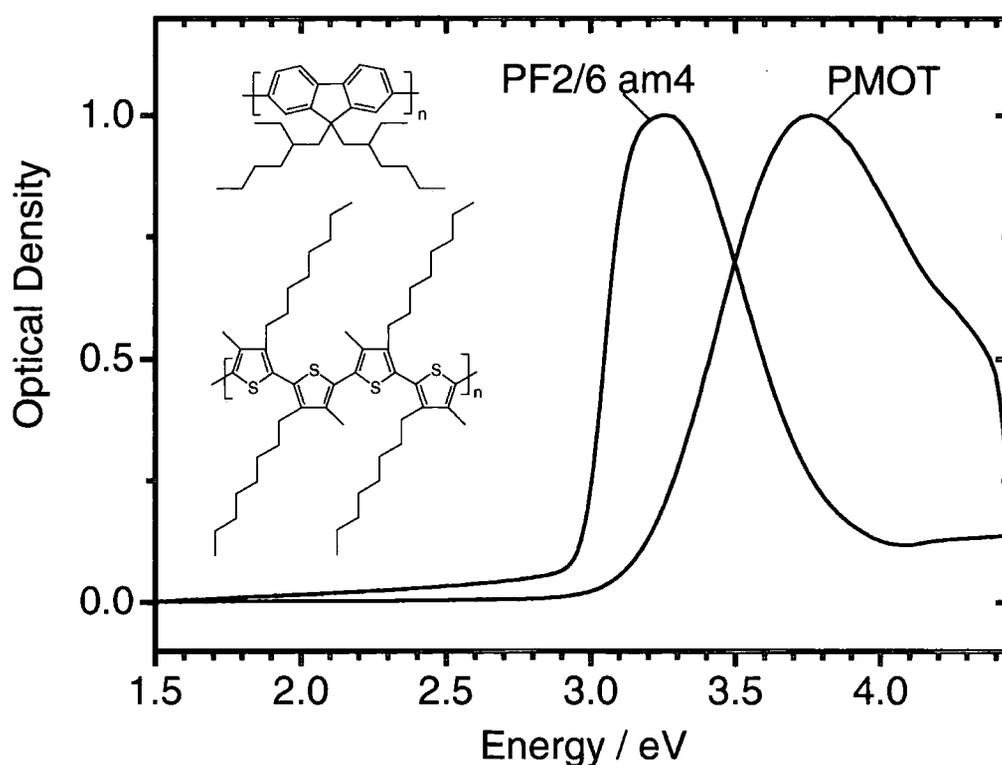
Figure 3.1 Absorption spectra of thin films of PF2/6am4 and PMOT. *Inset:* The chemical structure of PF2/6 (above) and PMOT (below).

Potsdam/Germany. The chemical structure of PF2/6 is shown in Figure 3.1. Since colour and intensity of the blue luminescence of polyfluorene are strongly susceptible to the influence of impurities, in particular keto chain defects[36], there have been attempts to modify the synthesis of PF2/6 in order to reduce these effects[51, 52]. The amine endcapped PF2/6 provided by R. Guentner exhibits a higher colour stability than plain PF2/6 and has been used for some of the presented polyfluorene measurements (with kind permission of C. Rothe, who carried out these experiments).

For the study of the role of keto defects in polyfluorene a series of fluorene/fluorenone co-polymers (PFO/PFl) was used, keto fractions ranging from 0.1 to 25 percent fluorenone in polyfluorene. These co-polymers as well as the polyfluorene (PFO) and polyfluorenone (PFl) homopolymers were thankfully received from P. de S. Freitas of the group of Prof. U. Scherf. The results obtained with them are shown in section 5. The chemical structure of the 9,9-bis(3,7,11-trimethyldodecyl)fluorene and 9-fluorenone repeat units they consist of can be found in Figure 5.1, section 5. Here is an overview of the polymers and co-polymers provided by P. de S. Freitas, who determined their molecular weights:

Table 1 Compendium of the series names, fluorenone input levels and molecular weights of all PFO/PFl co-polymers used in this study. Please note that the molecular weight of PFl, pure polyfluorenone could not be determined due to its

Name	Fluorenone Level / percent	Molecular Weight / 10^4*g*mol^{-1}
PFO (1)	0	9.3
PFO/PFl 2	0.1	1.8
PFO/PFl 3	0.2	1.2
PFO/PFl 4	0.5	1.7
PFO/PFl 5	1	2.0
PFO/PFl 6	2	5.6
PFO/PFl 7	5	1.2
PFO/PFl 8	10	1.7
PFO/PFl 9	25	2.5
PFl (10)	100	?

3.1.2. PMOT

The polymer family of polythiophenes offers the possibility to investigate the dependence of polymer luminescence on the structural properties of the emitter. This can be achieved by chemically modifying the structure of the polythiophene via application of different side chains

or via polymerisation of head-to-head instead of head-to-tail coupled repeat units. The blue emitting poly(3-methyl-4-octyl-thiophene) (PMOT) exhibits large torsion angles between the single repeat units. It has been investigated via time-resolved photoluminescence spectroscopy and photo-induced absorption measurements. The chemical structure of PMOT with two side chains attached to the backbone (C_8H_{17} and CH_3) is shown in Figure 3.1 in the head-to-head coupled variant. Its synthesis route is described in the literature[53]. The PMOT results are presented in section 4.

3.2. Sample fabrication

3.2.1. Solutions

All of the presented measurements were carried out either on solutions of conjugated polymers or on thin films. The first step was always the preparation of a solution, which happened under cleanroom conditions. Toluene was used as a solvent for polyfluorene type materials, chlorobenzene for PMOT. For solution measurements the concentration was usually adjusted to achieve a maximum optical density of ~1. In all other cases, i.e. for concentration dependent measurements, the explicit values will be given in the text. As the concentrations for film samples have an effect on the thickness of the film they were held constant at: 15 milligrams of PF2/6 per milliliter toluene, 20 milligrams of the PFO/PFl co-polymers per milliliter toluene and 45 milligrams of PMOT per milliliter chlorobenzene.

3.2.2. Spin coating and sample storage

Film samples were fabricated using a spin coating apparatus: Spectrosil discs of 12 mm diameter were covered with film solution and spun very fast (at 2500 rpm) for 60 seconds leaving a thin layer of solvent-free polymer on the disc.

Polymer films, especially polyfluorene type, are most subject to degradation. As spin coating takes place in an air atmosphere, an oxide layer forms immediately at the surface. Additionally, oxygen is present in the bulk of the film because the precursor solution is prepared in air and contains oxygen. The photooxidation of the film then takes place quickly in the presence of UV light, which is the reason why – for the most recent measurements, presented in section 4 – films were fabricated in "yellow" light, kept in dark and measured immediately.

3.3. Sample characterisation

3.3.1. Film thickness

Sample thicknesses were measured using a TENCOR Alpha Step Stylus. The values obtained could be found in the range of 40 to 100 nanometers, depending on the concentration of the precursor solution and the polymer. The accuracy of the alpha-step measurements was low: Film-to-film variations within the same sample batch could amount up to ±10 nm. However, even single films could not be fabricated smoother than ±5 nm. The necessity of cutting the film by hand (using razor blades) prior to the determination of the thickness worsened the accuracy of the measurement additionally. Absorption spectroscopy of the films produced a much more reliable and reproducible characterisation.

3.3.2. Absorption spectra

Absorption spectroscopy of films and solutions was carried out using a LAMBDA 19 (PERKIN ELMER) double beam spectrometer. Normalised spectra of a PF2/6 and a PMOT film are shown in Figure 3.1. Depending on the sample the maximum optical density was located between 0.2 and 0.7 (for films) with a value of 0.1 to 0.4 at 355 nm, which was used as the excitation wavelength.

For the temperature dependent PMOT absorption spectra recorded by C. Rothe (section 5) the spectrometer was fitted with a liquid nitrogen cryostat.

3.4. Steady-state photoluminescence measurements with the FLUOROMAX

3.4.1. The setup

Steady state photoluminescence measurements were carried out using a spectrometer (Fluoromax 3, JOBIN YVON), which could be fitted with a displex closed cycle helium cryostat (the same as for photoinduced absorption measurements). The setup of the instrument included a continuous excitation source (a Xenon lamp). The excitation slit could be adjusted to

achieve intensities in the low milli- to the microwatt range. The luminescence of the excited sample was then collected perpendicular to the excitation beam and, after monochromation, detected using a photomultiplier tube. Measured spectra were intensity corrected with the characteristic spectral response curve of the photomultiplier tube (for emission scans) or the emission profile of the Xenon lamp (for excitation scans).

3.4.2. Measurements

The Fluoromax offered the possibility to quickly record steady state emission (scan over emission wavelengths) and excitation spectra (scan over excitation wavelengths) of solution and film samples. For these purposes, fluorescence cells (all four windows made of quartz, content 3 ml) were used to contain the solutions. Thin films could additionally be examined at low temperature down to 10 K by fitting them into the helium cryostat.

The problem encountered in particular for film measurements was the high intensity of scattered excitation light, which distorted the spectra. Therefore the amount of scatter had to be minimised prior to scanning. As the maximum of excitation light is collected when the film faces both excitation source and detection optics at an angle of 45 °, a reduction could be achieved by slightly turning the film sample out of this position or by collecting emission through the back of the quartz disc carrying the film sample. However, the problem could never be solved completely and scatter was always observed as soon as a spectrum scanned across the excitation wavelength.

3.5. Time-resolved photoluminescence spectroscopy

3.5.1. The setup

The extremely sensitive apparatus used for time-resolved luminescence spectroscopy (TRS) was set up by C. Rothe.

The excitation of the (solution and film) samples was provided by the third harmonic of a pulsed Nd:YAG laser (SL312, EKSPLA) with a pulse width of 150 ps and an output frequency tuneable between 1 and 10 Hz. At the laser wavelength of 355 nm (3.5 eV) the output energy per pulse could amount up to several millijoules. In order to avoid undue sample degradation, this had to be reduced by beam splitters, neutral density filters and a polarisation filter. Finally,

the sample was excited by 2 mJ down to a few μJ per pulse (measured using a pulse power meter Nova, OPHIR OPTRONICS), the cross section of the laser beam being about the size of the area of a film sample.

The cryostat utilised for film measurements was a displex closed cycle helium apparatus with a lowest temperature of ~ 15 K. The usual combination of rotary and turbo pump created the necessary dynamic vacuum (10^{-3} Torr at room temperature to 10^{-5} at low temperature) inside the sample chamber.

Two mirrors focused the luminescence emitted by the excited polymer sample onto the entrance slit of a monochromator (Triax 180, JOBIN YVON SPEX). A 380 nm cut-off filter provided the necessary protection of the detection optics against scattered laser light. To record even weakest phosphorescence spectra a gated red-enhanced CCD camera (4 Picos, Stanford Computer Optics) was employed for detection. The sensitive time gate (defined by delay time and exposure) was controlled via computer. Whereas for the measurements presented in section 5 and 6 an electrical trigger was provided by the laser, for section 4 an electro-optical trigger (via photodiode) was applied, which reduced the signal jitter from 300 ps to the diode response time. The camera itself exhibited a response time of 4 ps.
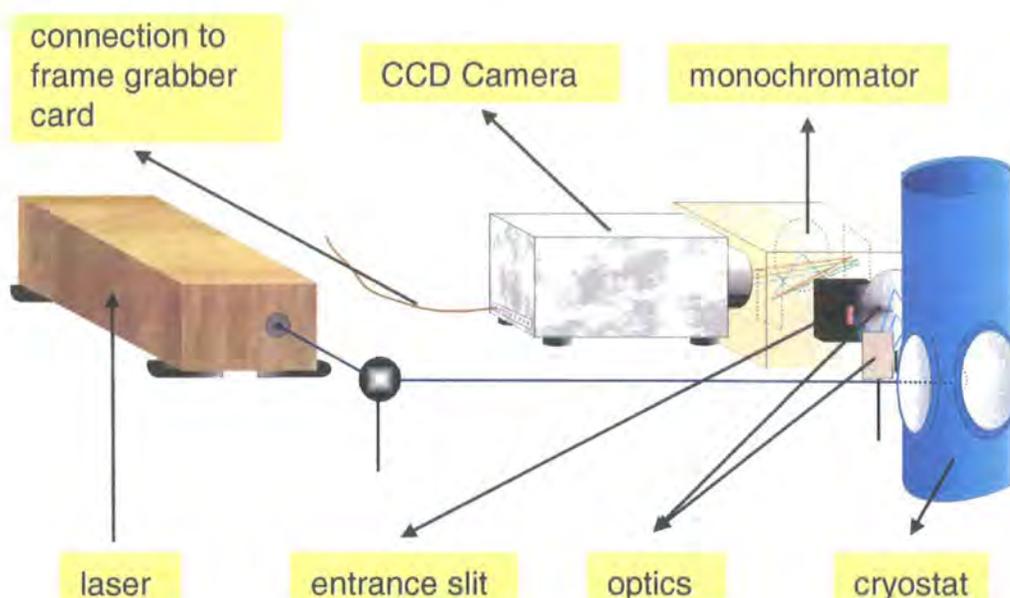
Figure 3.2 Setup of the TRS experiment, presented with the permission of C. Rothe[17].

3.5.2. *Measurements*

The setup described above provided the possibility of a thorough examination of the emission of polymer samples, which involved polymer solutions as well as thin films. Whereas the former

were degassed prior to measurement and then studied at room temperature in a quartz degassing cell, the latter were fitted into the cryostat and studied under dynamic high vacuum.

First of all, photoluminescence spectra were recorded. Here, the temporal resolution allowed for the distinction between prompt fluorescence (PF) and delayed fluorescence (DF) (or phosphorescence (Ph)) spectra. The former were usually recorded in the first microsecond or (with the electro-optical trigger applied) within the first 25 nanoseconds – for each spectrum an average over 20 laser shots was taken. DF and Ph detection took place after this time window with varying delay and gate times (up to 90 ms after excitation); for each spectrum 100 pulses were averaged. A spectral resolution of one nanometer could be achieved. The background spectrum, which was always taken before the start of a measurement, was automatically subtracted from the measured spectrum.

Decay curves of all three investigated kinds of luminescence were measured by varying the delay and gate time of the camera. Here, one has to distinguish between integrated measurements (mostly used for PF), where the gate time is much longer than the luminescence lifetime, and differential measurements, where the lifetime exceeds the gate time, which then has to be adjusted for each data point in order to prevent the luminescence signal from vanishing at longer delay times (used for DF and Ph).

Furthermore, the excitation dose dependency of PF, DF and Ph signal was determined within the energy range of the laser (from a few to 2000 µJ). This required the use of different neutral density filters and subsequent measurements of the pulse energy.

Of course, all of the above experiments could be carried out for both films and solutions. Additionally, films were studied at temperatures from 300 K down to 15 K using the helium cryostat.

3.6. Time-resolved photo-induced absorption spectroscopy

3.6.1. The setup

As explained in the theory section, the excitation of a conjugated polymer leads to the formation of excitons S_n, which quickly relax back to S_1 or T_1 states. Then a metastable phase sets in until the excitons are decayed to the ground state S_0. During this period, the absorption of a photon can transfer the exciton back to a higher excited state. The absorption signal is then proportional to the total population of the investigated type of exciton regardless of whether they emit or

decay non-radiatively. Hence, a photo-induced absorption (PIA) experiment was set up to monitor the decay of non-emitting excited states i.e. triplet excitons in the visible spectrum.

Similar to the TRS measurements, the types of examined samples included degassed solutions and thin films. Again, solutions were studied in a quartz degassing cell at room temperature and films (under dynamic vacuum) in a closed cycle helium cryostat (LEYBOLD) with quartz windows and a minimum temperature of 10 K. The excitation of the samples was provided by exactly the same laser like for the TRS using the same range of pulse repetition rates (depending on the lifetime of the excited state) and output energy (measured by a pulse power meter Nova, OPHIR OPTRONICS). Again, the excitation area matched approximately the area of a film sample.

At an angle of ~ 20 ° to the laser beam, the output of a 200 W tungsten lamp served as the absorption probe beam. Since optimised results are obtained when the excited sample area matches the probed area, the broad, continuous beam had to be focused by a lens. A 435 nm cut-off filter and a water filter protected the sample from undue degradation. Having passed the sample the white beam was collected by a further lens and mirror onto the entrance slit of a monochromator (BENTHAM, TM 300). The monochromated light was detected by a fast silicon PIN diode (S5052, HAMAMATSU) combined with a homebuilt transimpedance amplifier. The response of the system was restricted to the visible spectrum, as can be seen in Figure 3.3.

Although the fall time of the diode amounted to only a few nanoseconds, the temporal resolution of the set up was limited to the order of 10 µs by the amplifier. Using scattered excitation light of the known pulse width the instrument response function was measured at 20 µs (not shown here). Finally, the voltage signals were monitored by means of a digital oscilloscope (TDS 350, TEKTRONIX), which was triggered electrically by the laser. After averaging the decay curves on the oscilloscope (256 pulses for each measurement) they could be transferred to computer using a LABVIEW program, which was modified for this purpose.

3.6.2. Measurements

The setup described above was mainly used to investigate triplet and excimer states in solutions and films of PF2/6 am4 and PMOT down to temperatures of 10 K (for films). Due to several technical problems only a few of the measurements have gone to publication, most were of test character. This section is to point out what has been measured at all, even if it is not presented in this thesis, and which problems have been encountered.
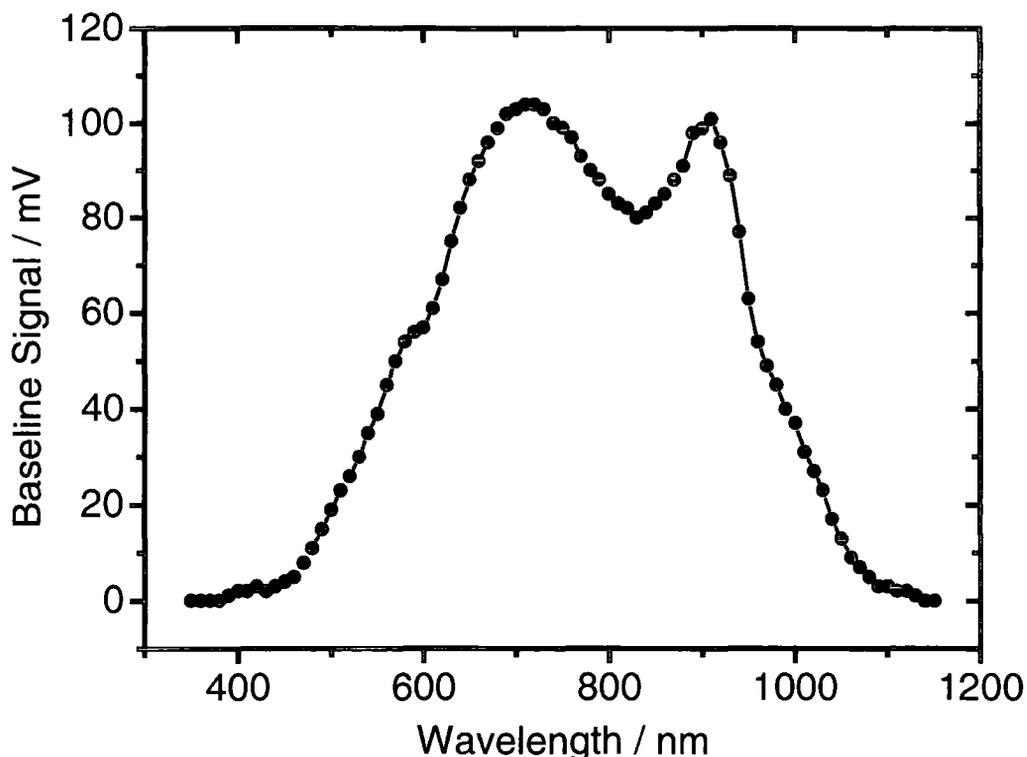
Figure 3.3 Spectral response of the PIA system: The wavelength dependent output of the Si
PIN diode irradiated by the tungsten lamp, measured on the TDS 350 oscilloscope; the
white light was monochromated using the TM 300 monochromator.

Mostly, decay curves of rarely or non-emitting excited states have been recorded. Prior to such a
measurement, the wavelength of maximum absorption of the examined excited state was
determined and compared to the literature. This maximum is located around 800 nm for the
PF2/6 triplet-triplet absorption (varying between film and solution) and around 670 nm for the
PMOT signal. The nature of the latter has been analysed in section 4.

Depending on the optical density of the polymer sample, absorption signals of up to 1 % (at t=0
after excitation) could be observed. Thin films usually exhibited a weaker absorption than
solutions. PF2/6 absorbed slightly stronger than PMOT. Noise levels for decay curves amounted
to approximately 5 % of the initial absorption (after averaging, which took about half a minute
at a repetition rate of 10 Hz). Although this corresponds to only about 0.05 % of the baseline
signal without absorption, the noise level created resolution problems relatively independent of
the sample temperature, especially for the determination of lifetimes of long-lived exited states.
Despite the attempt to replace the diode detector with a coolable photomultiplier tube, no
significant improvement of the background noise could be achieved.

The confirmation if the observed signal originated from triplet excitons or from another excited
state was accomplished by a comparison to the literature (PIA maximum wavelength and

spectra) and to signals obtained from TRS e.g. the decay kinetics of phosphorescence had to coincide with the decay kinetics of PIA in the case of an observation of triplet excitons.

Scanning the monochromator across various wavelengths, photo-induced absorption spectra could be measured. The signals obtained were corrected according to the spectral response of the system shown in Figure 3.3. However, the duration of exposure of polymer samples to radiation plays a crucial role for their degradation, in particular for thin films. Since the process of recording a single decay curve took comparatively long (30 s) and during this time samples were illuminated by a combination of UV laser pulses and an intense continuous beam of white light, sample degradation only allowed for the recording of very coarse spectra of not more than 10 to 20 nm steps. The high intensity of the white light was necessary to maintain reasonable signal-to-noise levels especially in spectral regions with a low detector response. On the other hand, it caused a heating of the samples, which was noticeable at low temperatures – a low temperature of 10 K was usually raised to 14 K by radiation.

The effect of sample degradation or alteration by interchain processes during recording process could be noticed when a decay curve at one wavelength was repeated and decay kinetics found to be changed to a degree depending on the polymer investigated. Since these processes are fastest right at the beginning of the measurement – they happen even during the recording of the first decay curve – the obtained spectra and decay curves can hardly be recognised as accurately reflecting the properties of the investigated polymer. An example series of decay curves, one recorded shortly after the other, is presented in Figure 3.4. The polymer under investigation is the polythiophene MS-Y. The whole measurement required only 7 minutes, while the decay signal was monitored at different oscilloscope time scales in order to capture long and short time decay. However, a general trend regarding the decay kinetics can be observed with time, which I attribute to the degradation of the polymer film caused by laser light and the white probe beam despite the use of several UV and IR filters. The observed *irreversible* decay changes proceeded slower but were still present when low laser intensity was used. It cannot be excluded that they are accompanied by spectral shifts as well but the detection of such changes lies beyond the capabilities of the experiment as spectra are not recorded instantly but require the recording of several decay curves. This is a serious disadvantage of PIA measurements of thin polymer films and was always observed, to a degree dependent on the polymer studied. Commonly, polymer solutions were much less subject to degradation or morphological alteration e.g. as the reservoir of excitable molecules is constantly renewed due to convection and diffusion in the solution container. Nevertheless, the objects of investigation in the context of this thesis were actually thin films, as these are understood to be the precursors of PLEDs. One way to overcome or at least alleviate the observed effects might be by using a pulsed probe beam to prevent the polymer molecules from continuous irradiation.
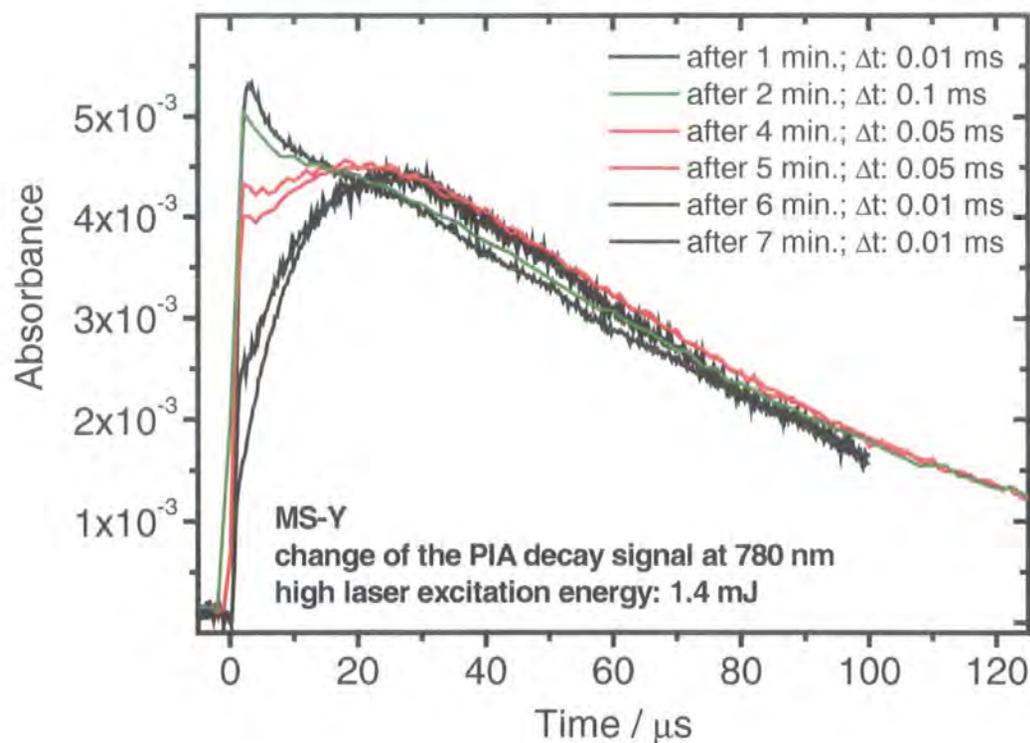
Figure 3.4 PIA decay curves of a thin film of the polythiophene MS-Y, monitored at 780 nm. The time at which the signal was recorded is stated in the figure legend in minutes after the first irradiation of the film sample. The legend also shows a measure for the time resolution of the oscilloscope. The fast part of the decay can be observed shrinking until it has disappeared after about 7 minutes. The inset depicts the chemical structure of MS-Y.

The second problem, posed by time resolution, was tried to solve as PMOT signal lifetimes were found to be of the order of 50 µs and less. However, all attempts to improve the situation, e.g. the use of a faster amplifier or the use of photomultiplier tubes instead of the diode, failed for various reasons – the fast amplifier created a noise level far too high for measurement purposes and for the photomultiplier tube variant the weak link was the connection to the oscilloscope. Hence several features of the examined decay kinetics were beyond resolution, which is the reason why the PIA setup will have to be arranged in a completely new way.

4. Long-lived photo excitations in PMOT

4.1. Introduction

When studying the photophysical properties of conjugated polymers one comes across significant variations of essential characteristics such as the energy[54], mobility and lifetime of excitons, energy and quantum yield[55] of the fluorescence, ISC rate[29] or the mechanisms responsible for delayed fluorescence[19, 56]. As these properties depend on a wide range of structural parameters of the investigated polymer the influence of a single parameter is rather difficult to identify. The polymer family of polythiophenes offers the possibility for a systematic study[29, 55, 57]. While the structure of their backbones is always a polythiophene, different side chains can be attached to the repeat units thereby tuning the torsion of the polymer chain and modifying interchain interactions. Moreover, head-to-head coupled repeat units can force a twist of the chain out of planarity – eventually, this leads to a tuning of the polymer luminescence via altering the effective conjugation length. High torsion angles cause the spectrum to blue-shift and the luminescence quantum yield to drop[55]. In fact, the concept of effective conjugation length has been fully developed during studies of polythiophenes.

The low PLQY of the blue-emitting polythiophenes impedes efficient device applications since most of the input energy is lost to non-radiative decay channels competing efficiently with radiative decay. These include singlet separation to free charges or geminate pairs, the formation of interchain aggregates[58] and excimers[59], internal conversion at impurities or chain distortion sites and, of great importance in polythiophenes, high ISC rates[60] to the triplet manifold due to the presence of the sulphur atom in every repeat unit. The nature of these processes is reflected in the nature and kinetics of long-lived excited states – this section is based on a study of long-lived photoexcitations in the blue emitting poly(3-methyl-4-octyl-thiophene) (PMOT), which has been published jointly by C. Rothe, A.P. Monkman and myself in two separate papers[4, 61].

4.2. Abstract

Using time-resolved photo induced absorption and gated emission spectroscopy, *long-lived photo-excitations* of the solid-state conjugated polymer poly(3-methyl-4-octyl-thiophene) (PMOT) have been detected and analysed at *different temperatures*. Whereas at 15 K

phosphorescence and delayed fluorescence are observed, at ambient temperatures the delayed emission, redshifted with respect to the prompt fluorescence, is assigned to excimer fluorescence. Via photo-induced absorption, we observe triplet-triplet absorption at 15 K and, at room temperature, excitations with extremely long lifetimes of 300 ms at 289 K are detected. These are allocated to triplet excimer formation.

4.3. Experiments

Thin films of PMOT were studied by time-resolved photoluminescence spectroscopy (carried out by C. Rothe, see section 3.5) and photo-induced absorption (see section 3.6). The inset of Figure 3.1 shows the chemical structure of head-to-head coupled PMOT. For further information about the polymer please see section 3.1.2. The process of fabrication of the thin polymer films studied is described in section 3.2.2 and sample thickness as well as a PMOT absorption spectrum can be found in section 3.3.

4.4. Low temperature observations and discussion

Depending on the sample temperature different types of delayed luminescence can be observed in solid-state films of PMOT. The lower part of Figure 4.1 presents the *prompt fluorescence* (PF) and delayed luminescence (CCD delay of 3 µs) recorded at 15 K. Clearly, the latter spectrum consists of a high- and a low-energy portion. The former of these is located around 2.66 eV isoenergetic to the low temperature PF spectrum. Therefore it is attributed to delayed emission from the $S_1^0 \rightarrow S_0^n$ transition (*delayed fluorescence*, DF) of PMOT. The low-energy part exhibits a shape similar to PF and DF but is red-shifted to these emissions by about 0.7 eV. As the peak energy (at 1.95 eV) agrees with the energy of the triplet exciton as observed by Monkman et al.[62] for solutions of PMOT in benzene (2.2 eV), this emission is attributed to the spin forbidden $T_1 \rightarrow S_0$ transition and termed *phosphorescence* (Ph). Note that a perfect agreement between both energy values cannot be expected because of the red-shift, which is usually encountered when comparing solid state Ph to solution, e.g. for MeLPPP[6, 62] and PF2/6[62, 63]. The offset between PF and Ph of 0.7 eV is characteristic for conjugated polymers exhibiting phosphorescence.
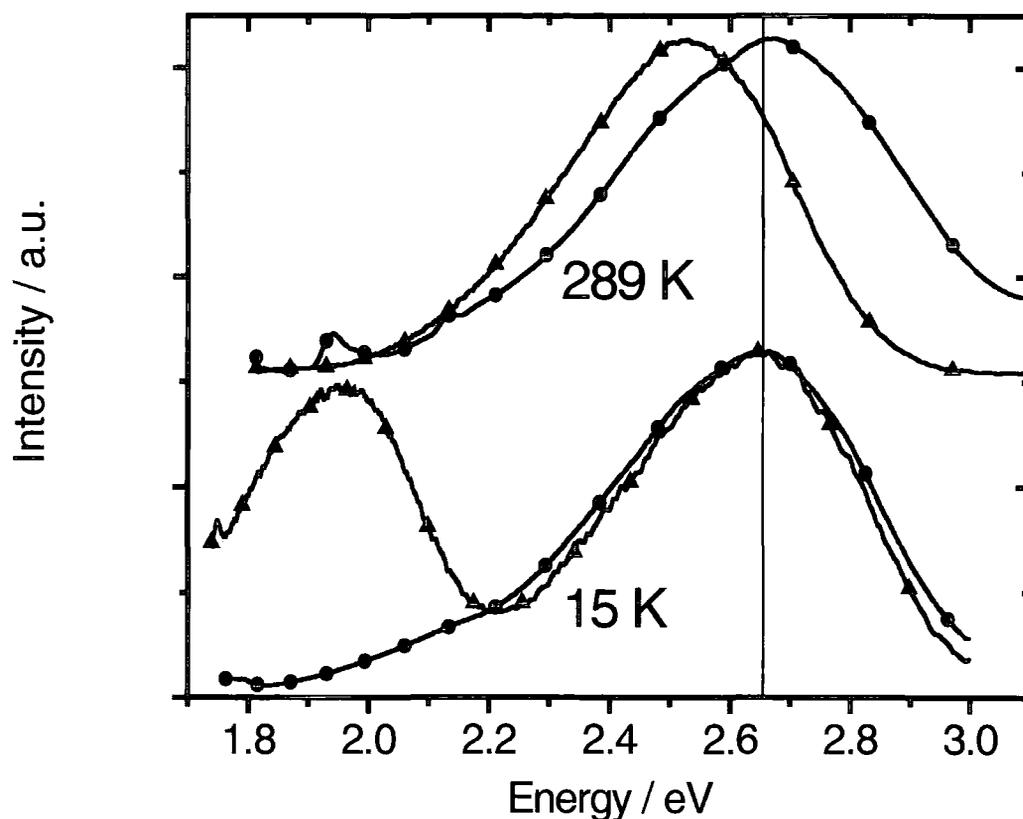
Figure 4.1 Comparison of normalised prompt (●) and delayed (▲) luminescence spectra at 289 K (3-100 μs) and 15 K (3-1000 μs).

Figure 4.2 b) shows the *integral decay kinetics* of DF and Ph at 18 K – it presents an integrated measurement as the data points have been obtained by C. Rothe from spectra taken at various delay times but all with the long gate time of 5 ms. As long as the DF shown in Figure 4.2 is still measurable the Ph signal decays slowly. However, the double logarithmic scale is used to show that the *long time* Ph decay obeys a power law with a slope of -1. This corresponds to a slope of –2 for the differential Ph decay.

Using the same type of PMOT samples (thin films as described in section 3.2) as in the TRS experiment, PIA measurements were carried out under similar experimental conditions (dynamical high vacuum, 15 K). The energy of the $T_n \leftarrow T_1$ transition of PMOT was taken from Burrows *et al.* 1.85 eV[60] (determined for a solution of PMOT in chlorobenzene; the value corresponds to a wavelength of 670nm) and found to match approximately the $T_n \leftarrow T_1$ energy of the investigated films. Figure 4.2 a) presents the decay kinetics of the PIA signal – the experiment has been carried out with virtually no gate time and is therefore a representative of differential measurements. If PIA really monitors the decay of the triplet manifold the decay curve should be proportional to the first derivative of the Ph kinetics obtained from TRS, which is apparently the case, see Figure 4.2 a). Observing emitting triplet excitons (Ph) and triplet-

triplet absorption at the same time is a valuable means to prove the validity of both measurements and the reliability of the obtained decay kinetics.
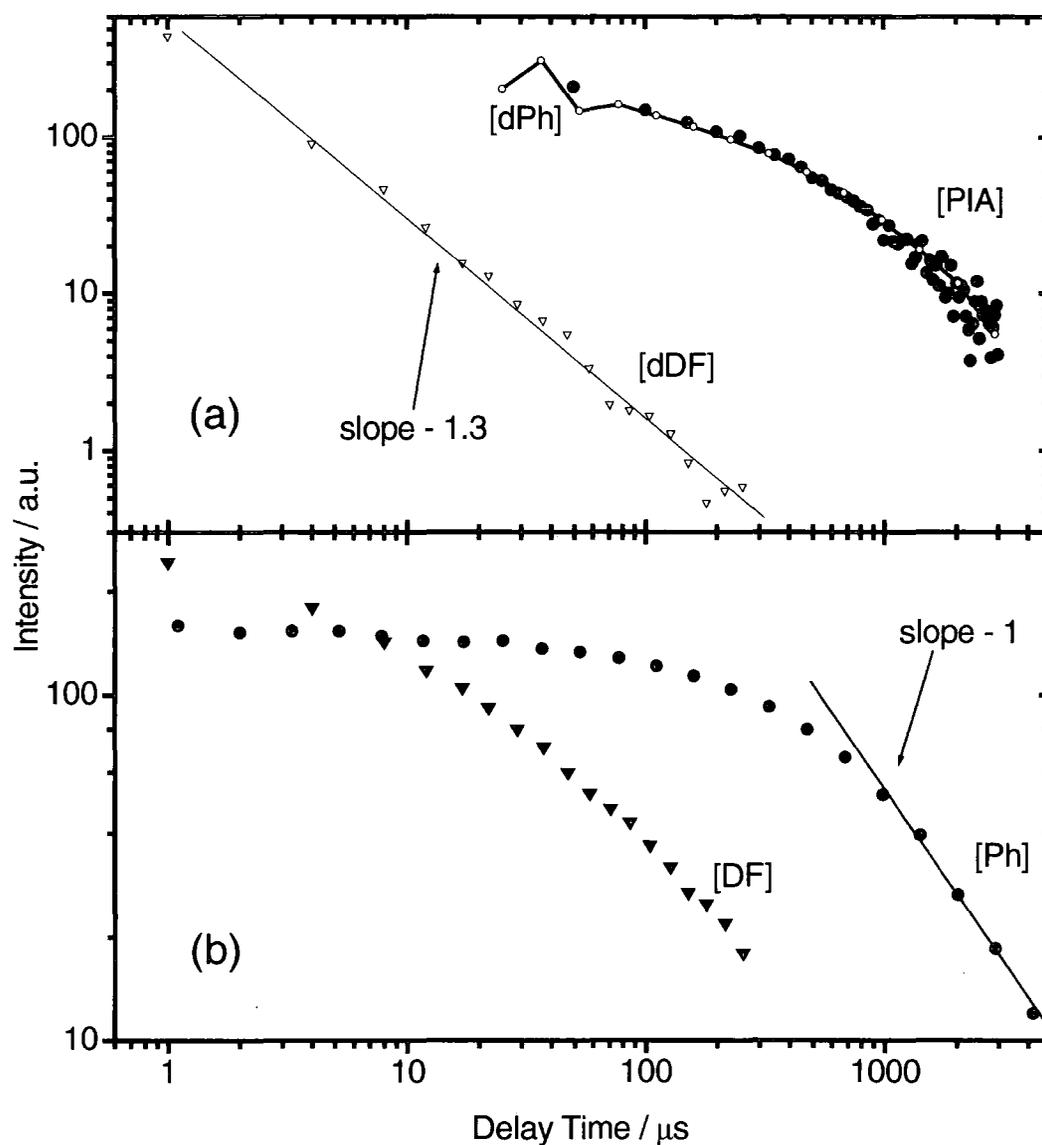
Figure 4.2 (a) Double logarithmic presentation of the kinetics of the photo-induced transient absorption signal recorded at 670 nm at 15 K (♦); the first derivative of the Ph decay curve (-∘-) is proportional to the PIA signal; the first derivative of the DF (∇) signal can be fitted to a power law with a slope of -1.3. (b) The integral kinetics of the DF (▼) and Ph (●) emissions of PMOT at 18 K; the long time Ph obeys a power law with a slope of -1.

Which photophysical mechanism is responsible for the observed delayed fluorescence? The DF kinetics derived from the measurement shown in Figure 4.2 cover only two orders of magnitude in time. C. Rothe recently improved the experiment to cover eight orders of magnitude in time, which proved to reveal much more information about the physical processes involved in the delayed fluorescence of PF2/6 (not published). Still, the first derivative of the DF integral

kinetics obeys a power law with a slope of -1.3. Such power law kinetics are characteristic for delayed fluorescence arising from the thermally activated recombination of *precursor* species.

Two types of these species have been identified to cause DF in other conjugated polymers such as thin films of MeLPPP[19] or in PF2/6 films, where a slope of -1.4 was observed at 20 K[7]. DF in the former polymer has been attributed to the delayed recombination of *geminate pairs* (GP)[19, 64]. Another possibility for DF emission encountered in polyfluorene is the *annihilation of triplet excitons* (TTA)[56]. One can distinguish between GP and TTA by comparing the excitation dose dependency of DF to those of triplet signals such as the Ph. In the case of TTA the excitation dose dependency of the DF is expected to be the square of the Ph dependence whereas for GP recombination both Ph and DF intensity should depend linearly on the excitation dose.
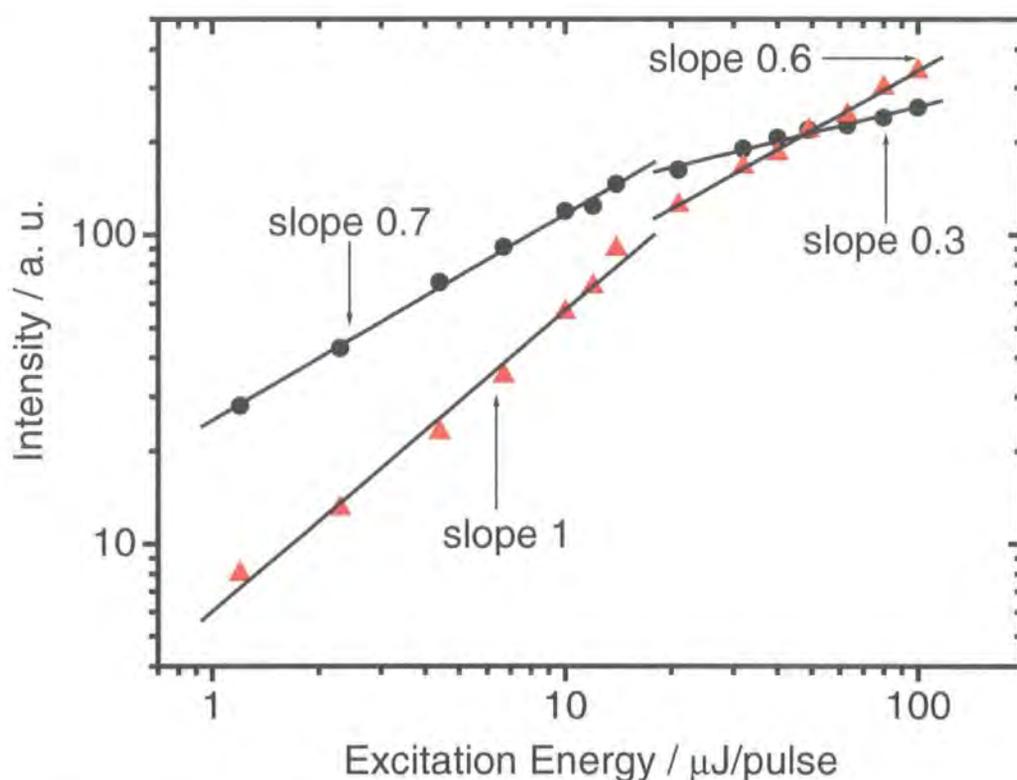
Figure 4.3 Dependencies of delayed luminescence (Ph ●, DF ▲) intensity on the laser pulse power at 20 K on a double logarithmic scale.

As can be seen in Figure 4.3 the slope of the Ph in a double-logarithmic plot was measured to be 0.7. This sublinearity might be seen as an evidence for the occurrence of a nonlinear quenching process for triplet excitons – such as singlet-triplet annihilation (STA) or TTA. Now a DF slope of 1 would favour geminate pair recombination while 1.4 would stand for triplet-triplet annihilation as the origin of DF. Apparently, the signal is linear for low excitation doses (Figure 4.3). These observations are somewhat contradictory as the DF seems to arise from geminate pair recombination but simultaneously the Ph signal is subject to nonlinear quenching, which suggests the existence of a quenching mechanism only for triplets – such as TTA. Perhaps this

contradiction can be explained by DF arising partly from GP and partly from TTA with an increasing influence of TTA as the excitation dose rises. Indeed, this assumption is supported by the fact that the slope of the DF signal of 1 does not properly fit the experimental data. Instead, it increases with rising excitation dose. Above ~ 7 µJ/pulse, the behaviour of the DF curve might be approximated by the square of the Ph data, especially as their *turning points* between high and low excitation dose coincide at 20 µJ/pulse.

Such *turning points* have also been observed in PF2/6[7] and are attributed to a non-linear absorption phenomenon (bleaching) at very high laser intensity. Consequently, the polymer sample is saturated with excited triplet states and the dependency of DF and Ph signals after the turning point supports the assumption of the previous paragraph: Both signals show sublinearity with a DF slope of 0.6, which is double the Ph slope of 0.3 – TTA seems to be the DF mechanism at high excitation doses.

Summarising the above, it is difficult to identify one source of DF from the available data. At low excitation dose the linearity of the DF signal indicates GP recombination although in this case the Ph signal should be linear as well. At excitation doses above 20 µJ/pulse all available data suggest TTA. Unfortunately, no decay kinetics have been measured in this excitation regime to provide further evidence of a connection between singlet and triplet exciton signals. Additionally, the PIA experiment is not able to distinguish between TTA and GP: On the one hand geminate pairs cannot be detected with the system used because they absorb in the infrared outside the detection range and on the other hand triplet excitons and their corresponding PIA signals exist no matter if they are mobile (and cause TTA) or immobile and the DF is caused by GP recombination.

4.5. Room temperature observations and discussion

Now attention shall be turned to the long-lived photoexcitations encountered at *room temperature*. Figure 4.4 illustrates the temperature dependence of the delayed photoluminescence of PMOT. The black data points have been obtained by integrating the delayed spectrum (1-100 µs) over the spectral range from 1.65 to 2.15 eV (compare to Figure 4.1) – they represent the thermal behaviour of the phosphorescence signal. Obviously, *no phosphorescence* is observed at temperatures above 180 K, which can be interpreted as a direct result of intensive triplet quenching due to the increasing phonon activity at higher temperature. This is reflected in the room temperature spectrum of the delayed emission, shown in the upper part of Figure 4.1.

Observing the DF signal across the same temperature range should result in a similar graph. The corresponding data set has been obtained from delayed spectra (1-100 µs) integrating from 2.2 to 3.0 eV. At first, the signal seems to be decreasing slightly with rising temperature but, unlike the Ph curve, it remains almost constant between 70 and 160 K followed by a *steep rise* starting at 220 K. No matter if TTA or GP is the source of delayed fluorescence in PMOT – this is a completely untypical thermal behaviour for DF as singlet excitons should be quenched by internal conversion similar to triplets. A consideration of spectra and decay kinetics can help to resolve this contradiction:

First of all, the emission *spectra* will be analysed. Note that the red measurement points shown in Figure 4.4 were obtained by integration over the spectral range from 2.2 to 3.0 eV and thus the resolution of temperature dependent spectral changes is minimal. Comparing the room temperature delayed spectrum (peak at 2.5 eV) to the DF spectrum at 15 K (peak at 2.7 eV) the former is *red-shifted* by about 0.2 eV. This shift occurs between 100 and 200 K unnoticed by the integral measurement of Figure 4.4, which therefore shows the *sum* of the DF and the shifted luminescence signal in the red data points.
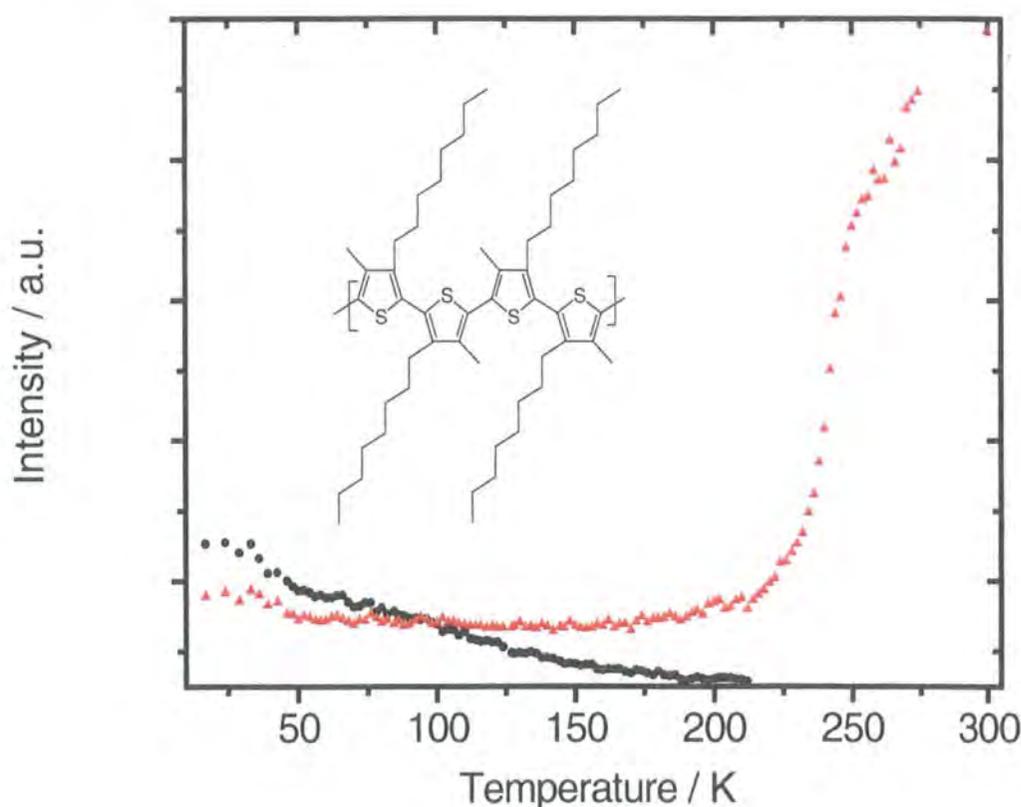
Figure 4.4 Temperature dependence of the integrated (1–100 µs) PMOT delayed luminescence. Symbols ▲ and ● refer to DF/EF and Ph, respectively. The inset shows the structure of head-to-head coupled PMOT.

There are several indications that the high temperature emission arises from a source completely different from long-lived singlet excitons – excimers (hereafter the emission will be referred to

as EF). As mentioned before, there is a red shift between high and low temperature delayed emission – this entails that the EF spectrum is *not isoenergetic* to the room temperature PF. Moreover, the shape of the EF peak is almost perfectly a *Gaussian* in contrast to the slight hump that is visible at the red side of the PF peak both at high and low temperature. Gaussian shaped emission bands are typical for excimer fluorescence as has been explained in section 2.6.1.

Second, the *decay kinetics* of the DF/EF emission change from power law at 15 K (Figure 4.2) to double exponential at room temperature (Figure 4.5) with characteristic times o f (1.0 ± 0.2) and (11.0 ± 2) µs. As an exponential behaviour is expected when no non-radiative channels are involved in the decay process[65] the room temperature emission cannot originate from migration-controlled processes such as TTA or geminate pair recombination but must originate from isolated emission sites e.g. traps, aggregates or excimers. Due to the similarity of the spectral shape of PF and EF traps are excluded as the origin.
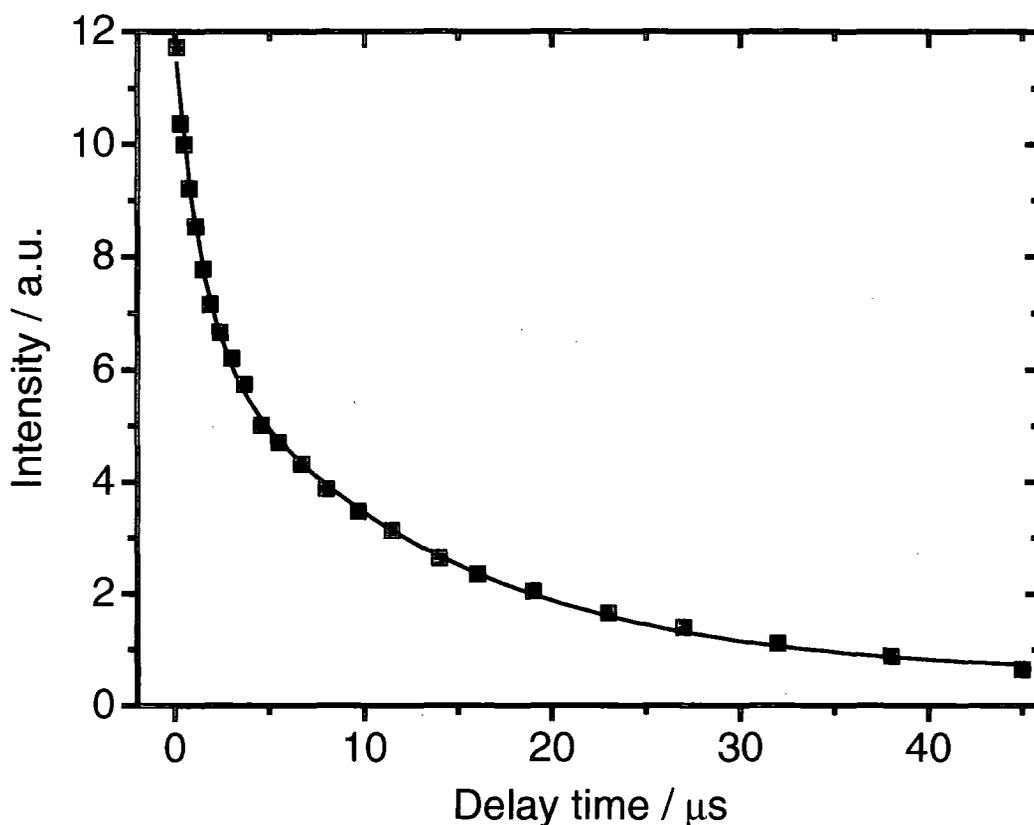
Figure 4.5 Integral kinetics of the PMOT delayed emission recorded at 289 K. The solid line represents a double exponential fit with time constants 1.0 and 11 µs.

Remain aggregates or excimers. As it is evident that the room temperature and low temperature emissions are different signals, one can attempt to explain the combined DF/EF *thermal behaviour*. The temperature region where the red-shift from DF to EF occurs happens to be exactly the region where the DF/EF signal remains constant. Below 100 K only DF is detected – as would be expected from the Ph behaviour the signal is slightly decreasing with rising

temperature. Above 200 K the data points represent only the EF – here, the increasing luminescence signal indicates a source of luminescence which is *thermally activated*. The formation of both, aggregates and excimers requires activation that can be provided in the form of thermal energy. As is shown in Figure 4.4 about one third of the final intensity is detected at ~ 240 K allowing an estimate of the activation energy of the underlying physical process to be ~ 20 meV. For emitters with a non-dissociative ground state such as aggregates one would expect the emission to persist even if the polymer sample is cooled down to 15 K unless the emission process itself does require thermal activation. The latter is surely not the case as it would contradict the exponential decay kinetics of the EF signal.

Instead, the experimental results make sense when excimers are assumed as the EF emitters. Their association regime continues at least up to room temperature apparent from the rising luminescence intensity. The onset of excimer dissociation is expected to occur at much higher temperatures as it would entail non-exponential decay kinetics[9].

How can the *double* exponential decay be explained? One possibility is the existence of two different but equally probable *excimer configurations*. Three arguments can be used to support this assumption:

1. The formation of excimers involves the overlap of π and π^*-orbitals. Hence, common excimer geometries, e.g. for anthracene, involve a cofacial arrangement of at least two aromatic rings (benzene or thiophene) from different chains or chain segments[66]. Due to the asymmetry of the thiophene ring one would expect cofacial configurations in such a way that the sulphur atoms overlap. As is explained in the introduction of this section, side chains play an important role for the photophysical properties of a polythiophene. In the case of PMOT, these are arranged asymmetrically – an octyl chain on one side and a methyl group on the other. When two thiophene rings overlap, these side groups can either match or they can be arranged such that octyl overlaps with methyl. Consequently, slight differences between the different *excimer configurations* arise regarding the radiative decay constant or the luminescence wavelength, the former being caused by two degrees of symmetrically forbidden decay.

Of course, this is only one possibility to obtain two slightly different excimers. Numerical calculations have not been carried out to support these specific configurations but the idea should be made clear.

2. As predicted by the former argument, a *red-shift* of the EF spectra from 2.54 eV (488 nm) to 2.52 eV (491 nm) is observed within the first few microseconds – this matches the time where the decay kinetics (Figure 4.5) show the transition from the shorter radiative decay to the longer. After that, the energy of the emission peak remains constant indicating that actually two states are observed, which are located at slightly different energy levels.
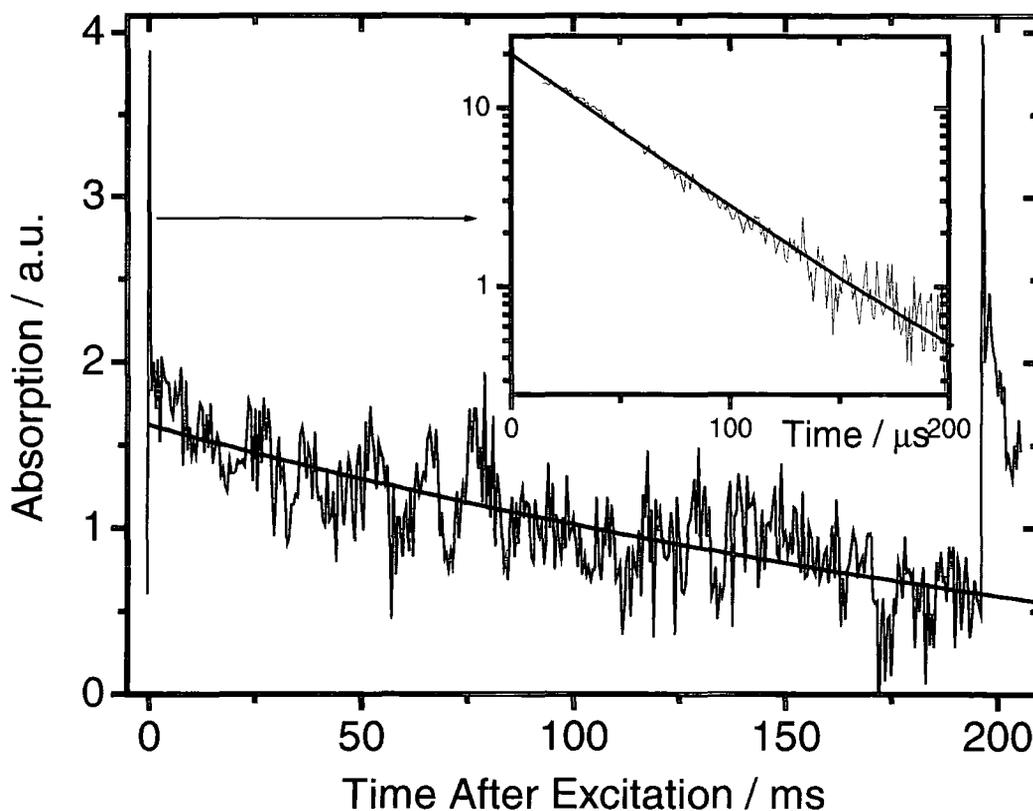
Figure 4.6 Photo induced transient absorption signal recorded at 1.9 eV (650 nm) at 280 K with 5 Hz repetition rate. The solid line represents a mono-exponential fit curve with 300 ms characteristic time. The inset shows the first 200 μs enlarged in a semi-logarithmic scale. In this case the signal can be well fitted exponentially using a decay time of 50 μs.

3. The double exponential decay has not only been observed by time-resolved photoluminescence spectroscopy but also by photo-induced absorption of thin PMOT films at room temperature. The lifetimes of the *emitting* excimers (1 and 10 μs) are too short to be detected with the temporal resolution of the PIA setup (limited to > 10 μs). Nevertheless, a PIA signal was detected at 670 nm exhibiting extremely long lifetimes. Figure 4.6 presents the corresponding decay kinetics and obviously they are double exponential – despite the poor quality of the measurement two lifetimes of (50 ± 5) μs and (300 ± 150) ms can clearly be distinguished. Which other excited state detectable in this spectral range could be so extremely long-lived but triplets? Although no corresponding excimer phosphorescence signal could be detected it is very likely that the PIA decay kinetics belong to the *triplet counterparts* of the emitting excimers. Qualitatively, they show the same decay kinetics, only the lifetimes have become exponentiated by ISC from the singlet to the triplet excimer state. As in Figure 4.5 half of the signal arises from the fast and half from the slow contribution, supporting the assumption of two excimer configurations with equal probability of formation (see 1.). Indeed, Subudhi *et al.* showed that PIA is a suitable experiment to detect triplet

excimers for α,α-dinaphthylalkanes[59] and similarly discovered exponential decay kinetics.

An on-chain triplet concentration can be ruled out as the origin of high temperature PIA signal for the various reasons: The PIA signal detected at 15 K corresponds to the emission of phosphorescence. Both signals are *proportional* – hence, triplet-triplet absorption decreases with rising temperature like the Ph. The temporal resolution and sensitivity of the TRS experiment would suffice to detect Ph if there was any, especially when exponential decay kinetics are observed pointing to an *isolated decay of immobile species*, unaffected by external quenching. Instead, the *lack of an emission* corresponding to the PIA signal indicates the observation of an excited state for which radiative decay is much more strictly *forbidden* than for triplet excitons – here, most probably the spin forbiddeness of a triplet state is combined with the symmetry forbiddeness of the excimer decay. Furthermore, the long-lived PIA signal is not observed at 15 K and apparently arises from excited states requiring *thermal activation*.

Finally, it must be noted that the PIA spectrum of room temperature films does not match that of room temperature PMOT solution or low temperature films. While the peak of the latter is found at 670 nm the former seems to be blue-shifted up to 600 nm and broadened. Unfortunately, the quality of the PIA measurements did not allow to record a presentable spectrum. However, such differences are expected as no excimers occur at low temperature. Furthermore, the formation of intrachain excimers – the parallel arrangement of neighbouring thiophene rings of the same chain made possible by a flexible bond between the repeat units – which could be encountered in solution as well, is highly unlikely due to steric hindrance provided by the side chains and the torsion of the chain. Even for a polythiophene like PMOT with a strong tendency to form chain coils this type of excimer formation is more likely encountered in polymer solutions rather than solid state.

4.6. Conclusion

In this work the photophysical properties of the conjugated polymer PMOT have been analysed with respect to its long-lived photo excitations as observed in the solid state. Two temperature regimes with entirely different properties can be distinguished. At temperatures below 100 K phosphorescence and delayed fluorescence are detected. They exhibit properties similar to those found in the conjugated polymers MeLPPP[6] and PF2/6[63]. The origin of the DF cannot clearly be assigned to geminate pair recombination or TTA as contradictive results are obtained depending

on the excitation dose regime. Whereas GP recombination seems to be probable for low doses TTA is favoured in the high dose regime.

The room temperature observations are different in so far as now delayed emission as well as photo induced transient absorption originate from excimer formation. A thermal activation of estimated 20 meV is required for excimer association. As a consequence of the asymmetry of the repeat units of PMOT, it is proposed that two equally represented configurations of singlet excimers are formed, leading to double exponential decay of their emission at room temperature. Both of them undergo ISC to form triplet excimers, which are observed using PIA measurements with lifetimes in the millisecond range at 300 K.

Excimers have previously been observed in polythiophenes. Seeing the presented study in the context of general photophysical properties of this family of conjugated polymers, one can explain their *high ISC rates* (about 60 % for PMOT[29]) as a consequence of excimer formation. Considering the intensity of EF emission these excimers are efficient exciton traps – moreover they are sufficiently isolated from the external quenching mechanisms to undergo ISC and form triplet states.

5. Investigation of fluorene-fluorenone co-polymers and the origin of keto emission

5.1. Introduction

Polyfluorenes are a widely studied family of conjugated polymers on account of their saturated and bright blue emission, which makes them interesting materials for applications in electroluminescent devices. Partly, this owes to their inter-system crossing rate, which is low[67] as in most homo atomic conjugated polymers. Here, their intrinsic structural variability might be useful – polyfluorene morphologies as different as the so-called β-phase[48] or the liquid crystalline phase, which exhibits polarised emission[50], have been observed and studied extensively with prospects for PLED applications.

Despite these promising findings there is a phenomenon impeding commercial polyfluorene devices: Instability of emission intensity and colour. A broad green emission band appears in photoluminescence spectra but especially affects electroluminescence[36, 68]. Its presence does not only distort the luminescence colour but is additionally accompanied by a reduction of the quantum yield. In the literature this emission has sometimes been attributed to excimers and, recently, with more convincing evidence, to *keto* defect sites[36, 68, 69]. The latter with their characteristic *carbonyl* groups can form via photo-oxidation of polyfluorene chains (formation of *fluorenone* repeat units), which explains why the unwanted emission is enhanced in aged or degraded thin films[70]. In these samples signals typical for carbonyl groups could be detected via infrared spectroscopy. However, their effect on polymer luminescence is only vaguely explained – keto defects themselves might act as exciton traps but also the formation of homo- or heteromolecular excimers or dimers might play a role. A systematic investigation of the problem is difficult as in samples of "pure" polyfluorene the background level of keto contamination strongly varies with time as it is supposed to arise from chemical polymer degradation. The rate of degradation again varies with the conditions of sample preparation and storage. The error of estimating this level is especially high as usually very low keto concentrations are encountered – still, they entail remarkable changes in the photo- and electroluminescence of a polyfluorene sample.

As a first approach, the quenching of the delayed luminescence of PF2/6 am4 due to ultraviolet radiation was investigated with the result that the overall photoluminescence is affected by

degradation and, in addition to delayed fluorescence, the green emission band appeared. The spectra are not shown here but resemble those presented in section 5.3. Secondly, P. de S. Freitas of the research group of Prof. U. Scherf kindly provided a series of co-polymers synthesised from 9,9-bis(3,7,11–trimethyldodecyl)fluorene and 9-fluorenone repeat units (PFO/PFl) with a broad range of fluorenone fractions[27]. The chemical structure of the fluorene and fluorenone repeat units can be found in the inset of Figure 5.1. The co-polymers served to simulate a controlled degradation of polyfluorene with the additional possibility to observe phenomena only visible at very high fluorenone levels. Techniques used for these investigations include steady-state and time-resolved photoluminescence spectroscopy, steady-state absorption and excitation spectroscopy as well as a flash photolysis experiment carried out by my supervisor, Prof. A.P. Monkman. Attention has been paid to dependencies of the signals on keto level and temperature as well as, for solutions, on concentration. It must be noted that the presented data and discussion will be published in the near future but are still incomplete and subject to further analysis.

5.2. Absorption

Regarding the question whether excimers are involved in the quenching processes the application of *absorption spectroscopy* might be useful. Excimers exhibit a dissociative ground state, stimulated by thermal motion an overlap between neighbouring orbitals, the formation of ground state excimers, only occurs statistically – invisible for absorption spectroscopy. In contrast to this, dimers possess a physical ground state and can always be detected via absorption spectroscopy. Still the exact experimental identification is difficult as already low keto levels can have an enormous quenching effect on the emission of polyfluorene but are hard to detect in any other way. As mentioned before, the series of fluorene-fluorenone co-polymers (PFO/PFl) provided by P. S. Freitas offers a wide range of fluorenone percentages (0.1 up to 25 percent), which overcomes this concentration problem. These polymers have been used to investigate the interactions between fluorene and fluorenone repeat units via absorption spectroscopy of solution and solid state samples.

5.2.1. Thin films

Figure 5.1 shows the normalised absorption spectra of thin films of the co-polymers. All samples exhibited a similar maximum optical density of 0.3 – 0.4 ensuring that no spectral distortions arise due to the normalisation procedure. Before this step, the spectra have been

converted from optical density A (in the decadic logarithmic scale provided by the absorption meter) to fraction of absorbed intensity I_A/I_0 (I_0 being the initial intensity of the incident light) using Lambert-Beer's law (Equation 2.1):

$$I_x = I_0 \cdot \exp(-\alpha \cdot c \cdot x) = I_0 \cdot \exp(-A \cdot \ln 10)$$

$$\ln \frac{I_x}{I_0} = -A \cdot \ln 10 \; ; \qquad -A = \ln \frac{I_x}{I_0} \Big/ \ln 10 = \lg \frac{I_x}{I_0}$$

$$\text{with} \qquad I_A = I_0 - I_x \quad \Big| \; (x = \text{sample thickness})$$

$$\frac{I_A}{I_0}(E) = 1 - \frac{I_x}{I_0}(E) = 1 - \exp(-A(E) \cdot \ln 10) \quad \Big| \; (E \dots \text{energy of } I_0 \text{ photons})$$
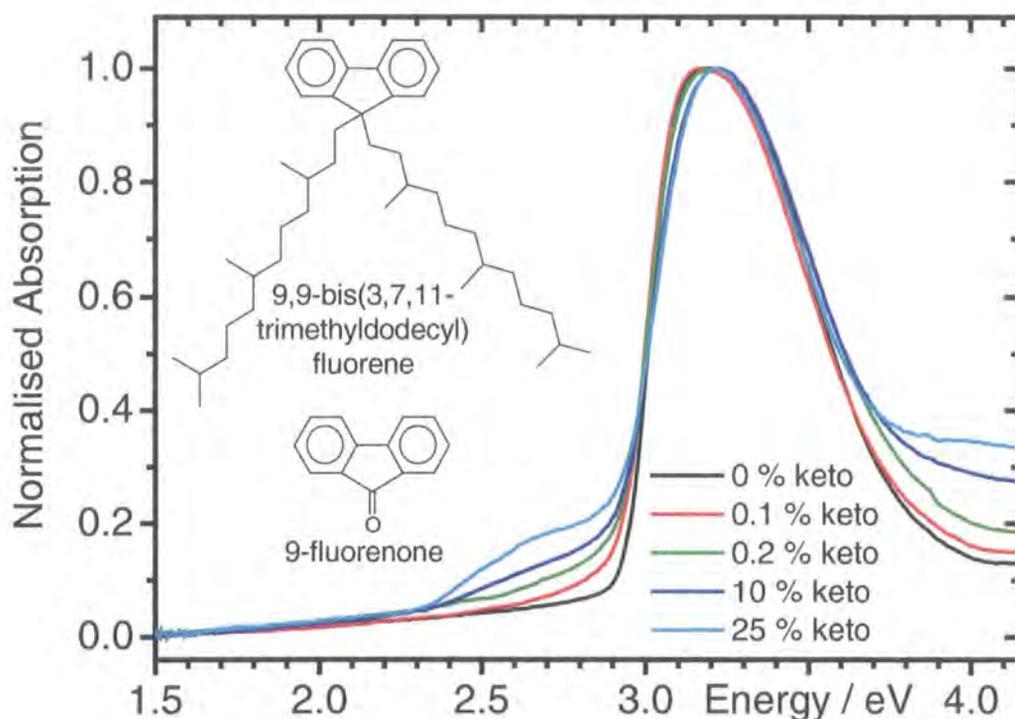
Figure 5.1 Normalised absorption spectra of thin films of PFO/PFl co-polymers. The legend illustrates the keto fractions present in each sample. *Inset:* Chemical structures of the fluorene and fluorenone repeat units of the PFO/PFl co-polymers.

The normalised spectra of I_A/I_0 in Figure 5.1 have been obtained from the PFO/ PFl co-polymers synthesised using 25, 10, 0.2 and 0.1 percent fluorenone as well as the corresponding poly(9,9-bis(3,7,11-trimethyldodecyl)fluorene) (here referred to as PFO) homopolymer. The shape of the homopolymer absorption is representative for all commonly used polyfluorenes such as poly(9,9-diethylhexylfluorene) (PF2/6) even though the peak in the absorption spectrum of the

latter (compare Figure 3.1) appears to be broader at its blue side. Characteristically, it shows one maximum within the detection range, which is located at 3.2 eV and known to correspond to the 0-0 singlet transition of polyfluorene[71].

The co-polymers exhibit the same absorption peak but also additional features attached as less intense shoulders to the red (2.65 eV) and blue side (4.0 eV) of the PFO absorption maximum. A systematic increase in both additional signals can be observed as the fraction of keto repeat units rises.

To complete the picture, a comparison of these results with absorption spectra of pure polyfluorenone would be necessary. Unfortunately, the polyfluorenone synthesised by P. de S. Freitas does not dissolve in common solvents such as toluene or chlorobenzene and, therefore, no film or solution samples of this polymer have been available for study. In the literature, one finds absorption spectra of the corresponding monomer, 9-fluorenone, in solution for various solvents. They exhibit a pronounced solvatochromism but generally the singlet $\pi \rightarrow \pi^*$ absorption modes are found in the ultraviolet, extending down to ~3.75 eV (330 nm)[72]. Additionally, an absorption feature is found around 3 eV, which has been attributed to $\pi \rightarrow n\pi$ absorption[73], from which a fluorenone triplet state is directly populated. Unfortunately, the latter reference goes back to 1966, which means that it had to be taken from another paper and could not be checked. However, this absorption feature is found here and it will be shown later that it is very probable to arise from direct triplet absorption of fluorenone, even if the exact assignment of a $\pi \rightarrow n\pi$ transition cannot be confirmed completely.
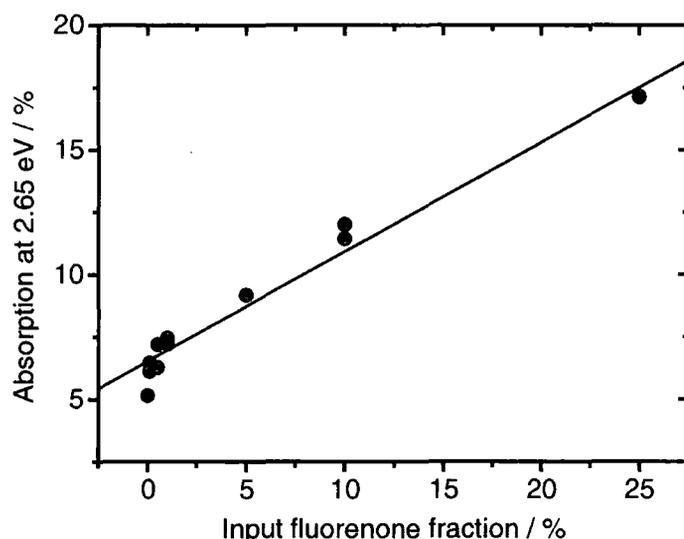
Figure 5.2 The fluorenone triplet absorption at 2.65 eV increases linearly with the fluorenone level input during co-polymer synthesis. The straight line represents a linear fit as guide to the eye. All values ± 2 %.

As the fluorenone percentages of the investigated co-polymers are rather low, the length of fluorenone segments of the co-polymer chains will statistically not exceed 2 or 3 repeat units (for 25 % fluorenone) and, therefore, bear monomer or oligomer character. Taking into account

the solvatochromism of the fluorenone absorption spectra and possible red-shifts caused by the extended conjugation length one attribute the "blue" shoulders of the co-polymer spectra to the $\pi \rightarrow \pi^*$ singlet excitation and the "red" shoulders to the $\pi \rightarrow n\pi$ triplet excitation of fluorenone. The latter has been confirmed via excitation spectroscopy, see section 5.4.

Finally, Figure 5.2 shows that the intensity of the "red" shoulder increases linearly with the percentage of fluorenone repeat units in the sample, although the first and lowest data point is slightly offset the linear fit. However, this data point does not correspond to one of the co-polymers but to PFO – it reflects the level of PFO absorption and not of fluorenone. Apparently, it is not zero – the proximity of the PFO absorption peak causes the offset of the linear fit. The linear dependency can be taken as evidence that the fluorenone/fluorene ratio input during the synthesis of the co-polymers is maintained in the resulting co-polymers. Each of the data points represents the value of the absorption at 2.65 eV of spectra normalised like the spectra shown in Figure 5.1.

5.2.2. Solution

The absorption spectra of solutions of PFO/PF1 7 (5 % fluorenone) in toluene have been investigated for various concentrations, in mg per ml: 2, 0.4, 0.08 and 0.016. The polymer exhibits a molecular weight of 10^4 g/mol. As expected, the fluorenone absorption bands at 2.65 and 4.0 eV were found in solution as well, their intensity depending linearly on the solution concentration (not shown here).

As the recorded spectra resemble the film spectra shown in Figure 5.1 they are not presented here. More important information has been obtained form steady-state emission and excitation spectra of the same set of solutions – these measurements reveal much more pronounced effects of the fluorenone repeat units than detectable by absorption spectroscopy (sections 5.3 and 5.4).

5.3. Steady-state photoluminescence emission

Using the FLUOROMAX spectrometer described in section 3.4, steady-state photoluminescence spectra have been recorded of thin films as well as of solutions of PFO and PFO/PF1 co-polymers for various keto levels. Whereas solution spectra have been obtained for room temperature only, thin films have additionally been studied at low temperatures of 160, 80 and 40 K. For solutions, special regard has been paid to the concentration dependence of their photoluminescence emission.
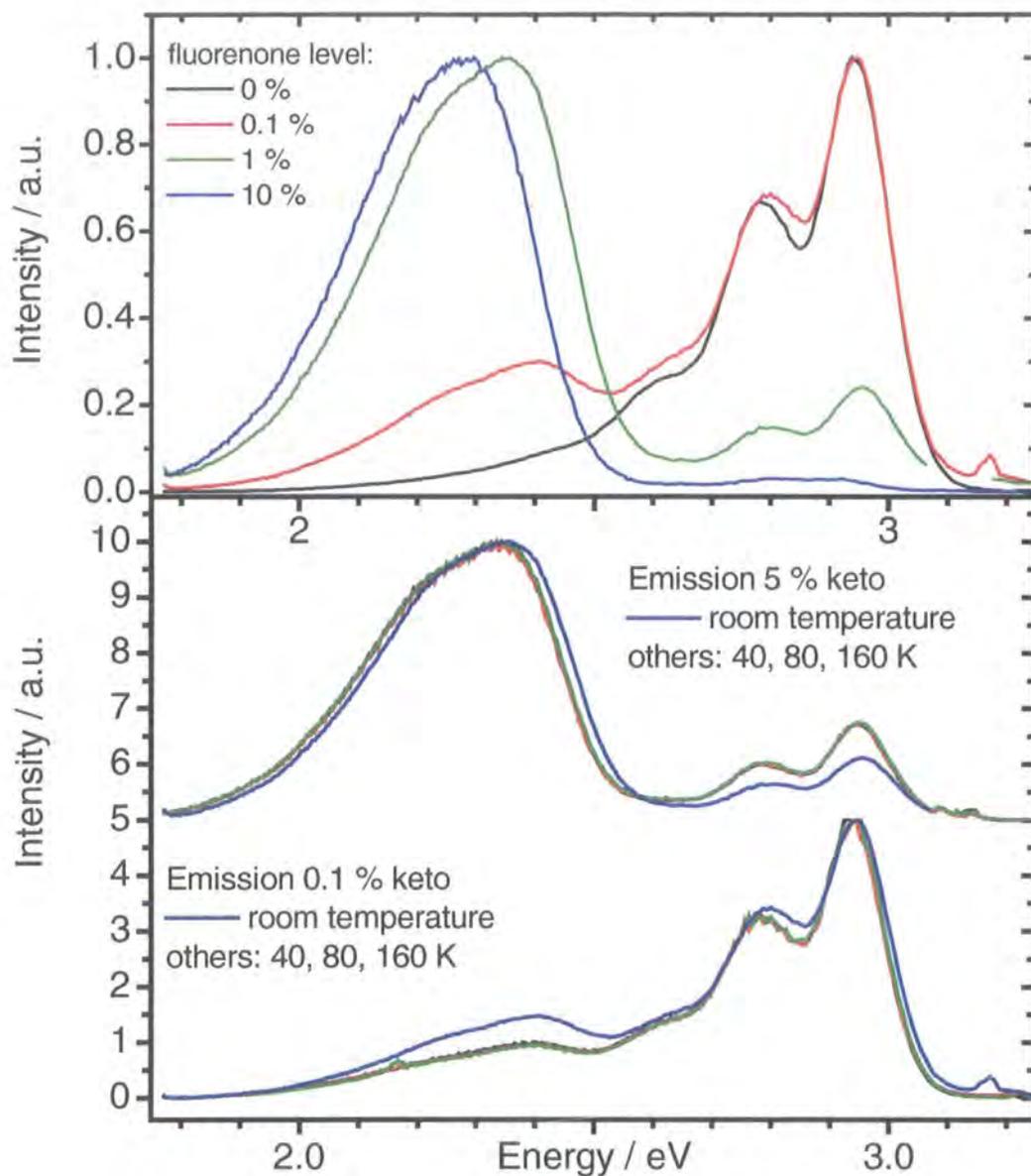
Figure 5.3 Steady-state photoluminescence spectra of thin films of PFO/PFl co-polymers *above:* recorded at room temperature for PFO/PFl containing 0.1, 1 and 10 % fluorenone as well as the PFO homopolymer. *below:* recorded at four different temperatures for PFO/PFl 7 (5 % keto, top curves) and PFO/PFl 2 (0.1 % keto, bottom curves).

5.3.1. Thin films

Figure 5.3 (top graph) presents the *room temperature* steady-state photoluminescence spectra of thin films of PFO/PFl co-polymers containing 0.1, 1 and 10 % fluorenone repeat units as well as the emission of the PFO homopolymer for comparison. All spectra were recorded using an excitation at 355 nm or 3.5 eV to ensure the comparability of these measurements with results

obtained from the TRS experiment, which utilises an Nd:YAG laser beam of 355 nm as excitation source.

Fluorenone Content / Percent	0	0.1	1	10
PFO Intensity / PFO + Keto Intensity *spectral range:2.8 – 3.0 eV*	1	0.75	0.16	0.03
Keto Intensity / PFO +Keto Intensity *spectral range:2.2 – 2.4 eV*	0	0.25	0.84	0.97

Table 2 A compendium of the intensity ratios between PFO prompt fluorescence and keto emission for thin films of different keto levels.

Two main emission features can be distinguished: First of all, a structured signal occurs between 2.6 and 3 eV – its intensity decreases rapidly with rising fluorenone content. Depending on the investigated polymer, it consists of two or three modes separated by 180 meV, which corresponds to the characteristic frequency of a C=C stretch mode. This emission is identified as prompt fluorescence (PF) from the first excited singlet state of PFO and represents the only feature in the spectrum of PFO.

For the co-polymers, an additional, rather unstructured band is detected between 2 and 2.5 eV. It increases and red-shifts by about 150 meV as the fluorenone level rises. This emission is commonly attributed to keto defects but still its origin remains unclear. It will be the objective of this study to reveal its nature.

It should be noted that the dependence of the relative intensities of PFO and keto emissions on the fluorenone content of the sample is *not linear*, see the table above. Obviously, the PFO prompt fluorescence is markedly quenched for low keto levels, so that almost all of the photoluminescence is keto emission already at 1 %. Furthermore, the quantum yield decreases with rising keto content. Both observations indicate that energy is transferred from PFO singlets to excited states that exist in connection with fluorenone, in accordance with the common observations on the luminescence of degraded polyfluorene samples.

The low temperature photoluminescence spectra shown in the bottom graph of Figure 5.3 exhibit the same dependencies on keto level as their room temperature counterparts. Additionally, two temperature effects are observed: As cooling freezes out chain motion giving rise to more planarity of the polymer molecules, their effective conjugation length rises. This causes a slight red-shift of the spectra. Second, an increase of the absolute intensity of PFO prompt fluorescence is observed with decreasing temperature (about 30 % more going from 300

to 40 K) while keto emission remains stable. Figure 5.3 presents normalised spectra to illustrate the enhanced PFO/keto ratio. The transition between the high and low keto emission regime must occur between 160 and 300 K as no remarkable spectral change is observed below 160 K. Unfortunately, the coarse thermal resolution of this measurement inhibits a more exact estimate.
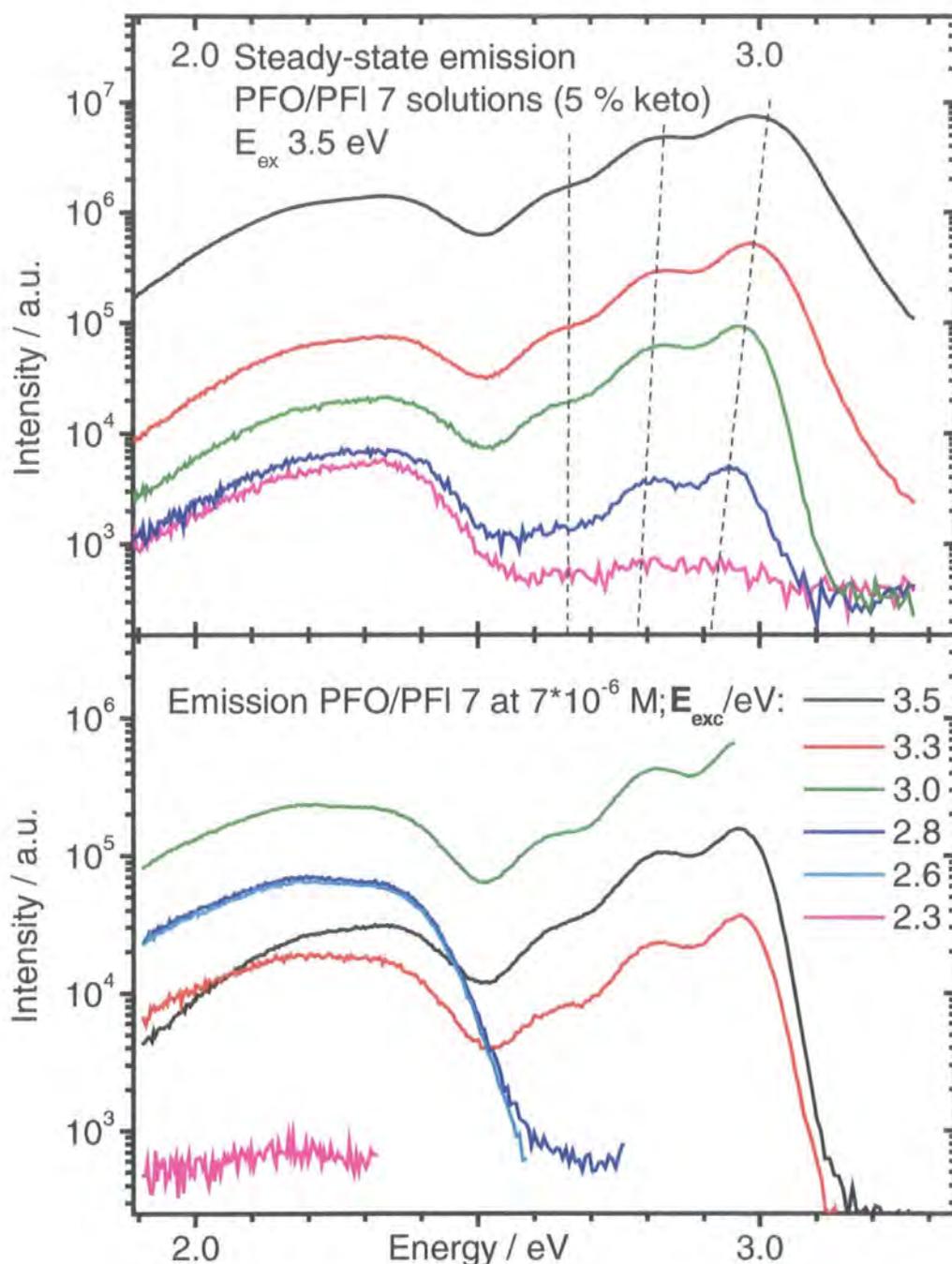
Figure 5.4 *above:* Room temperature steady-state photoluminescence spectra of toluene solutions of PFO/PFl 7 (5 % fluorenone) at concentrations of — $2.7*10^{-7}$ — $1.3*10^{-6}$ — $7*10^{-6}$ — $3*10^{-5}$ — $1.7*10^{-4}$ M. The dashed lines are guides for the eye to indicate the red-shift of the PF. *below:* The photoluminescence of the PFO/PFl 7 solution from above (at $7*10^{-6}$ M) excited with different photon energies.

5.3.2. Solution

The steady-state photoluminescence spectra of PFO/PFl solutions and their dependence on the keto level were comparable to that of the thin films. Here, main interest was focused on their concentration dependence in order to detect possible interchain effects involved in the keto emission process.

Figure 5.4 (top graph) presents the room temperature spectra (excitation at 3.5 eV) of toluene solutions of PFO/PFl 7 (5 % keto) for concentrations ranging from $2.7*10^{-7}$ up to $1.7*10^{-4}$ M. They exhibit a pronounced concentration dependence in so far that the PFO/keto ratio decreases simultaneously with the emission intensity as the density of polymer chains increases. The nature of the underlying physical processes has been further investigated via excitation spectroscopy, see next section.

Additionally, a red-shift of the PFO prompt fluorescence is observed as the concentration of the solution is increased – although for all investigated samples excitation at 3.5 eV remains constant as there is little shift in the absorption band. The phenomenon affects the first PF mode (total shift: 0.06 eV) stronger than the second (0.01 eV) while for the third mode hardly any shift can be detected due to the presence of keto emission. Again, further experiments are required before assumptions can be made about the origin of this effect: As can be seen in the bottom graph of Figure 5.4, the photoluminescence of a medium concentrated ($7*10^{-6}$ M) toluene solution of PFO/PFl 7 also depends on the photon energy utilised for excitation with respect to emission intensity as well as the shape of the spectrum. Far more photoluminescence (both PF and keto) is emitted upon exciting the sample at 3.0 eV – however, 3.3 eV does not simply yield the intermediate spectrum between 3.5 and 3.0 eV but lead to a reduced PF with simultaneously (at least partly) enhanced keto emission. As expected, only the latter is detected for every excitation wavelength below the PF emission spectrum. Such extraordinary behaviour can only be illuminated by further investigation via excitation spectroscopy.

5.4. Steady-state excitation spectra

Excitation spectroscopy is useful for the assessment of absorption features. In the investigated case, PFO singlet absorption at 3.2 eV was encountered in the co-polymer samples accompanied by absorption signals related to fluorenone, presumably fluorenone triplet absorption at 2.65 eV and fluorenone singlet absorption at roughly 4.0 eV. The same PFO/PFl samples as in section 5.3 were studied using the FLUROMAX in the excitation spectroscopy mode.
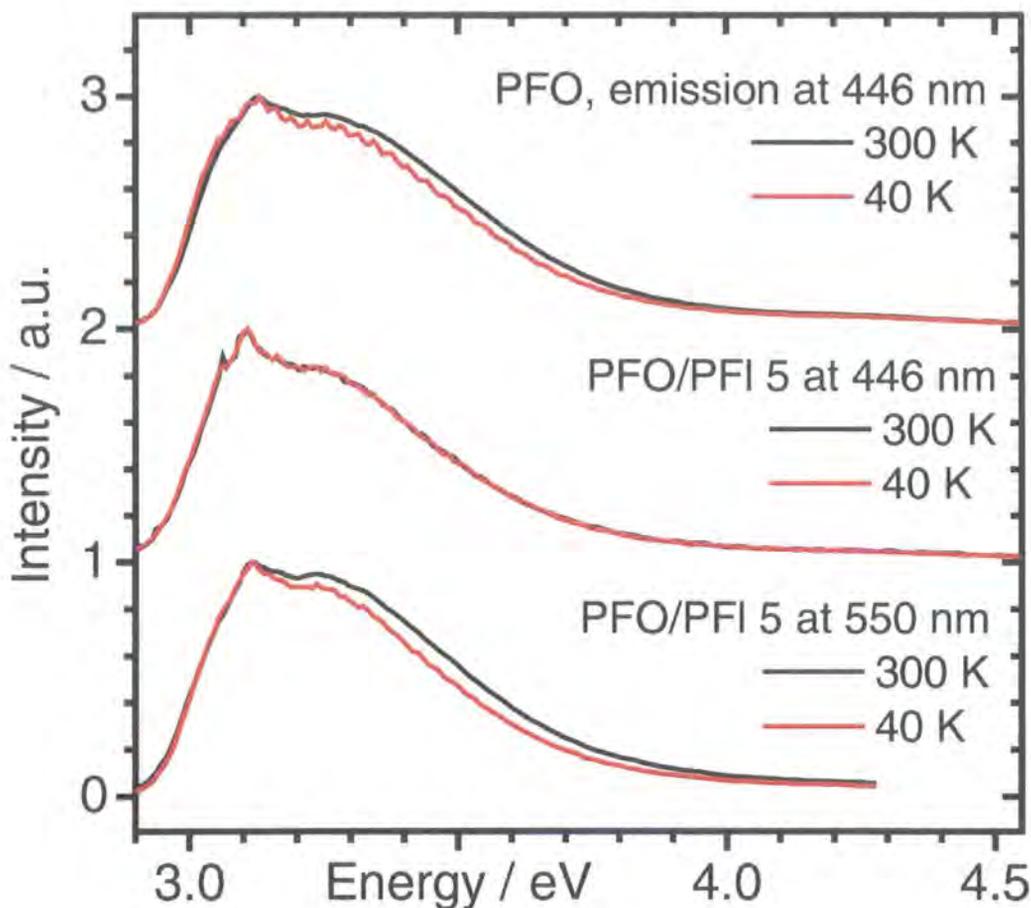
Figure 5.5 Steady-state excitation spectra of thin films of *(top)* PFO homopolymer, emission at 446 nm (2nd PF mode) monitored at 300 and 40 K *(middle)* PFO/PFl 5 (1 % keto), emission at 446 nm monitored at 300 and 40 K *(bottom)* PFO/PFl 5, emission at 550 nm (keto peak) monitored at 300 and 40 K.

5.4.1. Thin films

Figure 5.5 shows steady-state excitation spectra of thin films of PFO and PFO/PFl recorded at emission wavelengths of 440 nm (2.82 eV, corresponding to the second mode of the prompt fluorescence of PFO) and 550 nm (2.38 eV, in the middle of the keto emission peak) for 300 and 40 K. Apparently, no major changes occur upon varying these parameters apart from the increase of PFO emission with lower temperature, which has already been observed in the emission spectra, see previous section. No direct keto excitation is found for thin films of PFO/PFl as the curves in Figure 5.5 match only the PFO absorption band observed in the corresponding film absorption spectra. A slight difference between excitation and absorption signals is encountered regarding the shape of the peak, which seems to consist of two parts for the former (a spike occurs at the red side) while the latter are always smooth. This finding will be further commented in the next section, which presents solution excitation spectra.

5.4.2. Solution

Figure 5.6 shows a compendium of concentration dependent excitation spectra acquired by FLUOROMAX measurements using PFO/PFl co-polymers dissolved in toluene.

Mainly investigated was the PFO/PFl 7 containing 5 % fluorenone, which exhibits strong keto emission but a still detectable intensity of the polyfluorene PF as its photoluminescence. The second mode of the latter (at 440 nm or 2.82 eV) has been monitored for Figure 5.6 a). Essentially, dilute solutions of PFO/PFl 7 ($2.7*10^{-7}$ M, corresponding to a maximum optical density of ~0.5 at 3.2 eV) exhibit excitation spectra identical to those of thin films of PFO or PFO/PFl, compare to previous section. These show only one peak located in the spectral range of the PFO singlet absorption (between 3.1 and 3.5 eV). As has already been observed for thin film excitation, this feature is slightly more structured than the corresponding absorption. There is no fluorenone contribution to the PF emission.

Upon increasing the concentrations of the PFO/PFl 7 solutions (by a factor of 5 for each presented graph), the formerly slightly structured peak at 3.2 eV splits into two: A sharp component at its red side (FWHM only 0.1 eV), which shifts to the red and a broader part that blue-shifts. However, this effect is not due to a concentration dependence of the excitation properties of the polymer but an artefact of the detection system instead. Shortly speaking, the extremely high optical density of the solution sample causes that the absorption of the excitation beam happens within the first millimeter of solution. Hence, all emission comes from this region, which, unfortunately, lies at least partly outside the area sampled by the emission collection optics. With increasing concentration this region gets smaller and smaller resulting in a decrease of the collected emission where absorption is strongest – in the spectra, this appears as a gap which broadens with concentration and finally affects the entire excitation band so that no more emission is collected – the shifting peaks at the gap sides shrink. The overall shape of the excitation spectrum does *not change* with concentration, which has been confirmed by using very thin fluorescence cells (spectra not shown here; they resemble those of dilute solution). Bearing in mind that the corresponding steady-state emission spectra (Figure 5.4, top graph) have been recorded exciting at 3.5 eV, the concentration dependent decrease of PLQY can be explained by this pseudo-gap in the excitation spectrum.

Attention is turned now to Figure 5.6 b) which deals with the actual objective of this study: Keto emission. It presents a series of excitation spectra analogous to Figure 5.6 a) but monitoring the photoluminescence of PFO/PFl 7 solutions at 520 nm (2.38 eV), in the middle of the keto peak. In order to cover the observed intensity range completely, spectra are shown on a logarithmic scale.
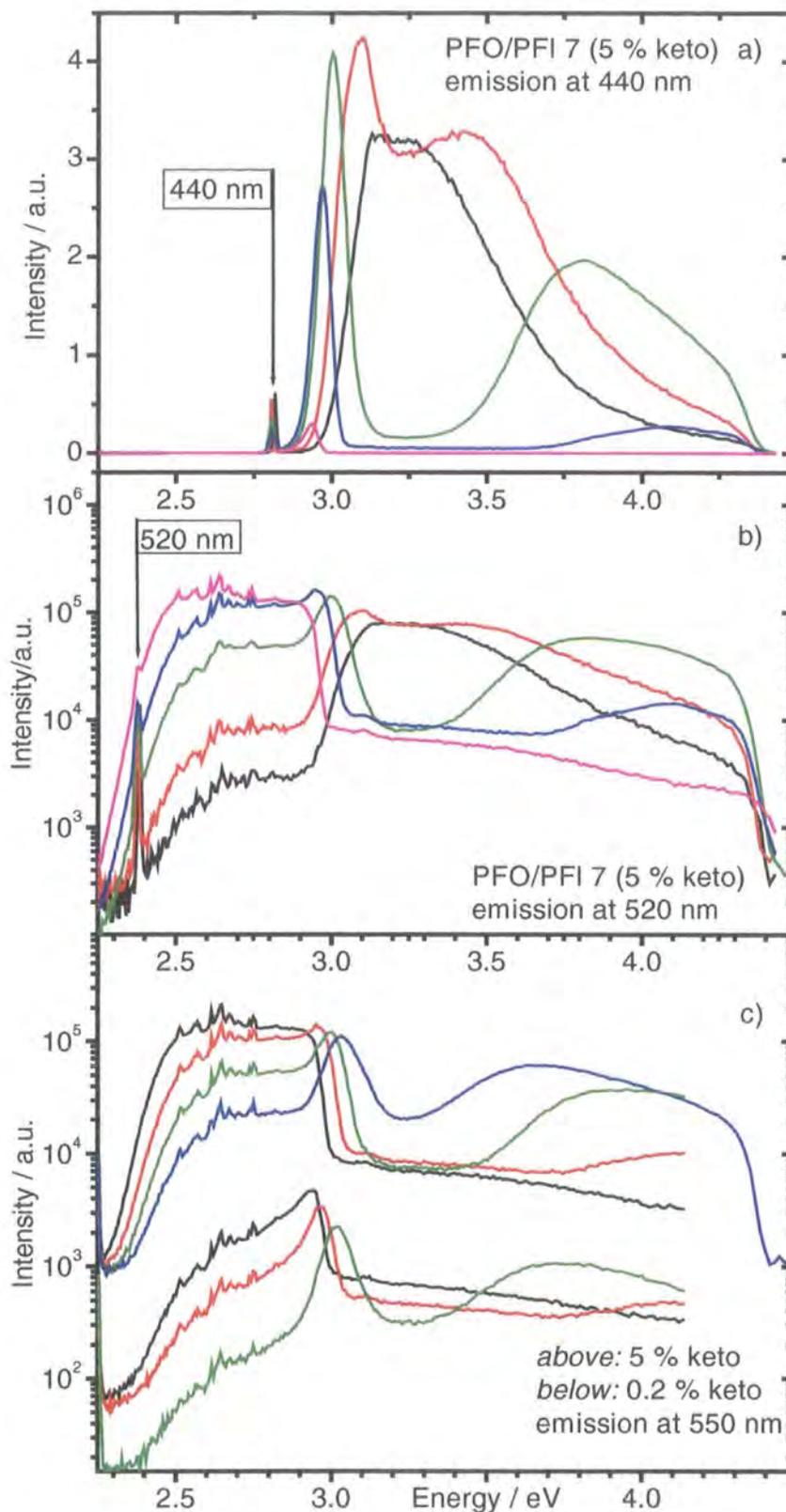
Figure 5.6 300 K steady-state excitation spectra of solutions of PFO/PFl 7 (5 % keto) at conc. of ▬ $2.7*10^{-7}$ ▬ $1.3*10^{-6}$ ▬ $7*10^{-6}$ ▬ $3*10^{-5}$ ▬ $1.7*10^{-4}$ M monitoring *a)* the 2nd PFO mode and *b)* the keto emission. *c)* excitation of the keto emission for toluene solutions of PFO/PFl 3 (0.2 % keto) and PFO/PFl 7 at conc. ▬ $1.9*10^{-6}$ ▬ $5.6*10^{-6}$ ▬ $2.8*10^{-5}$ ▬ $1.4*10^{-6}$ M.

Comparing Figure 5.6 a) and b), it is found that PFO absorption can excite keto emission. In fact, it represents the only excitation path for dilute solutions (as well as thin films of low keto content) – energy transfer takes place from PFO singlets to the excited states responsible for keto emission. The concentration dependence of keto excitation via PFO is identical to the direct excitation of polyfluorene PF (unfortunately, detection artefacts affect it as well).

Apart from PFO-keto energy transfer there is another path to excite keto emission – not via fluorenone singlet absorption, as this should be detected around 4.0 eV in addition to the PFO signal in similar resolution as for the absorption spectra, but via what is assumed to be *direct fluorenone triplet excitation*, see section 5.2. The corresponding signal exactly matches the triplet absorption peak observed in Figure 5.1 and grows about linearly in intensity as the concentration of the solution is increased. No artefacts affect this signal.

The spiky appearance of the peak is caused by the emission spectrum of the excitation source (Xenon arc lamp) and could not be removed completely despite normalisation of all excitation spectra with respect to the lamp emission profile. Summarising the above, there are two independent ways keto emission can be stimulated: Energy transfer from PFO singlets but also direct excitation of fluorenone triplets. Obviously, the presence of fluorenone triplets rather than singlets is linked to the emission.

For completion, Figure 5.6 c) presents concentration dependent excitation spectra for 550 nm (keto emission) that have been recorded using PFO/PF1 solutions containing different levels of fluorenone (5 and 0.2 %). PFO excitation with artefacts is observed for both as well as fluorenone triplet absorption. With respect to the former, fluorenone excitation is more intense for 5 % keto – as expected. Note that the spectra of 0.2 % have been divided by a factor of 10 for presentation purposes.

5.5. Time-resolved delayed luminescence in thin films

Using time-resolved photoluminescence spectroscopy (TRS) thin films of several polymers have been studied. Attention was paid to a systematic investigation of the PFO/PF1 co-polymers containing different levels of fluorenone involving PFO/PF1 8 (10 % fluorenone) and PFO/PF1 3 (0.2 % fluorenone). The results obtained are supplemented by similar measurements previously carried out for thin films of pure PF2/6 am4 by C. Rothe (these data are presented with his kind permission). The latter polymer was especially useful, as of all available pure polyfluorenes its photo- and electroluminescence is least affected by the presence of keto groups.

The following sections present results on the decay kinetics of the delayed luminescence of the polymers above. All measurements are differential; they have been obtained with variable delay and exposure times of the detector, the latter being about 1/10 of the former.

To each decay curve presented in section 5.5.3 belongs a set of spectra, from which the data points for the decay kinetics have been obtained via integration over an appropriate spectral region. These spectra have been given numbers in the order of their delay time, which are used to identify and compare spectra taken in similar time regimes. As the same recording routine has been utilised for all of the presented differential decay data same numbers always correspond to the same point in the decay curve; they are shown in the legends of Figure 5.7 and Figure 5.8.

5.5.1. Room temperature DF and keto emission spectra

Figure 5.7 shows some of the spectra of the delayed luminescence at room temperature. These have been selected to illustrate spectral changes occurring while recording the decay curve. The record number of the spectrum is show in the figure legend to simplify the identification of "early" and "late" spectra.

Basically, all consist of two parts, a rather structureless band at 2.2 to 2.3 eV and a more or less intense emission consisting of several modes at about 2.95, 2.8 and 2.6 eV. Located isoenergetic with respect to the PFO fluorescence the latter is recognised as the delayed fluorescence (DF) of polyfluorene. Apparent form the separation between its modes, this emission couples to the polymer backbone.

The broad red-shifted band has formerly been assigned to an emission linked to the presence of keto defects in PFO. As can be seen from the spectra presented in Figure 5.7, there is clearly a positive correlation between this emission and the fluorenone level in the sample, supporting the former assumption. However, the analysis of the spectra can yield even more information about the connections between sample chemistry and photophysics. First of all, the room temperature keto emission shifts from 2.3 to 2.2 eV with rising fluorenone level, an observation, which will be commented later after the low temperature spectra have been shown.

Regarding the spectral evolution with time, for PF2/6 am4, which shows almost plain DF after 90 ns, keto emission dominates the first spectra in a decay record. Similarly, the PFO/PF1 3 spectra mainly consist of the keto band, only at very long delay times the onset of DF is visible – PFO/PF1 8 cannot be considered for this matter as here band emission is observed throughout the complete decay measurement with only a weak contribution of what might be the third DF mode. It must be noted, that both emissions exhibit almost identical decay kinetics (see section 5.5.3) in the delayed luminescence regime but that keto emission actually starts shortly after the prompt fluorescence of PFO and dominates the PF spectra for high fluorenone concentrations.
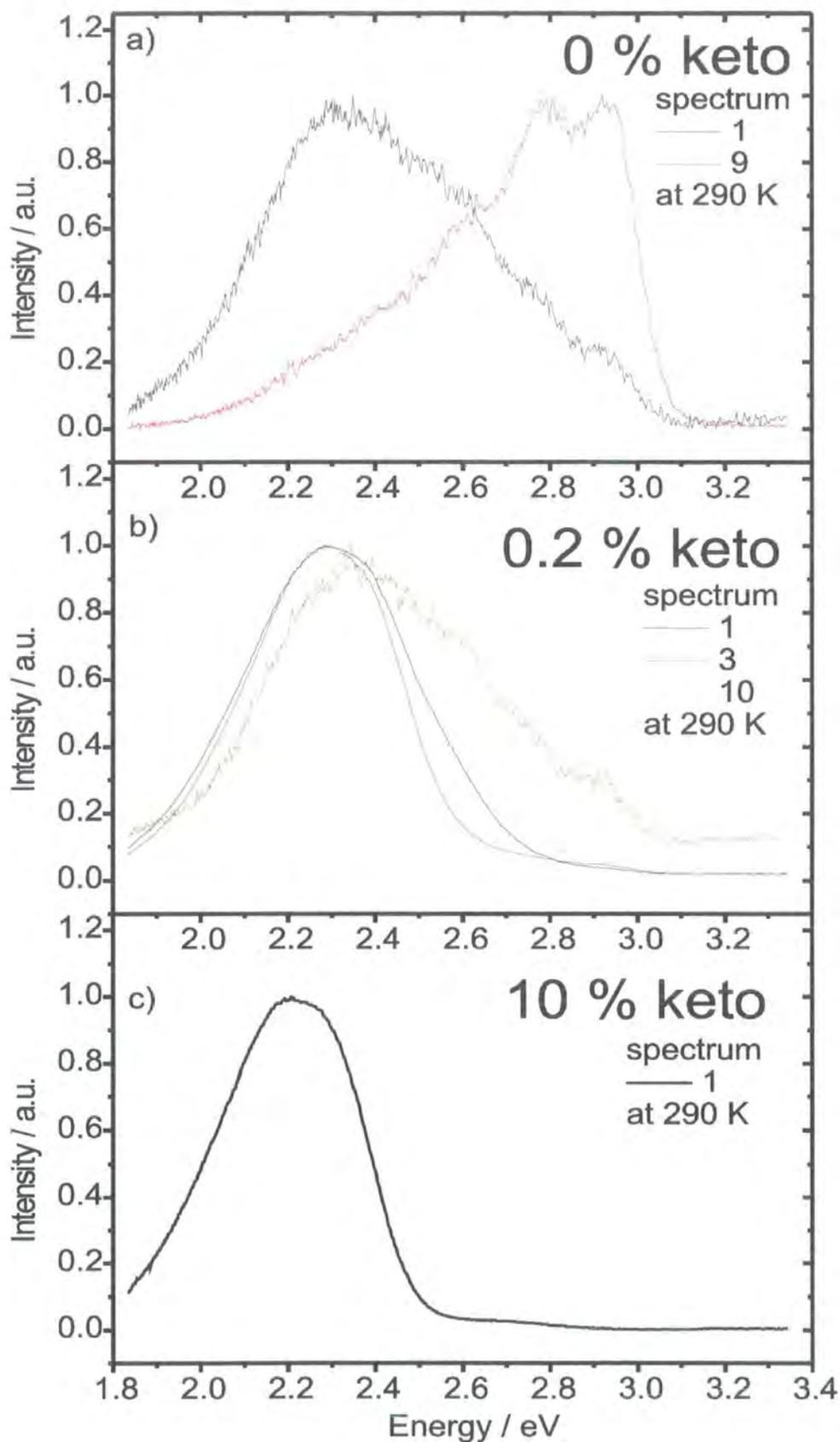
Figure 5.7 Room temperature spectra (normalised) of the delayed emission of thin films of *a)* PF2/6 am4, delay: ▬ 4.2 ns ▬ 89.2 ns; *b)* PFO/PFl 3 (0.2 % keto), delay: ▬ 4.2 ns ▬ 9.5 ns ▬ 126 ns; *c)* PFO/PFl 8 (10 % keto), delay: ▬ 4.2 ns.

What is actually meant by "high" concentrations becomes clear when comparing the intensity of the DF for the different polymers. Whereas DF decreases rapidly and spectra change completely from ~0 % keto (PF2/6 am4) to 0.2 % (PFO/PFl 3), the change is less significant between 0.2 and 10 % keto. Obviously, keto emission grows on cost of the DF very efficiently, as has already been observed for the PF. Therefore, 0.2 % can be considered as a high keto concentration, at 10 % fluorescence quenching is definitely saturated.

Please note that room temperature decay kinetics have been recorded for PFO/PFl solutions as well. The corresponding spectra showed keto emission and DF similar to the spectra in Figure 5.7. However, their lifetimes were shortened due to the high phonon activity and chain mobility in solution so that the decay kinetics obtained do not necessarily reflect intrinsic photophysical properties of the co-polymer. One important conclusion could be drawn from these measurements: Keto emission as well as DF are quenched in the presence of oxygen. Their intensity is enhanced upon degassing the solution investigated. Example spectra can be found in Figure 5.11 in the discussion section (5.7.2).

5.5.2. Low temperature DF, keto and phosphorescence spectra

Figure 5.8 shows again spectra of the delayed emission of thin films of different polymers with variable fluorenone concentration (PF2/6 am4, PFO/PFl 3 and PFO/PFl 8) but for the low temperature regime.

Again, DF and keto emission are observed but generally these signals are much longer lived compared to their room temperature counterparts in Figure 5.7. There are more differences:

a) Whereas for PF2/6 am4 keto emission was initially visible at 280 K, DF rising at later times, at 140 K DF is present form the beginning. Keto emission is even weaker and DF even stronger at 40 K – as these spectra do not change in the course of the decay measurement only those corresponding to the first data point of the decay curve are shown.

b) The same effect is observed for PFO/PFl 3. As here more fluorenone is present, keto emission is more pronounced than for PF2/6 am4. However, in contrast to the 290 K spectra, three modes of the PFO DF are clearly visible at 40 K after about 60 ns, making possible the recording of the DF decay kinetics at 40 K. An additional emission is observed at long delay times (>10 ms). It shows two modes at ~2.0 and ~2.2 eV, *separated by the 180 meV* characteristic for emission coupling to a ground state existing on a benzene ring, and is commonly attributed to PFO *phosphorescence* (Ph)[7]. PF2/6 am4 exhibits the same long-lived phosphorescence emission (spectra not shown here) although more intense.
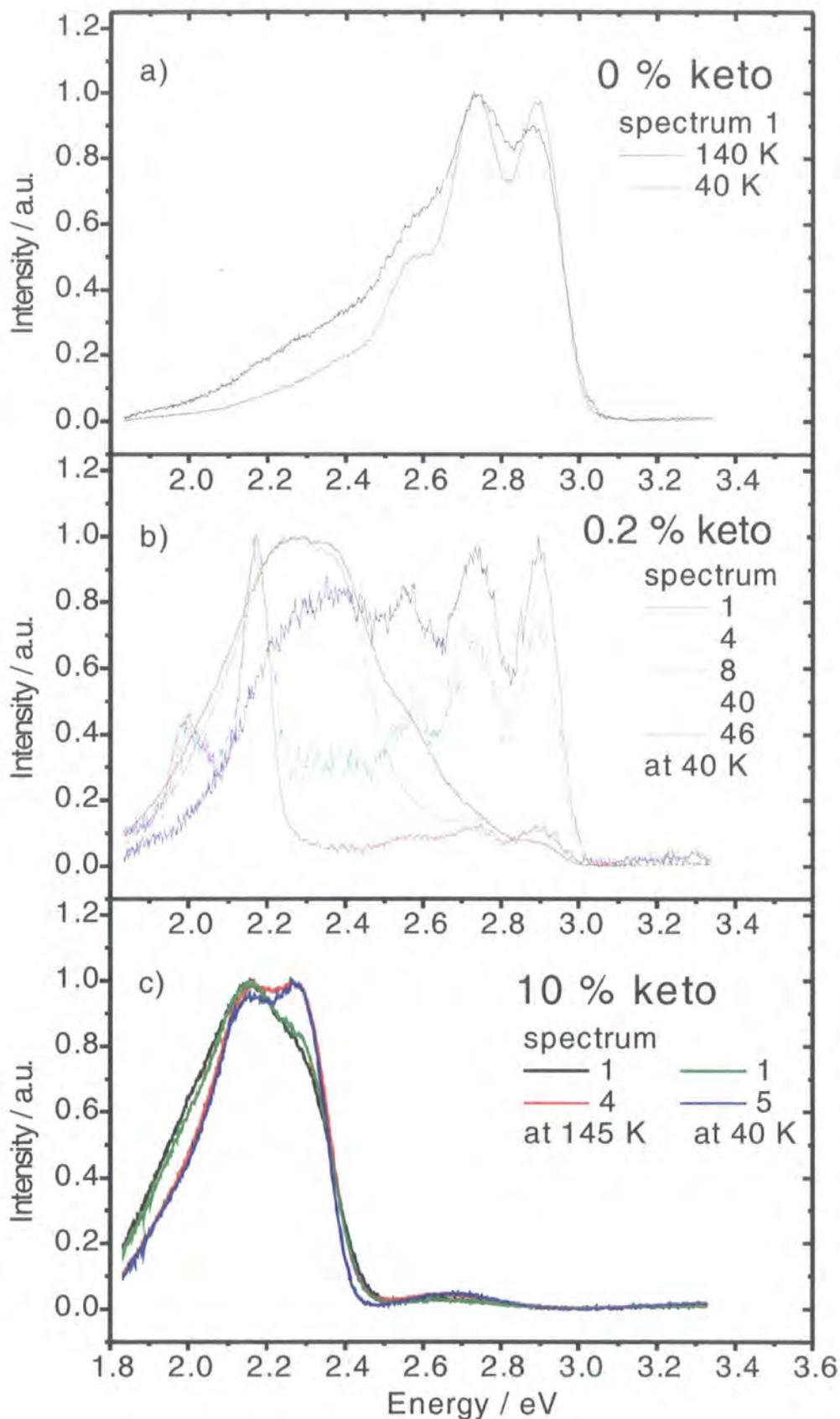
Figure 5.8 Low temperature spectra (normalised) of the delayed emission of thin films of *a)* PF2/6 am4 at ▬ 140 K ▬ 40 K (delay 4.2 ns); *b)* PFO/PFl 3 (0.2 % keto) at 40 K, delay: ▬ 4.2 ns ▬ 13.7 ns ▬ 60.9 ns ▬12.6 ms ▬ 126 ms; *c)* PFO/PFl 8 (10 % keto) at 145 K, delay: ▬ 4.2 ns ▬.13.7 ns, at 40 K ▬ 4.2 ns ▬ 18.9 ns.

c) At low temperature, PFO/PFl 8 with 10 % keto still shows much less DF than keto emission. The latter obviously consists of two parts, splitting into peaks at 2.3 eV and 2.1 eV, which exhibit different lifetimes. For 145 K as well as 40 K the peak at 2.1 eV is initially stronger than its bluish companion but this relation inverts for long delay times. Comparing these long-time spectra of 145 and 40 K, the 2.1 eV portion is slightly more pronounced for 145 K – altogether the relation between the 2.1 and 2.3 eV signals is very similar to that between keto emission and DF. The former are always *stronger at short delay times and for higher temperature*. No phosphorescence is encountered in PFO/PFl 8.

Summarising the above, the keto emission decreases with decreasing temperature. At low temperature and high fluorenone concentrations clearly two types of this emission at about 2.1 and 2.3 eV can be distinguished. The former is shorter lived and more pronounced at relatively high temperature. PFO phosphorescence is observed for long delay times but not at high fluorenone concentrations. It behaves similarly to the PFO delayed fluorescence.

5.5.3. DF and keto decay kinetics

Figure 5.9 shows a double logarithmic presentation of the decay kinetics of the DF and the keto emission found in thin films of the three polymers PF2/6 am4, PFO/PFl 3 and PFO/PFl 8 introduced in the previous sections. The curves have been corrected for fluctuations of the laser intensity as soon as the source of the emission – and with it the excitation dose dependency – was known.

All decay curves – of DF as well as keto emission and for all three polymers and the three investigated temperatures (room temperature, ~140 K, 40 K) – can be described in qualitatively the same way. They consist of mainly three parts.

The build-in of the signal does not belong to them but is a systematic error of the measurements: As mentioned above, these differential decay curves were recorded by a CCD camera with a different delay and exposure time for each data point and spectrum. The shorter the delay the shorter was also the exposure (about 1/10 of the delay). The camera, however, can only shut and open within 200 ps – thus for delays in the very low nanosecond range the intensity of the recorded emission is usually underestimated sometimes resulting in a pseudo-build-in of the decay curve.
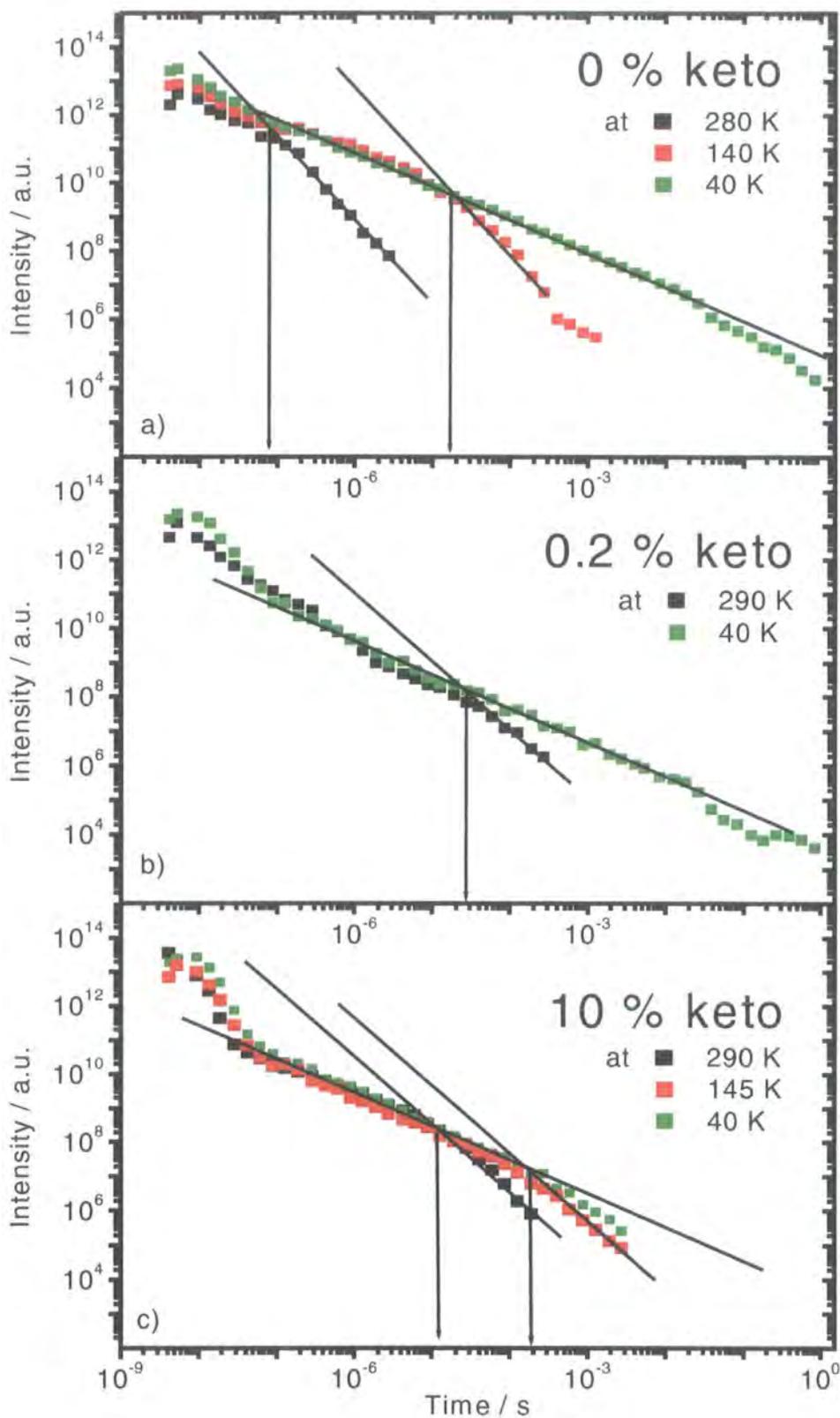
Figure 5.9 Decay kinetics of the delayed emission obtained from TRS of thin films of *a)* PF2/6 am4, DF at ■ 280 K ■ 140 K ■ 40 K; *b)* PFO/PFl 3 (0.2 % keto), keto emission at ■ 290 K ■ 40 K; *c)* PFO/PFl 8 (10 % keto), keto emission at ■ 290 K ■ 145 K ■ 40 K. The black lines are guides to the eye representing log-log slopes of -1 and -2 (for a): -2.5), respectively. The arrows mark turning points of the decay curves whenever applicable. a) is presented with kind permission of C. Rothe.

After that, a *fast decay* occurs with log-log slopes of the order of -3 or -4, which is followed by a region where the decay curve almost perfectly obeys a log-log *slope of -1*. At longer delay times, depending on the temperature at which the decay was recorded and the investigated polymer, a *transition from slope -1 to -2* is observed. The occurrence and the position of the corresponding turning points are extensively discussed in the following section as they reveal important information about the nature and the physical processes of the investigated emissions.

Naturally, for PF2/6 am4 only DF decay kinetics could be recorded as keto emission is hardly present in this polymer, see Figure 5.3. *Turning points occur faster with rising temperature.*
For PFO/PF1 3 containing 0.2 % fluorenone repeat units, keto as well as DF emission is present at room temperature and 40 K. However, the room temperature DF signals proved to be too weak to obtain a reasonable decay curve. Comparing keto and DF signals at 40 K, where one is an almost exact copy of the other, it might be assumed that this is the case for 290 K as well.

For PFO/PF1 8 containing 10 % fluorenone, DF decay curves are shown as well as those of the keto emission despite the poor quality of the data. The *keto graphs clearly exhibit the transition* mentioned above, turning times decreasing with rising temperature. One can only guess the same dependence for the DF curves although turning points can hardly be identified. However, obviously the DF lifetime decreases with rising temperature and, again, *DF and keto signals run parallel.*
As will be discussed in section 5.7.2, the observed slopes as well as the turning points can be interpreted making use of the hopping theory for excited states in conjugated polymers. The question is now: Which states are involved in the keto emission process? The following section is included in this thesis to provide additional information about the triplet excitons of both, fluorenone and polyfluorene.

5.6.   Triplet-triplet absorption spectra from flash photolysis

So far, only the singlet excitons of PFO have been investigated via steady-state luminescence and time-resolved spectroscopy techniques regardless the fact that keto emission can be excited via direct fluorenone triplet absorption. On one side, triplet excitons are connected to the emission process – on the other, energy transfer from PFO to keto can result in the same photoluminescence. The possibility that this is actually energy transfer from PFO to fluorenone triplets, must be taken into account.

In order to study the effects of keto defects on PFO triplet excitons, triplet-triplet absorption measurements have been carried out by my supervisor Prof. A. P. Monkman. They included two types of experiment: Photoinduced absorption (PIA, similar to the experiment described in 3.6) was utilised to obtain a T_1-T_n spectrum of a thin film of PFO in order to estimate the red shift between solid state and solution signals (shown in Figure 5.10). T_1-T_n spectra of polymer solutions were obtained from flash photolysis measurements. Here, the setup is similar to PIA: A pulsed electron pump beam excites a benzene solution, in which beside the polymer biphenyl is present, thereby creating biphenyl triplets of high energy. Via energy transfer from biphenyl to the polymer, the triplet exciton manifold of the latter is efficiently populated. A probe beam of white light is absorbed by these triplets, exciting them from T_1 into a higher energy level. The intensity of the absorption signal is proportional to the triplet concentration in the sample so that triplet decay curves and T_1-T_n spectra can be measured by monitoring the time and wavelength dependent induced absorption.
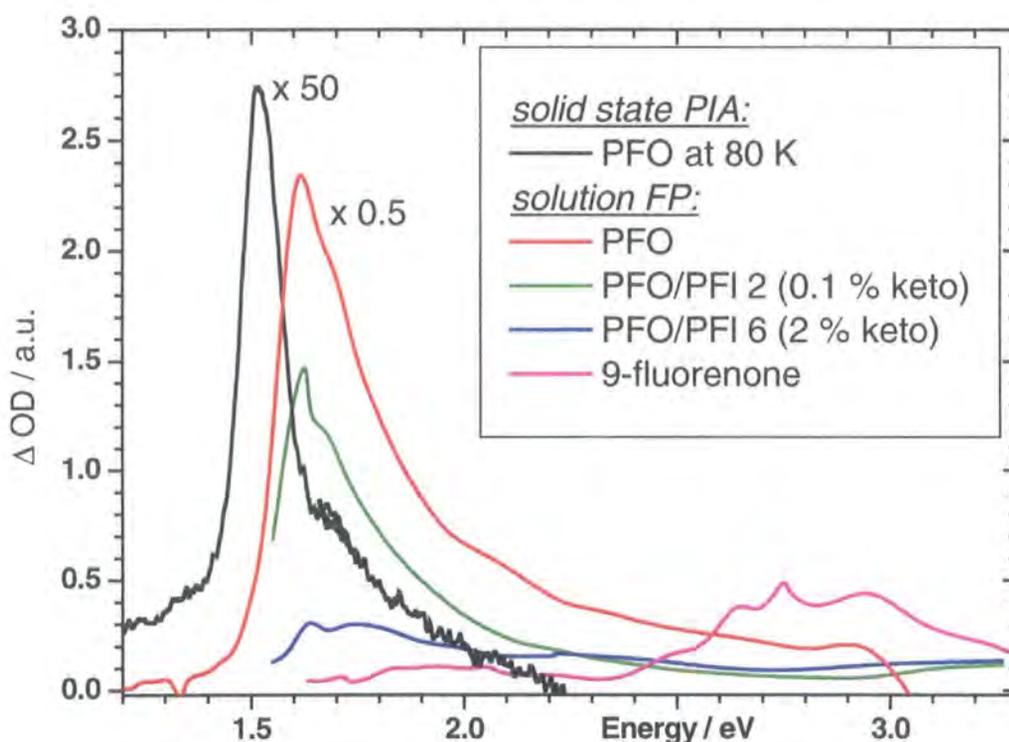
Figure 5.10 Triplet-triplet absorption spectra from flash photolysis (FP) of dilute solutions of PFO, PFO/PFl 2and 6 as well as 9-fluorenone in benzene (with 0.01 M Biphenyl as triplet generator). The PFO signal is strongly quenched upon introducing keto repeat units. For comparison, the red-shifted PIA spectrum of a thin film of pure PFO is shown at 80 K. Presented with kind permission from Prof. A.P. Monkman.

Figure 5.10 shows the T_1-T_n spectra for solutions of pure PFO, PFO/PFl 2 (0.1 % keto), PFO/PFl 6 (2 % keto) and – as pure PFl could not be dissolved – its corresponding monomer 9-fluorenone. The concentrations of the solutes in benzene (+0.01 M biphenyl): 10^{-4} M. As

expected, PFO triplet-triplet absorption is observed at 1.65 eV (for solution, solid state spectrum shifted to 1.5 eV) for pure PFO as well as for the co-polymers. The analogue for 9-fluorenone is located between 2.6 and 3.0 eV. The main information drawn from these data is that – comparing the intensities of the PFO triplet-triplet absorption signals among the polymers – the signal attributed to the PFO triplet manifold decreases much faster than it would be expected from the decreasing fraction of fluorene in the polymers. The presence of fluorenone strongly quenches PFO triplet excitons such that going from 0.1 to 2 % fluorenone only one third of the signal at 1.6 eV can be detected.

From the data of Figure 5.10 it can only be speculated if and how much of the fluorenone signal is detected in the co-polymer solutions. Still, the presented measurements provide an indication for the important role that triplet excitons play with respect to keto emission.

5.7. Discussion

5.7.1. Polyfluorene interchain interactions

Before discussing the results concerning keto defects in polyfluorene, the attention is turned to the excitation spectra of PFO/PFl solutions shown in section 5.4.2. Although these are distorted by inhomogeneous excitation of the sample, filtering the emission in regions of high optical density they still reveal an interesting effect.

It has been noted that the PFO part of absorption and excitation spectra coincide with respect to their spectral region and (roughly) their shape. However, their *fine structure* differs: Whereas the PFO absorption consists of one smooth band, the corresponding excitation spectra always exhibit a spike at the red side of the band (at about 3.1 eV, see Figure 5.5 and Figure 5.6). This observation has been made not only in the course of this study, for thin films as well as dilute and concentrated solutions of PFO/PFl co-polymers containing different keto levels, but is generally encountered for dilute solutions and films of various types of polyfluorene. The part of the spectrum which has been assigned to one PFO singlet absorption band (Figure 5.1) probably consists of *two components*.

There are several publications by Bradley *et al.*[48, 74-76] that report on *aggregation* combined *with long-range ordering* in annealed thin films of polyfluorene. Experimental evidence for such processes is mostly given in the form of solid state absorption (and photoluminescence) spectra, where changes are detected when the film samples have undergone thermal annealing. Following such treatment, an additional, very sharp absorption feature arises at 2.85 eV.

Some experimental findings indicate a relation between them and the excitation spike of untreated polyfluorene or PFO solutions. First of all, Figure 5.4 b) shows that one can excite a polyfluorene solution at 3.5 or 3.0 eV yielding qualitatively the same emission: Upon excitation at 3.0 eV even the tail of the first PF mode is clearly visible, the recording of the emission spectrum starting at 2.95 eV only on account of the detection system. Such a small Stokes' Shift is very unusual for a polymer but might rather be attributed to an aggregate state as these are rigid compared to a single polymer chain. Its lower limit could not even be detected. The excitation spike can be explained when all PFO singlet energy is efficiently transferred to aggregate sites on a time scale significantly shorter than the lifetime of PF emission. Thus the luminescence commonly attributed to polyfluorene PF would almost entirely be emitted from aggregate sites, in thin film as well as solution. When the aggregates, with their non-dissociative ground state, are directly excited, emission commences faster and is less subject to quenching entailed by a slight increase of intensity – the excitation profile shows a spike, which is not visible in the absorption spectrum but only arises due to different processes the excited states undergo *before* emission. In agreement with this, the rest of the absorption band remains unchanged compared to the corresponding excitation spectrum.

The spectral shift between Bradley's absorption feature and the presently discussed excitation spike can be caused by differences in morphology between the samples investigated[76, 77]. As mentioned above, the cited references report on the formation of macroscopically ordered structures, which might be seen as very long aggregates. Intensive annealing over a longer period of time is required to cause this change of film morphology. The aggregates that could form in a thin film *without* this annealing process are expected to occur statistically in places where neighbouring polymer chains are situated in very close proximity. There, they are proposed to form only between single repeat units resulting in a blue shift of their excitation profile. The same argument can easily be applied to room temperature solutions considering that the highest concentrations used for the studies presented in section 5.4.2 are still lower than those of the solutions used to spin-coat thin films.

Keeping in mind that the aggregates proposed are presumably low in concentration (without annealing treatment) their absorption is most probably hidden in the red end of the main PFO absorption band. To investigate this very interesting but as well speculative picture, the excitation and absorption spectra of solutions and thin films of PFO should be studied in greater detail, paying special attention to very highly concentrated and very dilute solutions as well as annealed thin films and thin films of PFO imbedded in the matrix polymer Zeonex. The latter is a matrix polymer which can be used to separate polymer chains and reduce interchain interactions.

From all of these considerations it should be expected that the different excited states also *emit differently* provided that their emission can be detected. As mentioned above the steady-state emission spectra upon excitation at 3.0 and 3.5 eV are equivalent – a result which does still

make sense when very fast energy transfer is assumed to occur from the high energy single chain to the low energy aggregate states. Here it is interesting to mention an experimental result obtained by C. Rothe using TRS measurements on films of PF2/6 am4 imbedded in Zeonex (not shown here). Indeed, accompanying the well resolved modes of the PF, a broader and slightly blue-shifted emission could be observed matching exactly the spectroscopic characteristics for single chain emission expected from excitation spectra. Still, this signal was rather weak. Consequently, the investigation of films with a lower PF2/6 am4 – Zeonex ratio or of different concentrations of pure PFO solutions will provide more detailed information about the nature of the single chain state. Furthermore, a better understanding of the relation between the two types of PFO chromophores can be achieved investigating solutions of PFO/PF1 as well as pure PFO in solvents of different polarity. Solvatochromism might reveal which orbital structures are involved in the formation of the observed excitations. Perhaps the aggregates proposed here have little in common with those observed by Bradley *et al.*. Further experiments will have to clarify this point as well.

Finally, I would like to state that I am aware of the speculative nature of the proposed aggregate picture drawn from only a side effect observed in the course of my study, one photoluminescence measurement and consultation with my supervisor. However, proving it true would entail serious consequences on the view to polyfluorene photophysics and, therefore, further investigations should be undertaken at least to negate the presented arguments.

5.7.2. The origin of keto emission

This section presents the interpretation of almost all of the experimental results obtained in connection with the study of fluorene-fluorenone co-polymers and attempts an explanation of the origin of keto emission well founded on experiment and recherché in the literature.

It has been confirmed via excitation dose measurements that the delayed fluorescence (DF) of PF2/6 am4 originates from triplet-triplet-annihilation (TTA) of polyfluorene triplets. Analysing the decay kinetics of this luminescence, one makes use of hopping theory: Having relaxed via internal conversion (IC) the triplet excitons migrate through the polymer via Dexter transfer. Many become quenched at impurities or via IC but some experience the distribution of available exciton sites as they perform downhill jumps (to sites of lower energy) with a temperature independent hopping rate[78] v_{ij} between sites i and j of energy ε_i and ε_j:

$$v_{ij} = v_0 \cdot e^{(-2 \cdot \gamma \cdot R_{ij})} \quad , \quad \varepsilon_j < \varepsilon_i$$

Equation 5.1
$$R_{ij} = \left| R_j - R_i \right|$$

where v_0 is a particle dependent prefactor, γ the inverse decay length of the localised wavefunction of the triplet and R_{ij} the spatial distance between the sites i and j. Once a local minimum is reached, the state of a triplet exciton is described as "frozen" because uphill jumps proceed much slower as these are rated with a Boltzmann-like expression[78]:

Equation 5.2
$$v_{ij} = v_0 \cdot e^{(-2 \cdot \gamma \cdot R_{ij})} \cdot e^{-\frac{(\varepsilon_j - \varepsilon_i)}{k_B \cdot T}} \quad , \quad \varepsilon_j > \varepsilon_i$$

with the above nomenclature, $k_B T$ being the thermal energy in Boltzmann terms. Statistically, triplets are then *immobile* for a period of time dependent on the temperature of the system. During this time they can undergo stable interactions with each other such as TTA, which leads to DF emission. According to Monte Carlo simulations[79] confirmed by experimental evidence[56] the latter emission decays with a slope of approximately -1 (in a double logarithmic plot).

After a temperature dependent duration, the average triplet has jumped uphill to the next exciton site, followed by another relaxation to a local minimum and further quenching of the triplet population. Triplet-triplet interactions are being broken up, resulting in a DF decay slope of -2[56]. The time when the transition between the -1 and -2 regimes takes place is termed *turning point* τ_C and exhibits the following temperature dependence (adapted from [79]):

Equation 5.3
$$\tau_C = v_0 \cdot e^{-\frac{c \cdot \sigma}{T^2}}$$

with k_0 as described above, σ denotes the width of the energy distribution of triplet sites, T is the absolute temperature and c is a parameter empirically determined via Monte Carly simulation s to be 2/3 for 3-dimensional and 0.9 for 1-dimensional motion[79]. Comparing DF and keto decay kinetics, almost identical behaviour is found, which means that the latter emission is also determined by *migration*. Combining the experimental results presented in this study with findings reported in the literature the photophysical processes leading to keto emission are proposed as follows:

Upon excitation at 3.5 eV (via laser or Xenon arc lamp) of keto-contaminated polyfluorene or PFO/PFl co-polymers, singlet excitons are formed on PFO chains or chain segments. They relax via IC and emit prompt fluorescence (PF) but – depending on the concentration of keto defects – a majority of them transfer their energy to keto sites (see excitation spectra). Which kind of transfer is involved here?

Let us consider that keto emission can be excited via *direct triplet absorption* (presumably $\pi \rightarrow n\pi$) as well. Beside this, singlet excitons transferring to defect sites will undergo intersystem crossing (ISC) before emission. The 9-fluorenone monomer exhibits an ISC rate

between 70 and 90 percent of the singlet excitons due to the presence of oxygen in the molecule providing a mixture of singlet and triplet excited states. Apparently, *fluorenone triplets* are the excited state that is finally required for keto emission. From the energetic point of view it is possible for a PFO singlet (energy 2.9 eV, see Figure 5.8 b)) to be converted to a fluorenone triplet (energy 2.3 eV[80]). Now, there are two possibilities for such a process to happen:

A) As oxygen atoms possess strong *electro negativity*, passing excitons might be trapped by their electron, the corresponding hole remaining delocalised on a polymer chain but centered at the oxygen atom. Such a state can be generated via Dexter electron or charge transfer. One must take into account that the singlet kinetics are dominated by Förster transfer and quenching as well as by radiative decay. As the time scales of these processes are much shorter than that of Dexter transfer (see theory section), the latter is somewhat improbable considering the small concentrations of fluorenone sufficient to generate keto emission.

On the other hand, such a scenario is likely to occur for the *electroluminescence* (EL) of polyfluorene where the formation of excitons via charge recombination requires time. This can allow single charge carriers to migrate to and be trapped at a keto defect site. The electron again can bind a hole to form an exciton at the keto site.

B) Another path opens up via *Förster radiative transfer*. Note that the PF emission spectrum of polyfluorene ranges from 2.5 to 3.05 eV (Figure 5.3) which gives a good spectral overlap with the fluorenone triplet absorption (2.4 up to at least 2.9 eV, Figure 5.1). How can this be brought into agreement with *spin conservation*? First of all, the triplet absorption represents a $\pi \rightarrow n\pi$ transition, which means that, during transfer, the triplet would be built up at the oxygen atom of the fluorenone repeat unit, which (on its own) exhibits a triplet ground state. Still, the very high ISC rate of fluorenone is an indication that the molecule possesses a high degree of mixing among singlet and triplet states. Thus the spin conservation rule is lifted and Förster transfer is possible e.g. highly efficient intramolecular singlet to triplet transfer has been reported for molecules of anthracene chemically joint to fluorenone[81]. –The singlet excited orbitals of polyfluorene interact radiatively with the orbitals of fluorenone resulting in a coupled transition of $S_n^m \rightarrow S_0^k$ for PFO (probably with n=1, m=0) and $T_n^m \leftarrow X_0^0$ for fluorenone (where X refers to a ground state of unknown multiplicity). The mechanism which is responsible for the trapping of the triplet exciton might still be the attraction of the electron by oxygen as suggested for A). This mechanism is more probable to occur under photoluminescence conditions in degraded PFO as here already low fluorenone concentrations can account for efficient transfer – Förster is larger than Dexter radius.

Whereas the former scenario is more probable to occur for EL conditions and the latter for photoluminescence (PL), in principle both of them are physically possible and, as they do not exclude each other, the transfer process in PFO/PFl will finally be a combination of both. It is a common feature of the suggested mechanisms that they populate the triplet manifold of the fluorenone repeat units and that these triplets exhibit a very low mobility as they are trapped by oxygen.

In section 5.2 it has been mentioned that the assignment of the red fluorenone absorption band to a $\pi \rightarrow n\pi$ triplet transition is not completely confirmed. Regarding transfer mechanism B) it must be noted that even if one only relies on the good spectral overlap of PFO emission and fluorenone absorption (if caused by triplets or not), the latter definitely originates from an at least partly allowed transition as it can be detected via absorption spectroscopy at low fluorenone concentrations. Hence, the suggested Förster transfer is allowed.
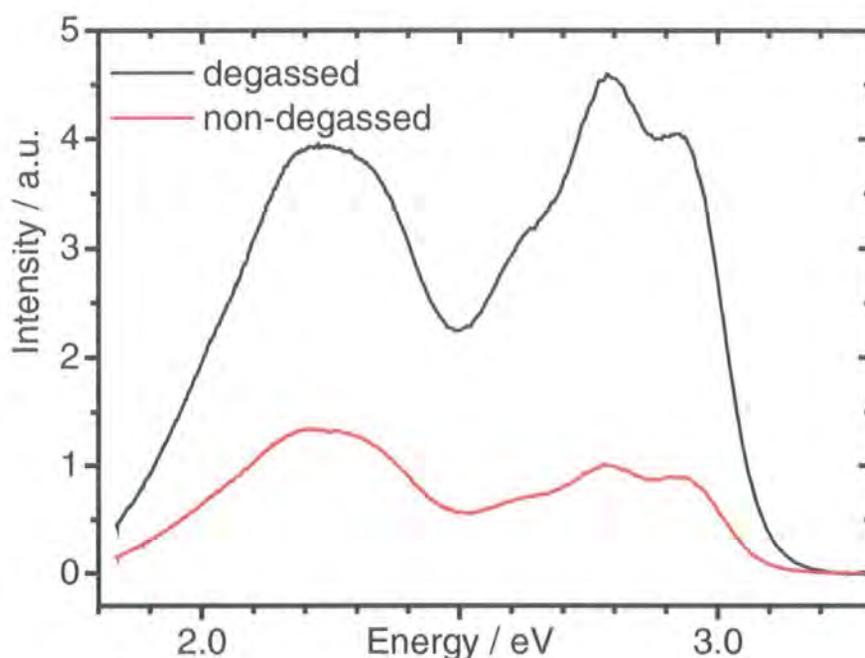
Figure 5.11 Two spectra of the delayed luminescence of a dilute solution of PFO/PFl 3 (0.2 % keto) recorded at room temperature under the same detection conditions (delay: 10 ns). The intensity of keto emission as well as DF grows upon degassing.

Continuing the thought that polyfluorene DF arises via *polyfluorene TTA* it has often been suggested that 9-fluorenone monomers (in various solvent environments) are likely to form excimers mediated by a *fluorenone TTA* process[72]. The orbitals of the triplet states on two adjacent fluorenone molecules interact with each other thus helping to overcome the potential barrier for excimer formation. The triplets annihilate into one excited singlet state causing the *irreversibility* of the excimer formation process. Strong dipole-dipole interactions between the polar fluorenone repeat units are responsible for the stability of the excited state. Thus, the

excimer is likely to emit as dissociation is weak. Should the observed keto emission be luminescence from fluorenone excimers then fluorenone triplet trapping must be reflected in *decay kinetics* of keto emission in analogy to the DF of polyfluorene. Experimental results support this point as (in the double logarithmic plots of Figure 5.9) slope regimes of -1 are observed, which are followed by slopes of -2. In agreement with hopping theory, the turning points between them occur much later (~10 μs at 40 K) compared to DF (100 ns at 40 K) due to the far lower mobility of fluorenone triplets. Despite such good agreement, the fluorenone TTA mechanism still has to be confirmed by measuring the excitation dose dependency of the keto emission, which should be quadratic as is observed for the DF. One indication of a triplet origin of keto emission is already given by the quenching of keto as well as DF emission in the presence of oxygen, see Figure 5.11. Additionally, this experimental result supports the assumption that the direct fluorenone absorption originates from triplet excitons.
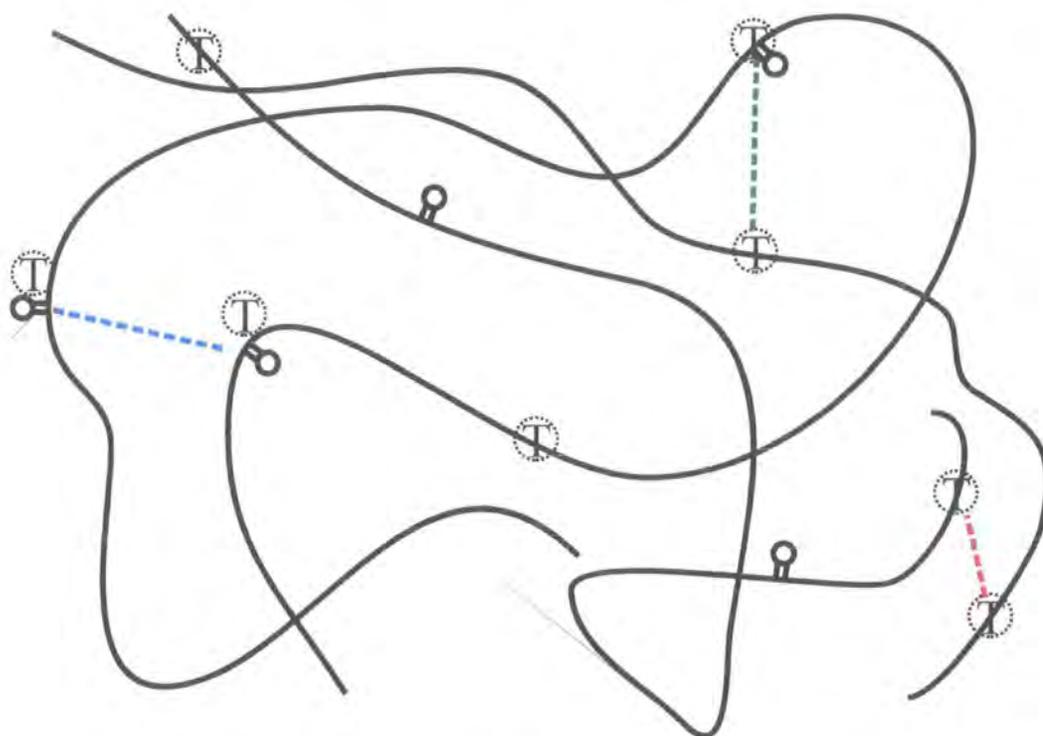
Figure 5.12 *Illustration of the proposed three types of triplet-triplet interaction in PFO/PFl:* The black lines represent polyfluorene chains, =O stands for a fluorenone repeat unit and each T for a triplet exciton. ▪▪▪ two PFO triplets feeling their mutual Coulomb attraction leading to DF emission via *TTA* ▪▪▪ in the presence of keto repeat units: A fluorenone and a PFO triplet attract each other mediating *exciplex* formation between the interacting chromophores ▪▪▪ two fluorenone triplets attract each other mediating fluorenone *excimer* formation.

However, the TTA picture described does not yet explain all of the observed emission features. Altogether three types of delayed luminescence have been identified in section 5.5: Delayed fluorescence, keto emission at 2.3 eV and another keto attributed emission at 2.1 eV. The third

could be separated from the second due to its slightly faster decay and different temperature behaviour. To explain this, the following is suggested (for an illustration, see Figure 5.12):

Two types of triplet are known to be present in PFO/PFl co-polymers: Fluorenone triplets (FT) (identified by a direct triplet absorption signal and proposed to be populated via energy transfer) and polyfluorene triplets (PFT) (DF and Ph have been observed for low keto content and low temperature). Hence, three types of triplet-triplet-interaction are possible: FT and PFT can interact with each other resulting in fluorenone excimer emission and DF, respectively, but also mixed FT-PFT interactions might be possible. In analogy to fluorenone excimers this mixed type of TTA might lead to *exciplex* formation:

As a consequence of overcoming the repulsion between the orbitals of a fluorene and a fluorenone repeat unit, stable physical bonds can form assisted by the strong electro negativity of the fluorenone oxygen atom leading to dipole-dipole attraction. Excimer and exciplex are supposed to exhibit similar properties with respect to their luminescence: Their ground states do not play a role as they do not exist; and the excited states are based on the same type of intermolecular interaction involving only the conjugated orbitals of the backbone and the n orbital of oxygen. In this way the similarity of the emission spectra as well as the decay and thermal behaviour of both of the keto assisted emissions can be explained.

Remains the question: Which emission belongs to 2.1 eV and which to 2.3 eV? This can be answered by comparing their dependence on keto level and temperature. While DF is mainly found at low temperature or low keto level, the emission at 2.1 eV favours low temperature and high keto level, and keto emission at 2.3 eV dominates at room temperature but still rather low keto level. Regarding of these relations between the three emissions it shows that the previously suggested triple TTA picture proves itself:

Polyfluorene triplets interact with each other, their recombination leading to DF emission. However, TTA is more likely to occur between polyfluorene and fluorenone triplets as the latter are immobile in contrast to the PFT, which can break up triplet-triplet interactions due to migration before any recombination and emission has set in. Thus already a low keto level leads to these mixed interactions and exciplex formation mediated by TTA. It is followed by keto emission at 2.3 eV that originates from the recombination of the exciplex singlet state. In analogy to this argumentation, high keto levels with an excess of fluorenone triplets entail the dominance of fluorenone excimer formation; the emission at 2.1 eV originates from the recombining singlet state.

The influence of temperature on keto emission is illustrated in Figure 5.13: After a short time PFO singlet excitons have reached a local minimum of site energy. If they are still not trapped, their further uphill migration in the sense of hopping theory requires a Boltzmann type thermal

activation. As a consequence, fewer singlets are keto-trapped and converted to fluorenone triplets at low temperature. Due to intrinsic PFO intersystem crossing there are also more fluorene triplets at long times after excitation, leading to more phosphorescence, delayed fluorescence and 2.3 eV keto emission in comparison to room temperature. In the latter case, depending on the concentration of keto defects, most of the PFO singlets are trapped at a keto site and due to the excess of fluorenone triplets many fluorenone excimers are formed, which emit at 2.1 eV.

Please note that the illustration of trap depths in Figure 5.13 does *not* attempt to compare the triplet energies of polyfluorene (2.15 eV, see Figure 5.8 b)) and fluorenone (2.3 eV[80]). Instead, Figure 5.13 refers to the fluorenone trap mechanism via electron attraction by oxygen described above and the distribution of triplet sites experienced by mobile fluorene triplets.
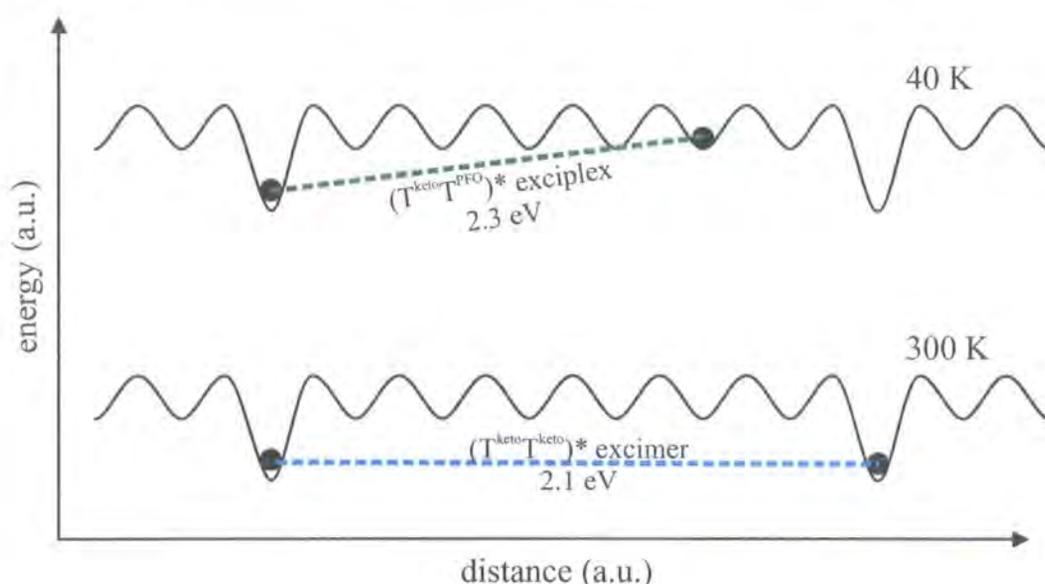
Figure 5.13 *Migration controls the triplet-triplet interactions involving keto repeat units: Above:* At low temperature trapped fluorenone triplets interact with "frozen" PFO triplets forming *exciplexes*, which emit at 2.3 eV. *Below:* At room temperature most PFO triplets become keto-trapped very fast due to thermal activation of their mobility. Fluorenone triplets mainly interact with each other leading to *excimer* formation with emission at 2.1 eV; a high keto concentration has the same effect.

The decay kinetics presented in section 5.5 for the keto emission have been tried to separate into two components corresponding to the 2.1 eV and 2.3 eV emissions. However, as these luminescence bands are located so close to each other, the quality of the data obtained has not been sufficient to clearly identify their decay kinetics and turning points. For this reason, the following discussion has to rely on the decay spectra of Figure 5.8 c), where the different keto emissions can finally be *separated by their decay kinetics* thus proving that *they originate from*

different excited states. It shows, that the TTA picture is also able to describe the decay behaviour observed in the delayed spectra presented in this section: Emission at 2.1 eV dominates the first spectra (when fluorenone repeat units are present) followed by keto luminescence at 2.3 eV and, later, DF. In analogy to the argument used previously, it is suggested that, in the presence of many keto defects, fluorenone-fluorenone interactions (excimers) are favoured and lead to emission in most cases thereby depopulating the fluorenone triplet manifold at early stages after excitation. Repopulation would require direct triplet absorption or the trapping of PFO singlets, which are not present after 1 ns except for those created via polyfluorene TTA. Due to an energy barrier (see paragraph above) PFO triplets, which have formed in the meantime via ISC of the remaining PFO singlets, cannot transfer directly to keto defects and the FT concentration decreases. Consequently, exciplex formation between PFT and FT is the favoured interaction now and after the decay of their luminescence there is a chance for DF.
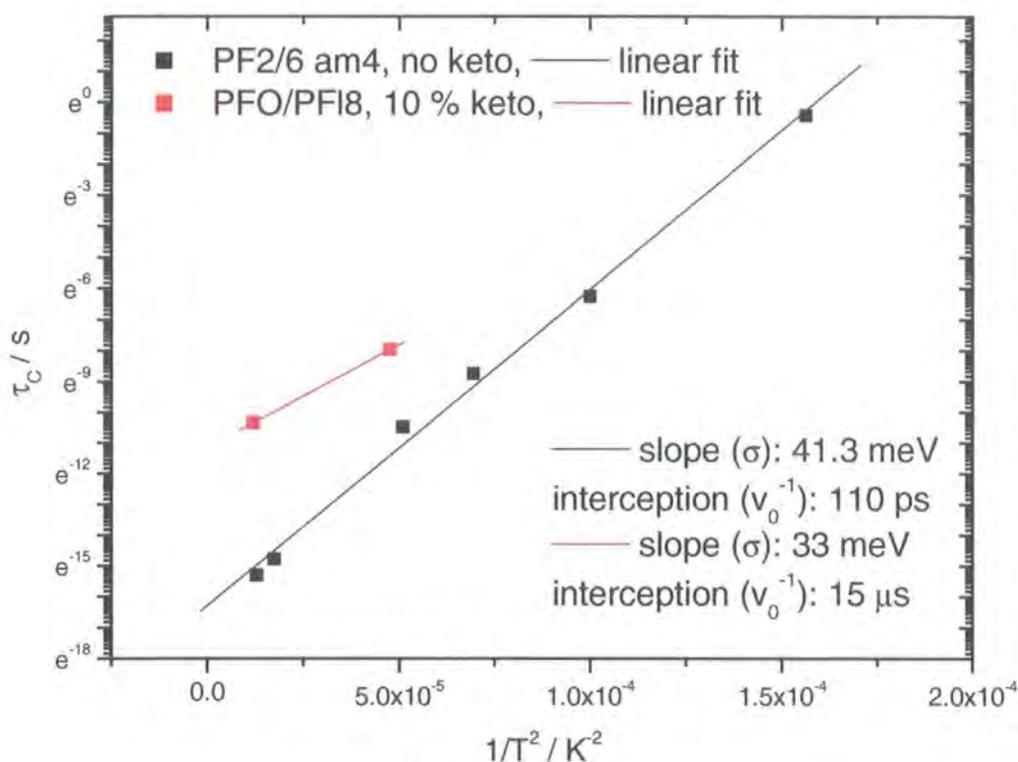
Figure 5.14 τ_c τ is the time of the transition between slope regimes -1 and -2 in the log-log decay curves of DF and keto emission. Its natural logarithm depends linearly on $1/T^2$, the interception with the ordinate representing the "attempt to jump" frequency v_0 between the emission precursors (linear fits yielding: — *1/110 ps* for the *DF of PF2/6 am4*, — *1/15 μs* for the *keto emission of PFO/PFl 8*) and the slope dependent on their trap depth σ (yielding: — *41.3 meV* for the DF of PF2/6 am4, — *33 meV* for the keto emission of PFO/PFl 8). The data and fit for the DF of PF2/6 am4 are presented with kind permission of C. Rothe.

As all of these processes are slowed down at low temperature, the emissions are separated best for high keto level at 40 K (Figure 5.8 c)). Still it proves to be difficult to measure their decay kinetics separately as their spectra overlap so closely, for the same reasons DF kinetics could not be measured. As an improvement of the decay measurements could provide the final proof of the above assumptions and the TTA picture, this has to be a matter of further investigations.

Finally, attention is turned to a qualitative analysis of the keto decay kinetics. For DF, the width of the site energy distribution for the annihilating triplets can be determined by plotting the turning time τ_C (between slopes -1 and -2) against $1/T^2$, assuming a 3-dimensional recombination process (c=2/3), compare to Equation 5.3 which describes the temperature dependence of τ_C. An analogous analysis in terms of hopping theory has been attempted for the decay kinetics of keto emission (Figure 5.14).

Two values of τ_C could be obtained from Figure 5.9 c). These have been plotted against $1/T^2$ (red data points and fit in Figure 5.14). The interception of the fit with the ordinate yields the jump rate (Equation 5.3). The result of $v_0=1$ jump/15μs for fluorenone triplets makes sense when compared to a fit for the DF of PF2/6 am4 ($v_0=1$ jump/110 ps, see Figure 5.14) as fluorenone triplets are suggested to be immobile. From the slopes of the fits a smaller width of the site energy distribution is found for fluorenone ($\sigma = 33$ meV) than for PF2/6 am4 ($\sigma = 41.3$ meV), which is about the same within the limits of accuracy of the experiment. Due to the lack of data, the error of the keto fit has to be assessed as rather high so that only the order of magnitude of the values obtained should be taken into account. In order to achieve more accurate results, the experiment should be repeated for more temperatures to improve the fit.

5.8. Conclusions

Based on the results of various spectroscopic experiments this section analysed the origin of keto emission in PFO/PFl co-polymers as model compound for photo-degraded polyfluorene. The relation between fluorenone repeat units and the green emission band found in polyfluorene samples has been established in the literature.

Three types of delayed emission could be identified such as delayed fluorescence emitted by excited polyfluorene singlet excitons created via TTA of polyfluorene triplets. Furthermore, the two types of keto luminescence (at 2.1 eV and 2.3 eV) were investigated via absorption, excitation, steady-state emission and time-resolved emission spectroscopy as well as flash photolysis. Keto emission can be excited directly via absorption of photons by fluorenone triplets. From the excitation spectroscopy it is also concluded that efficient energy transfer occurs from PFO singlets to fluorenone triplets, opening up a second route for keto emission.

The singlets are trapped at keto sites due to the electro negativity of the fluorenone oxygen atom. Fluorenone triplets are suggested to initiate fluorenone excimer and PFO-fluorenone exciplex formation via TTA. The physical bonds required for these interchain states supposedly involve the n-orbital of the fluorenone oxygen. The two types of keto emission could be clearly separated by their different decay kinetics and are, therefore, not just two vibronical modes of the same radiative decay.

This triple TTA mechanism is able to explain the observed three types of delayed emission as well as their relations regarding decay, temperature and keto level dependence. The TTA origin of keto emission is strongly indicated due to oxygen quenching of the luminescence in non-degassed PFO/PFl solution. In the literature, several references could be found that suggest fluorenone excimer formation via TTA. However, further experiments are required for the confirmation of the TTA picture such as the measurement of the excitation dose dependency of both keto emissions, which is expected to be quadratic. To imbed keto emission into hopping theory and gain qualitative information about fluorenone triplet migration processes, a more detailed study of temperature dependent decay must be carried out for keto emission. Moreover, the quality and analysis of the TRS decay measurements must be improved in order to separate the kinetics of DF and of the two types of keto luminescence.

In the course of this study, differences between PFO absorption and excitation spectra have been noticed. This observation has confirmedly been made by other persons as well. In contrast to the smooth single absorption band of PFO, the excitation spectrum appears with a spike at the red side of the band. Taking into account that the same emission (polyfluorene prompt fluorescence) is observed upon excitation at any point in the band as well as the extremely small Stokes' shift connected to it, the presence of aggregate states is proposed to occur statistically between single repeat units of polyfluorene. Parallels to ordered structures found by Bradley *et al.*[75] have been noticed. As the assumptions would also suggest that the prompt fluorescence of polyfluorene is emitted completely by aggregate states populated directly but also via extremely fast energy transfer from polyfluorene singlets, further investigations seem to be required. Studies of very concentrated and very dilute PFO solutions might be useful as well as experiments on annealed PFO films and films of PFO imbedded in matrix polymers. Especially the latter promise results as here already prompt emission could be observed, which might be attributed to fluorescence from single chain instead of aggregate states.

6. REFERENCES

1   J. H. Burroughes, D. D. C. Bradley, A. R. Brown, et al., Nature **347**, 539 (1990).

2   R. J. Visser, Philips J. Res., 467 (1998).

3   R. H. Friend, R. W. Gymer, A. B. Holmes, et al., Nature **397**, 121 (1999).

4   C. Rothe, S. Hintschich, A. P. Monkman, et al., Journal of Chemical Physics **116**, 10503 (2002).

5   Y. V. Romanovskii, A. Gerhard, B. Schweitzer, et al., Chemical Physics **249**, 29 (1999).

6   Y. V. Romanovskii, A. Gerhard, B. Schweitzer, et al., Physical Review Letters **84**, 1027 (2000).

7   C. Rothe, R. Guentner, U. Scherf, et al., Journal of Chemical Physics **115**, 9557 (2001).

8   M. Munowitz, *Principles of Chemistry*, London, 2000).

9   M. Pope and C. E. Swenberg, *Electronic Processes in Organic Crystals and Polymers* (Oxford University Press, Oxford, 1999).

10 H. Meier, U. Stalmach, and H. Kolshorn, Acta Polymerica **48**, 379 (1997).

11 S. Kishino, Y. Ueno, K. Ochiai, et al., Physical Review B **58**, R13430 (1998).

12 N. T. Harrison, G. R. Hayes, R. T. Phillips, et al., Physical Review Letters **77**, 1881 (1996).

13 A. J. Heeger, S. Kivelson, J. R. Schrieffer, et al., Reviews of Modern Physics **60**, 781 (1988).

14 H. Bassler, M. Gailberger, R. F. Mahrt, et al., Synthetic Metals **49**, 341 (1992).

15 S. Barth and H. Bassler, Physical Review Letters **79**, 4445 (1997).

16 S. F. Alvarado, P. F. Seidler, D. G. Lidzey, et al., Physical Review Letters **81**, 1082 (1998).

17 C. Rothe, (University of Durham, 2002).

18 H. S. Nalwa, (Wiley, Chichester ; New York, 1997), p. 4 v.

[19] D. Hertel, Y. V. Romanovskii, B. Schweitzer, et al., Synthetic Metals **116**, 139 (2001).

[20] P. W. Atkins, *Molecular Quantum Mechanics*, 1983).

[21] C. H. J. Wells, *Introduction to molecular photochemistry* (Chapman and Hall, London, 1972).

[22] M. G. Harrison, S. Moller, G. Weiser, et al., Physical Review B **60**, 8650 (1999).

[23] A. P. Monkman, H. D. Burrows, M. d. G. Miguel, et al., Synthetic Metals **116**, 75 (2001).

[24] T. H. Förster, (International Union of Pure and Applied Chemistry, 1972), p. 225.

[25] E. F. H. Brittain, W. O. George, and C. H. J. Wells, *Introduction to molecular spectroscopy; theory and experiment* (Academic Press, London, New York,, 1970).

[26] S. C. J. Meskers, J. Hubner, M. Oestreich, et al., Chemical Physics Letters **339**, 223 (2001).

[27] P. S. de Freitas, U. Scherf, M. Collon, et al., (2002).

[28] M. Wohlgenannt, W. Graupner, G. Leising, et al., Physical Review B **60**, 5321 (1999).

[29] H. D. Burrows, J. S. de Melo, C. Serpa, et al., Journal of Chemical Physics **115**, 9601 (2001).

[30] M. Wohlgenannt, K. Tandon, S. Mazumdar, et al., Nature **411**, 617 (2001).

[31] J. F. Rabek, *Photodegradation of Polymers* (Springer, 1996).

[32] T. H. Förster, in *10th Spiers Memorial Lecture*, 1959), p. 7.

[33] G. Cerullo, S. Stagira, M. Zavelani-Rossi, et al., Chemical Physics Letters **335**, 27 (2001).

[34] R. Richert and H. Bassler, Chemical Physics Letters **118**, 235 (1985).

[35] A. R. Buckley, M. D. Rahn, J. Hill, et al., Chemical Physics Letters **339**, 331 (2001).

[36] E. J. W. List, R. Guentner, P. S. de Freitas, et al., Advanced Materials **14**, 374 (2002).

[37] C. Rothe, S. I. Hintschich, L. O. Palsson, et al., Chemical Physics Letters **360**, 111 (2002).

[38] M. A. Baldo, D. F. O'Brien, Y. You, et al., Nature **395**, 151 (1998).

[39] M. A. Baldo, S. Lamansky, P. E. Burrows, et al., Applied Physics Letters **75**, 4 (1999).

[40] D. Dexter, Journal of Chemical Physics **21**, 836 (1953).

[41] R. Richert and H. Bassler, Journal of Chemical Physics **84**, 3567 (1986).

[42] S. A. Bagnich and A. V. Konash, Chemical Physics **263**, 101 (2001).

[43] A. P. Monkman, H. D. Burrows, I. Hamblett, et al., Chemical Physics Letters **340**, 467 (2001).

[44] R. W. T. Higgins, A. P. Monkman, H. G. Nothofer, et al., Applied Physics Letters **79**, 857 (2001).

[45] I. D. W. Samuel, G. Rumbles, and R. H. Friend, *Primary Photoexcitations in Conjugated Polymers* (World Scientific, New York, 1997).

[46] J. H. Hsu, W. S. Fann, P. H. Tsao, et al., Journal of Physical Chemistry A **103**, 2375 (1999).

[47] T. Q. Nguyen, V. Doan, and B. J. Schwartz, Journal of Chemical Physics **110**, 4068 (1999).

[48] A. J. Cadby, P. A. Lane, H. Mellor, et al., Physical Review B **62**, 15604 (2000).

[49] M. Tammer, R. W. T. Higgins, and A. P. Monkman, Journal of Applied Physics **91**, 4010 (2002).

[50] M. Grell, W. Knoll, D. Lupo, et al., Advanced Materials **11**, 671 (1999).

[51] T. Miteva, A. Meisel, W. Knoll, et al., Advanced Materials **13**, 565 (2001).

[52] S. Setayesh, A. C. Grimsdale, T. Weil, et al., Journal of the American Chemical Society **123**, 946 (2001).

[53] M. R. Andersson, W. Mammo, T. Olinga, et al., Synthetic Metals **101**, 11 (1999).

[54] A. P. Monkman, H. D. Burrows, I. Hamblett, et al., Journal of Chemical Physics **115**, 9046 (2001).

[55] M. Theander, O. Inganas, W. Mammo, et al., Journal of Physical Chemistry B **103**, 7771 (1999).

[56] D. Hertel, H. Bassler, R. Guentner, et al., Journal of Chemical Physics **115**, 10007 (2001).

[57] M. Theander, O. Inganas, and M. R. Anderson, Synthetic Metals **101**, 331 (1999).

[58] U. Lemmer, S. Heun, and R. F. Mahrt, Chemical Physics Letters **240** (1995).

[59] P. C. Subudhi and E. C. Lim, Chemical Physics Letters **56**, 59 (1978).

60   H. D. Burrows, J. S. de Melo, C. Serpa, et al., Journal of Chemical Physics **115**, 9601 (2001).

61   S. Hintschich, C. Rothe, and A. Monkman, Synthetic Metals **135-136**, 365 (2003).

62   A. P. Monkman, H. D. Burrows, L. J. Hartwell, et al., Physical Review Letters **86**, 1358 (2001).

63   C. Rothe and A. Monkman, Physical Review B **65** (2002).

64   B. Schweitzer, V. I. Arkhipov, U. Scherf, et al., Chemical Physics Letters **313**, 57 (1999).

65   J. B. Birks, *Photophysics of aromatic molecules* (Wiley-Interscience, London, New York,, 1970).

66   J. B. Birks, *Organic molecular photophysics* (J. Wiley, London, New York,, 1973).

67   H. D. Burrows, J. S. de Melo, C. Serpa, et al., Journal of Chemical Physics (2001).

68   V. N. Bliznyuk, S. A. Carter, J. C. Scott, et al., Macromolecules **32**, 361 (1999).

69   S. Panozzo, J.-C. Vial, Y. Kervella, et al., Journal of Applied Physics **92**, 3495 (2002).

70   E. Zojer, A. Pogantsch, E. Hennebicq, et al., Journal of Chemical Physics **117**, 6794 (2002).

71   G. Klaerner and R. D. Miller, Macromolecules **31**, 2007 (1998).

72   S. A. Rani, J. Sobhanadri, and T. A. P. Rao, Journal of Photochemistry and Photobiology a-Chemistry **94**, 1 (1996).

73   K. Yoshihara and D. R. Kearns, Journal of Chemical Physics, 1991 (1966).

74   M. Grell, D. D. C. Bradley, G. Ungar, et al., Macromolecules **32**, 5810 (1999).

75   M. Grell, D. D. C. Bradley, M. Inbasekaran, et al., Synthetic Metals **111**, 579 (2000).

76   M. Ariu, D. G. Lidzey, and D. D. C. Bradley, Synthetic Metals **111**, 607 (2000).

77   M. Grell, D. D. C. Bradley, X. Long, et al., Acta Polymerica **49**, 439 (1998).

78   B. Ries, H. Baessler, M. Gruenewald, et al., Physical Review B **37**, 5508 (1988).

79   B. Movaghar, M. Grunewald, B. Ries, et al., Physical Review B **33**, 5545 (1986).

80   R. S. Murphy, C. P. Moorlag, W. H. Green, et al., Journal of Photochemistry and Photobiology a-Chemistry **110**, 123 (1997).

[81]   H. D. Becker, C. Burgdorff, and H. G. Lohmannsroben, Journal of Photochemistry and Photobiology a-Chemistry **86**, 133 (1995).